Non-intrusive condition monitoring of power cables within the industrial sector

JH van Jaarsveldt

20569408

Dissertation submitted in fulfilment of the requirements for the degree *Magister* in Electrical and Electronic Engineering at the Potchefstroom Campus of the North-West University

Supervisor: Prof R Gouws

May 2015

Executive Summary

Condition monitoring (CM) of electrical equipment is an important field in electrical engineering and a considerable amount of research is dedicated to this field. Power cables are one of the most important parts of any electrical network and the variety of techniques available for CM of electrical cables is therefore no surprise. Electrical cables are exposed to operational and environmental stressors which will cause degradation of the insulation material. The degradation will continue to the point where the cable fails. Blackouts caused by failing cables will have an effect on the safety, efficiency and production of an electrical network. It is therefore important to constantly monitor the condition of electrical cables, in order to prevent the premature failure of cables. The research presented in this dissertation sets out to investigate CM techniques for power cables and to design and implement a basic cable CM technique based on the principles of partial discharge (PD) measurements.

A comprehensive literature study introduces the fundamental concepts regarding the CM of power cables. The basic construction of electrical cables, as well as the variety of different types is researched in order to lay a foundation for the research that follow. CM techniques for electrical equipment are investigated, with the emphasis on techniques used on cables. Conducted research led to the decision to focus on CM by means of PD measurements. PD as a phenomenon is investigated to be able to better understand the origins and effects of discharge activity. From there the focus shifts to the available techniques for monitoring the condition of electrical cables by means of PD measurements. The research conducted in the literature study chapter forms the basis from which the rest of the study is conducted.

Simulation models were used to study PD characteristics. The models are derived from engineering and mathematical principles and are based on the well-known three-capacitor model of PD. The simulations were performed in order to study the effects of discharge activity. The designed simulation models allows for a variety of PD characteristics to be studied. The simulations were performed in the MATLAB® Simulink® environment.

The research conducted in the dissertation was used to design an elementary CM technique which can be used to detect the presence of PD within electrical cables. The designed CM technique was used for the practical measurement of PD data. MATLAB® programs were designed in order to analyse the PD data in both the time- and frequency-domain. The analysis of the measured data revealed PD characteristics of the test specimen used for the measurements. The designed CM is used for the detection of PD activity within electrical cables and in combination with other techniques, may be used for complete CM of electrical cables. The experimental setup which was used to take practical PD measurements adds another dimension to the work presented in this dissertation.

Key Words: Condition Monitoring (CM), Partial Discharge (PD), Cross-Linked Polyethylene (XLPE), Non-intrusive, Simulation models, Apparent Charge

Opsomming

Kondisie monitering van elektriese toestelle is ’n belangrike komponent van elektriese ingenieurswese en baie navorsing is gefokus op dié veld. Elektriese kabels is een van die belangrikste komponente van enige kragstelsel en daarom is daar ’n groot verskeidenheid tegnieke beskikbaar vir die monitering van kabels. Degradasie van die isolasie materiaal van ’n elektriese kabel vind plaas omdat die kabel aan beide operasionele, sowel as omgewing-stresfaktore blootgestel word. Die degradasie kan lei tot kabels wat faal. Kragonderbrekings wat plaasvind a.g.v. kabels wat faal, sal die veiligheid, effektiwiteit, asook die produksie van ’n netwerk beïnvloed. Deur die konstante monitoring van kabels, kan kabels wat faal voorkom word. Die doel van die navorsing in hierdie verhandeling is om verskeie tegnieke van kondisie monitering, van toepassing op kabels, te ondersoek. ’n Kondisie moniteringstegniek wat gebruik maak van gedeeltelike ontlading metings moet dan ook ontwerp en geïmplimenteer word.

Die doel van die deeglike literatuurstudie is om grondslag aspekte van kondisie monitering vir elektriese kabels te ondersoek. Navorsing aangaande die konstruksie van elektriese kabels, sowel as die verskillende tipes kabels word ondersoek. Verskeie tegnieke van kondisie monitering was nagevors, met die fokus spesifiek op tegnieke wat op kabels van toepassing is. Navorsing het tot die besluit gelei om spesifiek te kyk na tegnieke wat gebruik maak van gedeeltelike ontlading om elektriese kabels te monitor. ’n Deeglike studie rondom gedeeltelike ontlading is uitgevoer sodat die proses en oorsake van gedeeltelike ontlading beter verstaan kan word. Die navorsing in die literatuurhoofstuk kan gesien word as die basis waaruit die res van die projek sal ontwikkel.

Simulasie modelle is gebruik om die eienskappe van gedeeltelike ontlading te ondersoek. Simulasie modelle is geskep deur gebruik te maak van Wiskundige beginsels, sowel as beginsels van Ingenieurswese. Hierdie simulasie modelle is gebaseer op die bekende Drie-kapasitor model. Die simulasie modelle is gebruik om die effek van gedeeltelike ontlading te ondersoek. Die modelle is ontwerp sodat ’n verskeidenheid eienskappe van gedeeltelike ontlading ondersoek kan word. Die simulasies is uitgevoer deur gebruik te maak van MATLAB® Simulink®.

Die navorsing wat in hierdie verhandeling voorgestel word, het gelei tot die ontwerp van ’n kondisie moniteringstegniek wat gebruik kan word om ontlading in kabels op te spoor. Die tegniek is gebruik om praktiese metings van gedeeltelike ontlading ontlading te neem. MATLAB® is gebruik om programme te ontwerp vir die ontleding van gemete data in beide die tyd- en frekwensie-gebied. Wanneer gemete data ontleed word, sal eienskappe van die gedeeltelike ontlading ontbloot word. Die tegniek word gebruik om ontlading te identifiseer en benodig die samewerking van ander tegnieke vir die volledige analise van die toestand van elektriese kabels. Die praktiese eksperimente van hierdie studie word gebruik as die skakel tussen teoretiese kennis en praktiese ervaring.

Kernwoorde: Kondisie monitering, Gedeeltelike ontlading, elektriese kabels, simulasie modelle

Acknowledgements

First of all I want to thank God for His grace and love.

Anlerie, my fiancé, I would like to thank you for your endless love and support throughout the years. I appreciate everything that you do for me sincerely.

Thank you, Dr. Rupert Gouws, for being my mentor over the past few years. I would like to thank you for all your support and critical remarks during this study

My loving family also deserves acknowledgement for their moral support and prayers.

MARTEC made it possible to be able to perform practical measurements for this study and for that I would like to thank them. Thank you for the guidance and the permission to use your equipment.

For financial support I would also like to thank the bursary department of IMPLATS as well as the National Research Foundation (NRF).

Table of Contents

List of Figures

List of Tables

Chapter 1 Introduction

The purpose of this chapter is to provide an introduction to the work presented in this dissertation. A literature background is provided to familiarize the reader with the concepts of the study. The formulation of a problem statement is one of the most important aspects discussed in this chapter. The problem statement will form the basis from which the rest of the study will stem. Research aims and objectives are also discussed in this section. The dissertation overview is also discussed. The work presented in this dissertation is in the final stages of publication and is documented in this chapter.

1.1. Background

Condition monitoring (CM) of electrical equipment is a field that, at the moment, benefits from a great deal of research due to the importance of monitoring the electrical condition of such equipment. Although research in the field of CM of electrical equipment dates back to the 1970s, the beginning of the 1990s saw most energy companies investing a lot of finances as well as time into CM techniques. According to Y. Han and Y.H. Song: "Condition monitoring can be defined as a technique or a process of monitoring the operating characteristics of a machine in such a way that changes and trends of the monitored characteristics can be used to predict the need for maintenance before serious deterioration or breakdown occurs" [**1**]. Time based maintenance was the common practice within the industrial sector before the use of CM techniques. Time based maintenance is performed according to a specific schedule, usually determined by a time schedule or according to running hours. Although time based maintenance is an important operation, it may cause many unwanted shutdowns and without knowledge, regarding the current condition of equipment, it may also require unnecessary manpower. Time based maintenance also reveals little to no information regarding the current condition of equipment and therefore may cause unexpected accidents.

Condition monitoring of electrical cables is essential, as the cables are exposed to a variety of environmental and operational stressors throughout their service life. The level of aging degradation can be evaluated by means of CM techniques [**2**]. Without the constant monitoring of the condition of cables, cables may fail prematurely and cause serious problems within the electrical network. Several factors must be considered when choosing a CM technique to monitor electrical cables. The intrusiveness of the chosen technique along with the characteristics of the cables being monitored are two of the most important factors to consider when choosing a CM technique for the monitoring of electrical cables.

A single technique may not be sufficient to completely characterize the condition of a cable and the insulation material of that cable. It is therefore important to use multiple CM techniques for the successful monitoring of electrical cables [**3**].

The need for CM techniques is mainly due to the health of employees and the safe operation of electrical equipment. CM techniques also have a positive economic impact, as the machines being monitored are often very expensive. A CM technique can be described as a system with four main parts. The four individual parts must function as an interlocking unit in order to guarantee the success of the CM technique. Figure 1-1 illustrates the main parts of a typical CM technique.

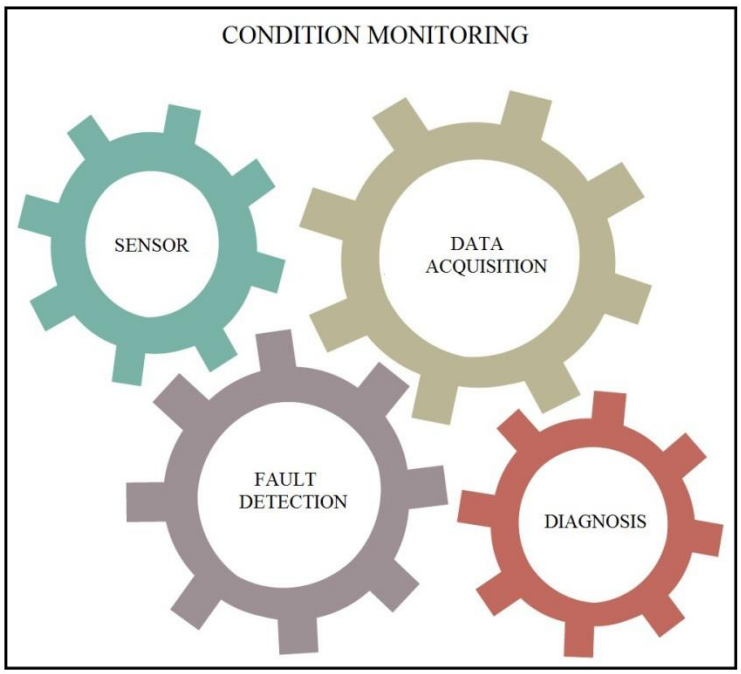

Figure 1-1: Main components of a CM technique

1.1.1. Sensor

The chosen monitoring method as well as the physical environment of the equipment being monitored will determine the type of sensor. The key requirements for any sensor are: the sensitivity of the sensor, affordability and the sensor being able to record data non-intrusively. Sensors are used to convert a physical quantity to an electrical signal [**1**].

1.1.2. Fault detection

Fault detection can be seen as the main objective of any CM technique. Fault detection can be described as the ability to determine whether an electrical fault is present in the equipment being monitored. Different methods for fault detection are available and will again be determined by the chosen CM technique as well as the environment of the equipment.

1.1.3. Data acquisition

The data acquisition unit is an important part of any CM technique, as it will be the link between the data obtained by means of the sensors and the analysis of data. The data acquisition unit is used for: amplification of the measured signals, correction of sensor failures and in some cases the conversion of measured data from analogue to digital [**1**]. The characteristics of the data acquisition unit will mainly depend on whether the data will be analysed on-line or off-line.

1.1.4. Diagnosis

The most important part of the CM technique is the analysis and interpretation of the measured data. The diagnosis part is used to identify trends, in measured data, as well as specific degradation mechanisms [**2**]. The analysis of partial discharge (PD) data is usually performed offline by specialists, although some techniques may perform online diagnosis by means of advanced technologies. It is however still vital to have the expertise of a specialist.

1.2. Problem statement

The purpose of this research project is to investigate the use of monitoring techniques for the condition monitoring (CM) of medium voltage electrical cables. Emphasis is placed on the use of partial discharge (PD) measurements for the condition monitoring of cross-linked polyethylene (XLPE) cables.

A literature study must be conducted in order to investigate the numerous available monitoring techniques. The literature study must include a thorough investigation regarding the construction of medium voltage electrical cables. The degradation of the insulation material of medium voltage cables is also important as this can be seen as the foundation of any CM technique. The literature study should include an in depth study regarding: the process of PD, the measurement of PD as well as PD measurements associated with electrical cables.

Simulation models need to be constructed in order to accurately simulate the occurrence of PD activity within the insulation material of a medium voltage XLPE cable. The simulation models will accommodate the investigation of various parameters on the characteristics of measured PD data.

A condition monitoring technique must be designed and implemented which can be used to monitor the electrical condition of a medium voltage cable. The CM technique must be designed with PD measurements as basis and must also adhere to industry standards involving CM techniques for electrical cables. A practical setup must be created in order to use the designed CM technique to measure and analyse PD data.

The problem statement can be summarized in three main objectives as illustrated in Figure 1-2. Each of these objectives has its own sub-problems and limitations.

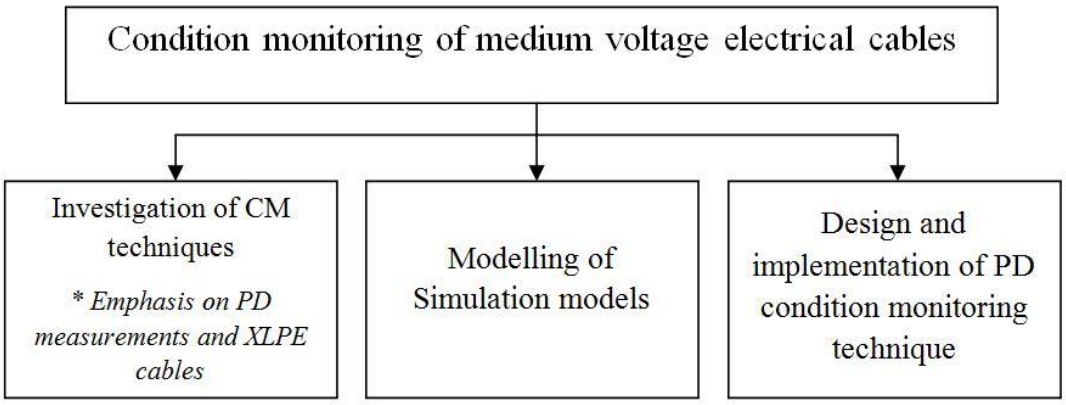

Figure 1-2: Project Breakdown

1.3. Research aim and objectives

The objectives are defined from the problem statement as an investigation of CM with specific focus on techniques for CM of electrical cables, the derivation of simulation models for the investigation of PD and the analysis of practical PD data.

1.3.1. Investigation of condition monitoring

The literature study involving cable CM concepts plays a vital role in the understanding of the phenomena and related subject matter. The first objective is to do comprehensive research on relating topics, including: electrical cables, CM techniques as well as PD.

1.3.2. Modelling

The derivation of mathematical models to be used for simulation purposes plays a vital role in acquiring much needed knowledge regarding the analysis of PD data. The validation of the models is based on the models being derived from mathematical and engineering principles. The MATLAB® Simulink® environment is identified as the platform for the development of the simulation models as well as the execution of the actual simulations.

1.3.3. PD analysis

The final objective of the research involves the analysis of practical PD data. The objective can be divided into sub-objectives, which must be completed for the successful completion of the PD analysis objective. The first sub-objective is to design and implement a non-intrusive condition monitoring technique which can be used to detect discharge activity within electrical cables. The design and implementation of MATLAB® programs which will be used for the analysis of the measured data will form the final part of the sub-objectives.

1.4. Dissertation overview

This section provides a brief overview of the dissertation. Chapter 2 provides a literature study regarding necessary theory relevant to the research. The first part of the literature study contains electrical cables. The study of electrical cables includes the construction of electrical cables and different types of electrical cables. The aging and degradation of electrical cables are also investigated in the literature study. The final part of the literature study provides an overview regarding CM. The main focus is on CM techniques related to electrical cables. Various techniques are investigated and the advantages as well as the disadvantages of each are discussed. CM techniques regarding the use of PD measurements are the main focus, as this will also form the basis of the research discussed in the rest of this dissertation.

Chapter 3 is dedicated to the mathematical modelling of two simulation models. Both simulation models are used to simulate the occurrence of PD due to a single void within the insulation material of an electrical cable. The main focus of this chapter is the mathematical derivation of the two models. The models are both based on the well-known three-capacitor model for PD. The physical models as well as the mathematical equations required to determine the parameters of each model are also discussed in this chapter.

Chapter 4 provides a detail design of a CM technique for electrical cables. The technique makes use of PD measurements to monitor the condition of the cable's insulation material. Each component of the monitoring system is discussed in detail within this chapter. The designed system is also compared to systems used in the industry and systems discussed in published research in order to validate the designed system.

Chapter 5 discusses the results obtained by means of the simulation models discussed in Chapter 3. The first part of the chapter will focus on the simulations of the basic three-capacitor model. The simulations performed by means of the comprehensive three-capacitor model are discussed in the second part of this chapter. The simulations are performed in order to gain knowledge regarding discharge activity within the insulation material of electrical cables. The simulations are also used to investigate the effect of certain parameters on the PD characteristics.

Chapter 6 outlines the discussion of the results obtained from practical PD measurements. The designed CM system was used to obtain practical PD data. The focus of chapter 6 is the analysis of the obtained PD data. MATLAB® was used to create two programs which can be used to analyse PD data in both the time- and frequency-domain. The analysis provided by these programs is used to determine the severity of the discharge activity and also to estimate the remaining life of the cable being tested. The verification process of the results is based on the comparison of results obtained from systems used within the industry to that of the designed system.

Chapter 7 concludes the dissertation by discussing the findings of the research. The conclusions include: the discussion of various CM techniques, the importance of CM, the use of simulation models to investigate the effect of PD, the designed monitoring system as well as the analysis of data obtained from practical PD measurements. Recommendations are also made for improvements and future work.

The appendices of this dissertation include a Turnit-in report, in order to verify the originality of the work presented in this dissertation. A research paper submitted to the SAIEE ARJ is also included in the appendices. This paper represents the work conducted throughout the project. A data CD is attached to the dissertation with additional information relevant to the study.

1.5. Publications

The research presented in this dissertation has been documented in a number of papers, each in a different stage of publication or evaluation for publication. The published papers together with the relevant abstracts are provided:

- H. van Jaarsveldt and Dr. R. Gouws, "Design of a non-intrusive cable condition monitoring technique by means of partial discharge," *Proceedings of the Southern African Universities Power Engineering Conference (SAUPEC 2013)*, January 2013, pp 92-97, ISBN 978-186822-631-3.

  Article abstract:

  The purpose of this paper is to discuss the design of a non-intrusive condition monitoring technique for medium- and high-voltage power cables. Partial discharge (PD) was used to design the non-intrusive condition monitoring technique, with specific focus on XLPE power cables. A simple A-B-C model was used to derive an equivalent circuit for partial discharge, due to a void in the insulation material of a power cable. The condition monitoring technique is based on the classification of PD activity according to 5 distinct levels of PD. The design of the condition monitoring technique is of such a nature that it can easily be adapted to be used for different input voltages as well as different types of electrical cables. This technique can thus be seen as an effective and useful technique of cable condition monitoring. Future work will include the use of the results discussed in this paper to aid the construction as well as calibration of a practical model. This model will be used to perform non-intrusive condition monitoring of power cables by means of PD measurements.

- H. van Jaarsveldt and Dr. R. Gouws, "Partial Discharge Simulations used for the Design of a Non-Intrusive Cable Condition Monitoring Technique," *Journal of Energy and Power Engineering,* November 2013, Volume 7, Number 11, ISSN 1934-8983

  Article abstract:

  The purpose of this paper is to investigate the effect of partial discharge (PD) activity within medium voltage cross-linked polyethylene (XLPE) cables. The effect of partial discharge was studied by means of a number of simulations. The simulations were based on the well-known three capacitor model for partial discharge. An equivalent circuit was derived for partial discharge due to a single void in the insulation material of a power cable. The results obtained from the simulations will form the basis of the design proses of a non-intrusive condition monitoring

technique. The technique is based on the classification of discharge activity according to five levels of PD. Future work will include the improvement of the simulation model by investigating the high frequency model of a power cable as well as the statistical nature of PD activity. This will improve the accuracy of the simulation results when compared to actual measurements. The work discussed in this paper will be used to construct and calibrate a practical model which will make use of PD measurements for non-intrusive condition monitoring of medium voltage electrical cables.

- H. van Jaarsveldt and Dr. R. Gouws, "Condition monitoring of medium voltage electrical cables by means of partial discharge measurements," *SAIEE Africa Research Journal,*
  Submitted - November 2013, Accepted – June 2014, Publication – December 2014, ISSN 1991-1696
  (Complete version of paper available in Appendix B)

  Article Abstract:

  The purpose of this paper is to discuss condition monitoring (CM) of medium voltage electrical cables by means of partial discharge (PD) measurements. Electrical cables are exposed to a variety of operational and environmental stressors. The stressors will lead to the degradation of the cable's insulation material and ultimately to cable failure. The premature failure of cables can cause blackouts and will have a significant effect on the safety of such a network. It is therefore crucial to constantly monitor the condition of electrical cables. The first part of this paper is focussed on fundamental theory concepts regarding CM of electrical cables as well as PD. The derivation of mathematical models for the simulation of PD is also discussed. The simulation of discharge activity is due to a single void within the insulation material of medium voltage cross-linked polyethylene (XLPE) cables. The simulations were performed in the MATLAB® Simulink® environment, in order to investigate the effects of a variety of parameters on the characteristics of the PD signal. A non-intrusive CM technique was designed for the detection of PD activity within cables. The CM technique was used to measure and analyse practical PD data. Two MATLAB® programs were designed to analyse the PD data in both the time-domain and frequency-domain.

The purpose of this chapter was to provide an introduction to the work presented in the rest of the dissertation. The most important part of this chapter is the formulation of a problem statement. The problem statement sets the scene for the rest of the study which is built around the formulated components of the problem statement. The problem statement was also used to formulate research aims and objectives.

Chapter 2 Literature Study

The purpose of this chapter is to provide a literature study regarding theory concepts related to the work presented in this dissertation. An overview of the literature is provided to create a clear image of the work discussed in this chapter. The main research topics discussed in this chapter includes: medium voltage electrical cables, aging and degradation of the insulation material of cables and CM techniques, with the specific focus on techniques used for the monitoring of electrical cables. CM techniques which make use of PD measurements are also discussed in detail.

2.1.Introduction

The research presented in this dissertation focused on partial discharge within the insulation material of medium voltage electrical cables. The research is structured according to a review of medium voltage cables, condition monitoring of medium voltage electrical cables and PD both as the phenomenon and PD used as a monitoring technique for electrical cables. Condition monitoring and PD is a vast sea of information and it can therefore be difficult to critically review sources in order to ensure that the research presented within this dissertation is both accurate and relevant. The sources used to shape and present the literature study of this dissertation were reviewed by means of the following steps:

- Recognise un-stated and invalid assumptions in arguments
- Distinguish facts from hypothesis
- Distinguish facts from opinions
- Distinguish an argument's conclusions from the statement that supports it
- Recognise what kind of evidence is relevant and essential for the validation of an argument
- Recognise how much evidence is needed to support a conclusion
- Distinguish between relevant and irrelevant statements and evidence
- Identify logical fallacies

2.2.Overview

The main focus of this chapter is to research the variety of concepts regarding CM of electrical cables. The overview of the literature study is illustrated in Figure 2-1.

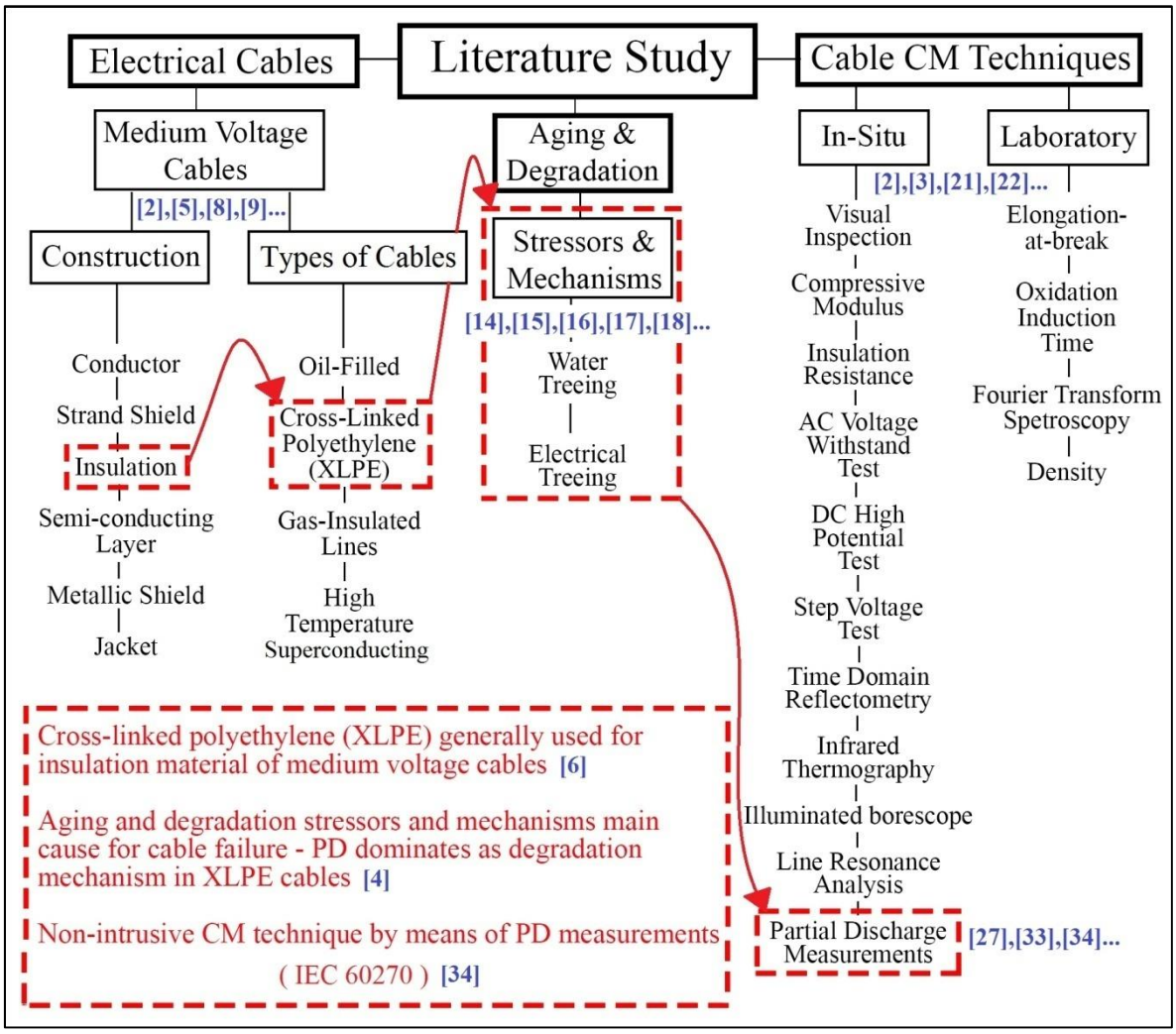

Figure 2-1: Literature study overview

The literature study is divided into three sub-groups. The first part of the literature study will focus on research regarding electrical cables, with the main focus on medium voltage cables. The construction of electrical cables as well as the numerous types of medium voltage cables will be discussed in this section. The second part of the study will focus on the aging and degradation of the insulation material of electrical cables. Stressors as well as mechanisms for aging and degradation will be investigated. The final part of the study will focus on CM techniques used for power cables. The techniques can be divided into two groups, namely: laboratory and in-situ. The focus will be on in-situ techniques, as these techniques can be used within the industry.

An in depth study was conducted on CM techniques which make use of PD measurements, as it is evident that PD is one of the main mechanisms for aging and degradation of medium voltage electrical cables [**4**]. The phenomenon known as PD will be discussed as well as the process of performing PD testing on medium voltage cables.

2.3. Electrical cables

2.3.1. Introduction

Electrical cables are an essential part of an electrical network and play a vital role in the safety of such a network, as failing cables may result in the death of employees as well as damage to expensive equipment. High voltage cables are generally used for underground transmission and distribution of electricity. For this reason, the conductor must be completely isolated, in contrast to overhead lines where air forms part of the insulation. Due to the fact that the conductor must be completely isolated, the cables are much more expensive than normal overhead lines [**5**].

Different types of electrical cables exist, each with their own advantages and disadvantages. Most electrical cables are single cored and therefore have their own insulation. The insulation of electrical cables is also used for mechanical protection by means of sheaths [**5**]. The general need in the industrial sector is to transmit three phase power. To be able to transmit three phase power via electrical cables a single three-core cable can be used, it is also possible to make use of three individual single-core cables [**5**]. Cross-linked polyethylene (XLPE) is the preferred insulation for power cables, both for distribution and transmission system applications [**6**].

2.3.2. Cable construction

The IEEE standard (100) defines nominal medium voltage (MV) as greater than 1 kV and less than 100 kV [**7**]. Medium voltage cables are generally used for distribution systems, power plants and industrial facilities. Distribution systems in residential areas also use medium voltage cables [**8**]. The basic construction of an electrical cable generally consists of an electrical conductor, typically copper or aluminium, covered by a polymer insulating material [**2**]. Typically electrical cables consist of six crucial layers. These layers include:

- Conductor
- Strand shield
- Insulation
- Semi-conducting layer
- Metallic shield
- Jacket [**8**].

Each of these components has a specific and vital function in an electrical cable. The manufacturers of electrical cables approve their cables for use, according to a number of criteria. These criteria include: The specified service life of the cable, the maximum ambient temperature of operation for the electrical cable as well as the specified operating voltage for the cable [**2**]. Figure 2-2 illustrates the basic construction of an electrical cable with the six crucial layers. There are two basic types of medium voltage cables: single conductor and three conductor cables. Single conductor cables have one conductor per cable, whereas three conductor cables have three individually insulated and shielded conductors [**8**].

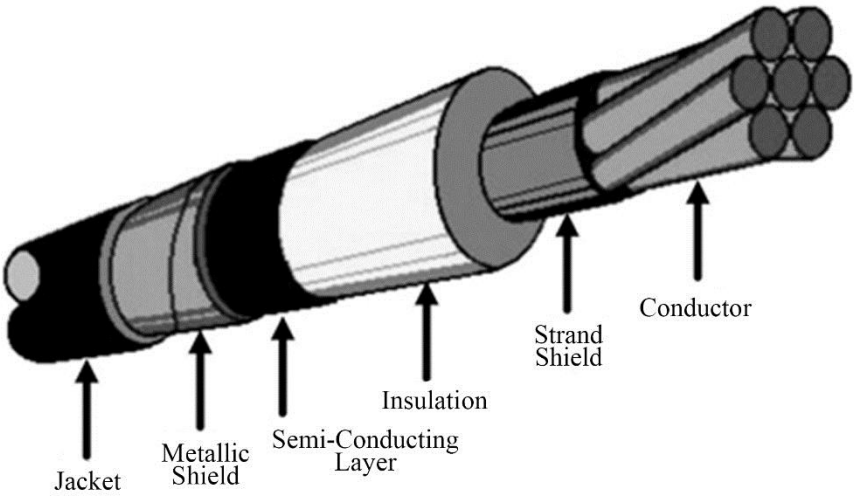

Figure 2-2: Layers of a basic electrical cable [**8**]

Conductor

The conductor can be seen as the heart of the cable, as the sole purpose of the conductor is to carry current. Copper and aluminium are two commonly used materials for the construction of the core. Copper cables are generally used for industrial applications and aluminium for utility purposes [**8**]. Different conductor configurations are used for different purposes, each with its own advantages as well as disadvantages. The four basic conductor configurations are: concentric, compressed, compact and solid [**8**].

Strand shield (semi-conducting layer)

The strand shield is a semi-conductive layer of the cable. The function of the strand shield is to shield the cable from any air that may be surrounding the conductor strands [**8**]. The strand shield is one of the most important layers of an electrical cable. Without the strand shield layer the air surrounding the conductor strands would ionize. This then can result in partial discharge (PD) within the cable. PD can deteriorate the insulation of a cable to the point of cable failure [**8**].

Insulation

The insulation layer in electrical cables is used to contain the voltage of the cable. The materials commonly used for cable insulation are: Ethylene Propylene Rubber (EPR) and Cross Linked Polyethylene (XLPE) [**8**]. XLPE is the preferred choice for the material used as insulation of electrical cables due to the various advantages of this material [**9**]. The insulation layer of the cable is susceptible to various aging and degradation mechanisms including: water treeing, electrical treeing as well as PD. The insulation layer of a cable has a standard operating temperature as well as an emergency operating temperature [**8**].

Outer semi-conducting layer

The function of the outer semi-conducting layer is similar to that of the strand shield. The main function is to shield the cable insulation from the air that is between the cable insulation and the metallic shield [**8**]. The air trapped within the cable can cause PD, thus it can be seen that the outer semi-conducting layer also serves a purpose to prevent PD within the cable.

Metallic shield

The metallic shield is the conductive metallic component of the cable's shielding system [**8**]. The metallic shield of a cable must always be grounded. The metallic shield of the cable must perform a number of important functions. The most important functions of the metallic shield include: to contain the electric field within the cable, to limit radio interference on the cable, to provide symmetrical radial distribution of the voltage stress among the insulation, to serve as a return path in the event of a short circuit and to act as a safety component, as the metallic shield reduces the risk of a shock. Figure 2-3 shows the five construction types generally used for the metallic shield.

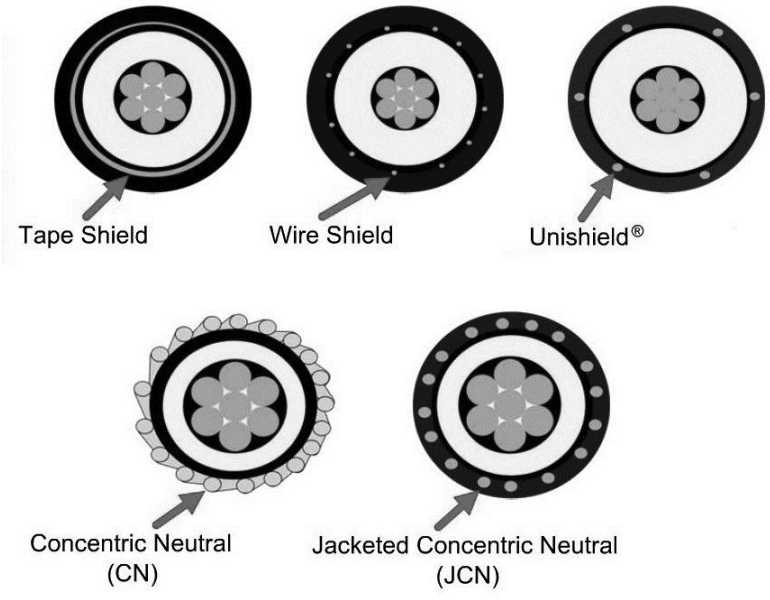

Figure 2-3: Metallic shield configurations [**8**]

There are five types of metallic shield constructions generally used for electrical cables. The five construction types include: tape shield, wire shield, unishield®, concentric neutral and jacketed concentric neutral. The metallic shield in concentric neutral and jacketed concentric neutral also act as the neutral for the cable.

Jacket

The jacket is one of the most important layers of an electrical cable as the jacket protects the cable from physical damage. The jacket of a cable can be made from a variety of materials, neoprene rubber or polyvinyl chloride (PVC) is generally used [**8**]. The function of the jacket as mentioned is to provide external physical protection for the cable. The jacket also provides a moisture seal for the cable. The moisture seal is very important as this protects the cable against degradation mechanisms such as water treeing and PD.

2.3.3. Types of electrical cables

Different types of electrical cables are used for different needs as well as due to a difference in environmental factors. As mentioned previously, the different types will each have an individual set of advantages and disadvantages. There are four main types used for high-voltage cables [**9**]. These types are: paper insulated oil filled (OF); cross-linked polyethylene (XLPE) insulated; oil filled, gas insulated and high-temperature superconducting cables [**9**].

Oil-filled cables

Oil-filled (OF) cables were the preferred choice for underground cables since 1920 [**9**]. This is due to the fact that paper is a somewhat fundamental insulator which yields good results. The insulation properties of paper are further improved when impregnated with oil [**9**]. The installation as well as the maintenance of OF cables are more complex than that of normal paper-insulated cables. Even though this may seem as a drawback for OF cables, they have a number of advantages over plain paper-insulated cables. These advantages include: voids are prevented by the oil and may eliminate cable breakdown; OF cables are much safer to use and thus add to operation safety of an electrical network and OF cables have higher power and voltage ratings [**9**].

Cables within the oil-filled group can be divided into two sub-groups, namely: self-contained and pipe-type. Self-contained OF cables are constructed with a durable plastic jacket. This jacket serves the purpose of the outer sheath of the cable and will also protect the cable from any physical damage. Figure 2-4 shows the cross section of a typical oil-filled cable.

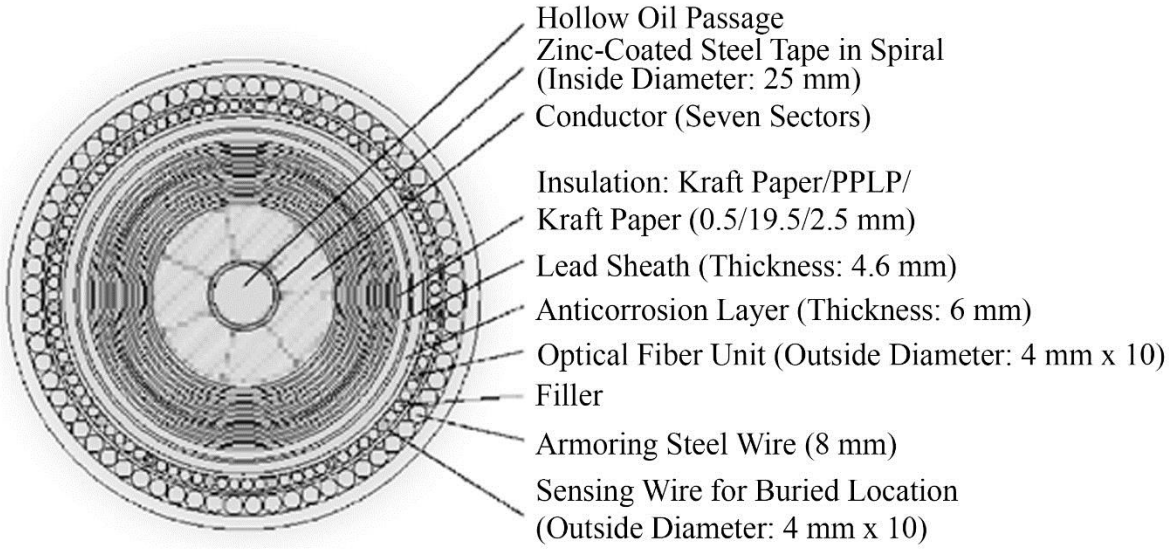

Figure 2-4: Cross-sectional view of oil-filled cable [**9**]

Three different constructions are available for self-contained OF cables [**9**]. The first construction type is a single-core with an oil duct within the core. The conductor of this type is the hollow core of the cable. The second type of self-contained OF cables is a single-core sheath channel. Other than with the first type this type of cable has a solid core. The oil duct is situated between the sheath and the insulation material of the cable. The final construction type for self-contained OF cables is three-core filler-space channel. This type of cable, as mentioned in the name, has three cores. The oil channels are located in the filling space section of the cable [**9**].

The pipe-type OF cables is housed within a steel pipe. These cables commonly have three conductor cores each with individual impregnated-paper insulation. Generally a pipe-type OF cable is pressurized to 1360 kPa [**9**]. Pipe-type OF cables has three main advantages over the self-contained OF cables: mechanically the pipe system is much stronger, the system requires fewer joints and the ampacity of the cable is improved due to an increased cooling ability [**9**].

Cross-linked polyethylene (XLPE) cables

The cross-linked polyethylene (XLPE) cable is the preferred type of electrical cable within the industrial sector. This cable was first designed with the use of polyethylene insulation. Later cross-linked polyethylene (XLPE) was used due to the fact that this type of cable has a higher heat tolerance. The maximum operating temperature for XLPE cables is 90ºC and the emergency temperature is 130ºC. The maximum temperature in the case of a short circuit is 250ºC [**9**]. Excluding the fact that cross linking contributes to higher operating temperatures it also improves: impact strength, dimensional stability, tensile strength and the resistance to chemicals, solvents and ageing.

A common degradation mechanism for electrical cables is the phenomenon of water treeing. Water treeing is also one of the most important failure mechanisms of medium- and high-voltage cables. This is where another advantage of XLPE cables is important, as the cross linking process prevents the water treeing effect on electrical cables [**9**]. The phenomenon of water treeing is illustrated in Figure 2-5. Section B and C in the figure are enlargements of the original water treeing shown in section A of Figure 2-5.

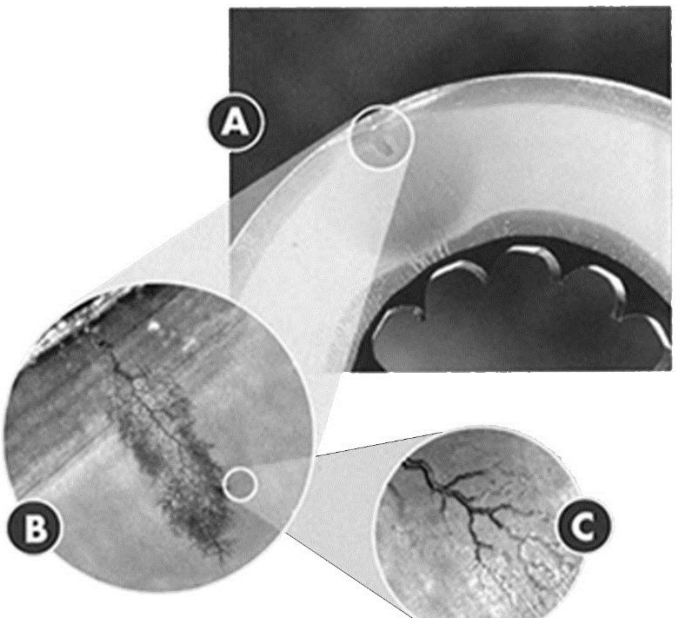

Figure 2-5: Water treeing phenomenon [**10**]

With added joints XLPE cables can be used for operation over long distances. No joints are required for operation over short distances. XLPE cables can also be used for successful DC transmission. The first high-voltage DC system which made use of XLPE cables was in Sweden during the year 1999 [**9**]. XLPE cables are rated up to 500 kV, with on-going research constantly leading to a reduced size of the thickness of the XLPE insulation needed for the cables [**9**].

Generally an XLPE cable consists of a low-resistance conductor covered with XLPE insulation. The cable is enclosed in a jacket which is used to protect the cable from the environment [**9**]. The jacket of the cable is assembled from different materials in order to form the finished jacket. These materials include: a metal screen around the insulation; a reinforcing sheath from aluminium and the outer sheath which is usually made from PVC [**9**]. Figure 2-6 shows the cross-sectional view of a typical XLPE cable.

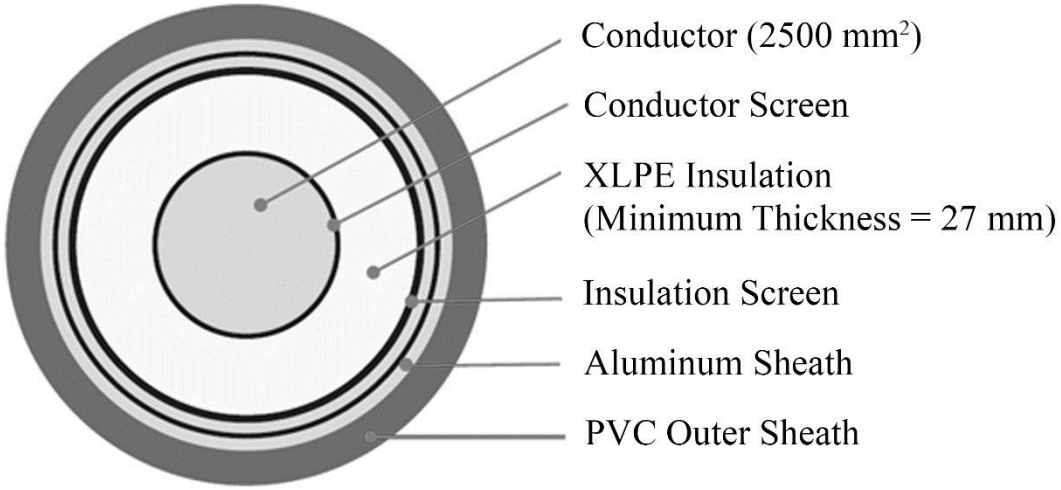

Figure 2-6: Cross-sectional view of a XLPE cable [**9**]

The construction of an XLPE cable is very important as poor construction can lead to a high percentage of cable losses. The current flowing through the core of the cable will induce parasitic currents in the sheath of the XLPE cable. The sheath currents flowing in the metal cable sheath can reduce the ampacity of a XLPE cable by as much as 40% [**9**]. To interrupt the path of this parasitic currents a bonding method is used. This is accomplished by bonding a ground to the sheath of the cable. This will then interrupt or completely eliminate the sheath currents [**9**]. Three main types of bonding are typically used in XLPE cables. These methods include: single-point bonding; multi-point bonding as well as cross bonding [**9**]. The best method of bonding is the cross bonding method, as this method will result in the highest possible cable ampacity. Cross bonding however has a disadvantage as the induced voltage on parallel lines will be higher than that of the other two methods [**9**].

Gas-insulated lines

Another type of electrical cable typically used for high-voltage transmission is gas-insulated lines (GILs). This type of cable was first introduced in the 1970s, with the main purpose of it being to connect switchgear in substations [**9**]. GILs consist of an aluminium envelope which houses the pressurized gas. The aluminium conductor and the insulator spacers are situated within the aluminium envelope of the line [**9**].

Overhead lines are not suitable for highly concentrated industrial areas and densely populated cities. In these areas XLPE and GILs are often the preferred choice for a transmission medium. GILs offer a number of advantages over conventional insulated cables. These advantages include: higher power ratings, longer operating distances, non-flammable, multiple grounding points and GILs also has a high short-circuit withstand capability [**9**]. The major drawback for Gas-insulated lines is that the manufacturing process is an expensive operation. The installation process of GILs is also more expensive than that of conventional insulated cables [**9**]. The cross sectional view of a typical hybrid GIL can be seen in Figure 2-7.

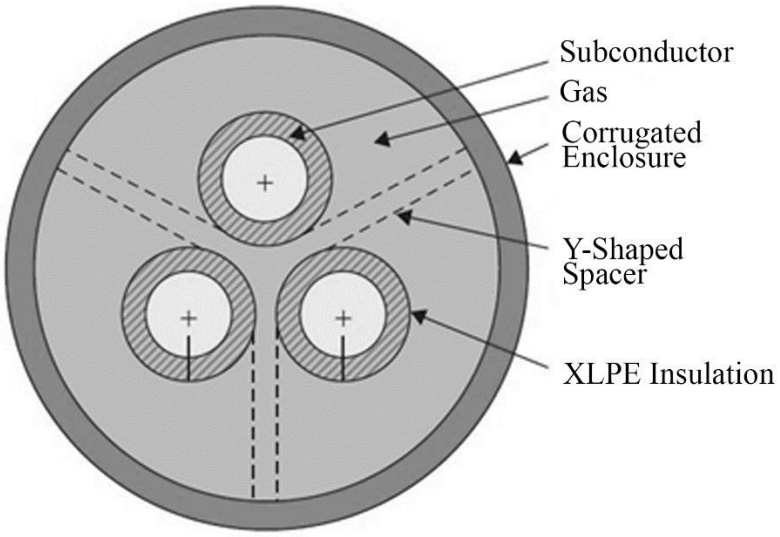

Figure 2-7: Cross-sectional view of a hybrid gas-insulated line [**9**]

The gas used for insulation in a GILs is usually Sulphur hexafluoride (SF6). The SF6 gas is used at pressures ranging from 0.29 MPa to 0.51 MPa at 20ºC [**9**]. Sulphur hexafluoride (SF6) is the most useful form of all the sulphur fluorides and is often used as a gaseous insulator in power breakers [**11**]. Air and SF6 are the two most popular gasses used for insulation. SF6 gas is commonly used as an insulation gas due to the fact that SF6 gas is relatively inexpensive [**11**]. The reason for SF6 being a good insulation gas is due to the fact that SF6 is an electronegative gas, with a breakdown strength nearly three times that of air. The gas is also non-toxic and non-flammable [**11**].

One major setback for GILs is that they are particularly susceptible to contamination by metal particles [**9**]. This contamination usually occurs when the cable is being installed and will lead to a reduced breakdown voltage of the line. A solution for this problem is to use hybrid GILs. A hybrid GIL has a composite insulation system. This means that the line makes use of both compressed gas insulation and also a normal XLPE insulation [**9**]. This then leads to the solution for the contamination problem of ordinary gas-insulated lines.

High-temperature superconducting cables

High-temperature superconducting (HTS) cables have a corrugated stainless steel tube for the core of the cable. Layers of HTS tape is wrapped around the core of the cable. The cryostat of the cable is formed by means of two coaxial corrugated steel tubes and is situated around the core. For cooling purposes liquid nitrogen flows through and over the core. The HTS material has to be cooled at about -196ºC [**9**]. XLPE is often used as the dielectric material in HTS cables. A typical HTS cable is illustrated in Figure 2-8.

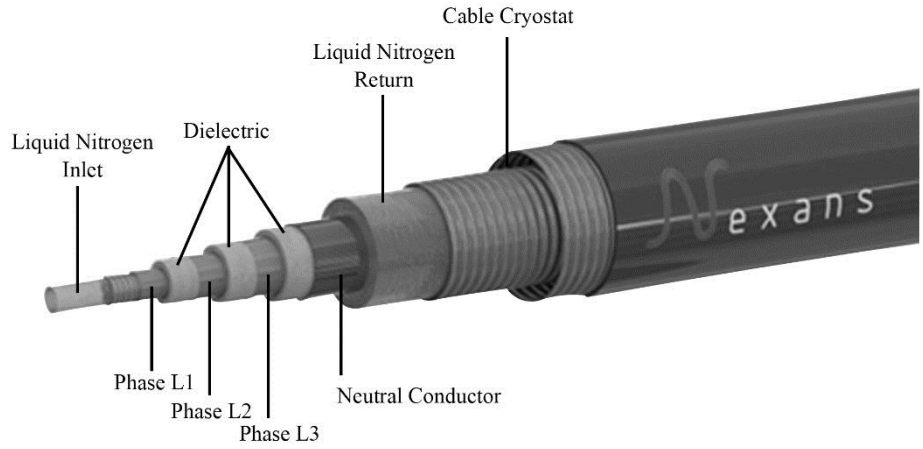

Figure 2-8: High-temperature superconducting (HTS) cable [**12**]

An HTS cable can tolerate short-circuit currents up to 20 kA. The conductivity of HTS ceramic materials, when cooled by liquid nitrogen, is a million times greater than that of copper at room temperature. HTS materials can also handle current densities 20 times greater than copper conductors [**9**]. A Major advantage of HTS cables is that they can distribute electricity almost without any losses. HTS cables are also seen as the solution for efficient, space-saving transmission of electricity in urban areas [**13**]. Low-temperature superconductors (LTS) also exist, although the low-temperature may be relative, as the material has to be cooled by liquid helium to very low temperatures [**9**]. LTS materials have several disadvantages including: reliability problems; high costs and the cooling process of LTS materials are very complex due to the low temperature. Contradicting to this HTS materials have better thermal stability; less complex cooling and also improved reliability [**9**].

On 19 January 2012 it was announced that the current longest high-temperature superconductor (HTS) cable in the world would be installed in the city of Essen, Germany [**13**]. RWE Deutschland AG would act as the leading partner for the project, while Nexans would be the manufacturer of the HTS cable for the project. The total costs for the project would be in the region of € 13.5 million, about R 190 million. The project would commence in the year 2013. It is believed that the large-scale use of HTS cables would be economically viable in the near future [**13**].

2.4.Aging and degradation of cables

2.4.1. Introduction

The insulation materials used in electrical cables degrades over a period of time. Many factors and mechanisms can be attributed to the degradation of cable insulation. Aging of solid insulation materials and systems are defined by the IEC and IEEE as the occurrence of irreversible deleterious changes that critically affect performance and shorten useful life [**14**]. Aging and degradation of electrical cable insulation are important aspects of electrical cable operation, as they may lead to cables failing prior to their estimated lifespan. Premature failing of cables directly affects the safety as well as the production in industrial processes. Degradation of electrical cables, used for distribution and transmission, is the result of a number of stresses affecting the cable. The stresses may include: electrical stresses; thermal; mechanical and environmental stress [**15**]. One of the main sources of electrical stress is due to switching surges, this occurs during the operation of a power system [**15**].

Cable systems within the industrial sector represent a large capital investment for electrical utilities and premature failing of electrical cables can result in loss of revenue [**16**]. Cable systems therefore must be highly reliable. Thus the quantification of degradation of cables is very important, as this can be used to determine the useful life of a particular cable [**14**].

2.4.2. Ageing and degradation stressors

Stressors can be characterized as environmental stressors or as operational stressors. The stressors are characterized into these two groups by means of the origin of the stressor. Environmental stressors are due to the environment in which a specific cable is located. Whereas, operational stressors such as: the cable current loading, electrical system transients or operating and maintenance activities are responsible for operational stressors [**2**]. A list of some of the most important aging factors for electrical cables is given in Table 2-1.

Table 2-1: Aging factors for insulation materials of electrical cables [**16**]

Thermal	**Electrical**	**Environmental**	**Mechanical**
Maximum temperature	Voltage (ac, dc, impulse)	Gasses (air, oxygen, etc.)	Bending
Low, high ambient	Frequency	Lubricants	Tension
Temperature gradient	Current	Water/humidity	Compression
Temperature Cycling		Corrosive chemicals	Torsion
		Radiation	Vibration

Aging stressors can be divided into environmental stressors or operational stressors. Table 2-2 below shows a list of the most important environmental and operational stressors.

Table 2-2: Environmental and Operational Stressors [**2**]

Environmental Stressors	**Operational Stressors**
Elevated temperatures	High voltage stress
High radiation	Material defects
High humidity	Water treeing
Moisture intrusion	
Accumulation of dirt and dust	
Exposure to chemicals	

2.4.3. Ageing mechanisms

The aging mechanisms affecting the conductor of an electrical cable usually develop slowly and are also not likely to occur. Aging mechanisms related to the insulation can develop fast and are also the reason for the majority of cable failures [**17**], [**18**]. Aging mechanisms can be the result of a number of aging and degradation stressors. Although different stressors result in different aging mechanisms, they all have the same aging effects, namely: decrease in dielectric strength, increase in leakage current and eventual failure. Table 2-3 gives a list of aging mechanisms as well as the stressors responsible for each mechanism.

Table 2-3: Stressors and aging mechanisms for cable insulation materials [**2**]

Material	**Stressors**	**Aging Mechanisms**	**Aging Effects**
Polymer materials (XLPE, EPR)	Elevated temperatures, Elevated radiation fields	Embrittlement, Cracking	Decrease in dielectric strength Increase in leakage currents Eventual failure
Polymer materials permeable to moisture	Wetting	Moisture intrusion	
M without a tree retardant additive	Wetting concurrent with voltage	Electrochemical reactions, Water treeing	
Polymers with voids or other imperfections	Voltage, Electrical transient	Partial discharge (corona), Electrical treeing	
Polymer materials (XLPE, EPR)	Physical contact, abuse during maintenance, operation, or testing	Mechanical damage: crushing, bending, tensile deformation	
Polymer materials (XLPE, EPR)	Installation Damage	Mechanical damage: crushing, bending, tensile deformation	

Water treeing

Most extruded cables used for distribution are exposed to moisture and thus are susceptible to ageing due to water trees [**16**]. Water trees are formed over a period of time in the presence of moisture, impurities or contamination at an electrical field [**19**]. Water trees within the insulation of an electrical cable may lead to the development of electrical trees. With the presence of electrical trees PD may occur. Water trees in electrical cables lead to higher harmonics due to the generation of nonlinear conduction currents. There are two main types of water trees, namely: Vented trees and bow-tie trees [**16**]. Figure 2-9 illustrate examples of both vented trees and bow-tie trees within the insulation of an electrical cable.

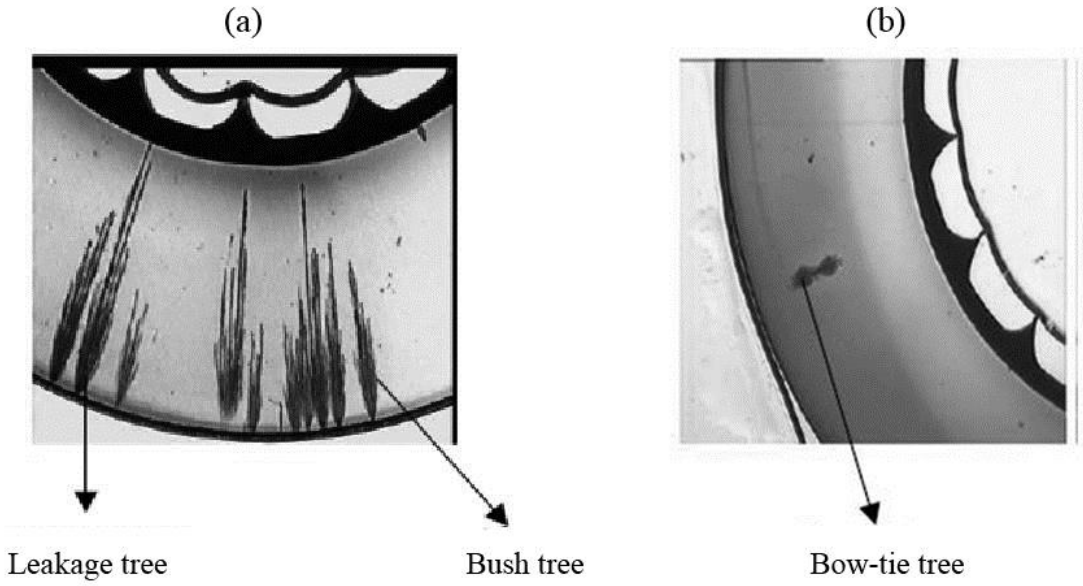

Figure 2-9: Water treeing: (a) vented trees and (b) bow-tie trees [**19**]

Vented trees are initiated at interfaces and will start to grow from the surface of the insulation material, inwards into the insulation [**16**]. All vented trees will grow in the direction of the electrical field. In some cases vented trees may grow through the entire thickness of the insulation. Vented trees are the more dangerous of the two types as this type of tree may cause cable failures [**19**].

Bow-tie trees are initiated by soluble contaminants or water-filled voids in the insulation of the electrical cable [**16**]. In contrast with vented trees, bow-tie trees grow from the insulation outwards towards the surface of the insulation [**19**]. As with the vented trees, bow-tie trees will also grow in the same direction as the electrical field and will grow in both directions. Although bow-tie trees have a faster initial growth rate than that of vented trees, they are not capable of growing to large sizes [**19**]. Bow-tie trees initiated by water-filled voids will have a typical length of some tens of a μm, thus they do not have a significant effect on aging of electrical cables [**16**]. Due to the restricted size of bow-tie trees they do not have the capability to cause cable failures [**19**].

Electrical treeing

Electrical treeing can occur from: eroded surfaces in a void, water trees and also stress enhancements without voids [**16**]. Electrical treeing can be divided into two phases. Phase one of electrical treeing is known as the initiation phase. The insulation of the cable gradually degrades due to the charge motion of each half cycle of the applied voltage. The degradation of the insulation can lead to the formation of small voids within the insulation. Figure 2-10 illustrates a typical electrical tree within the insulation of an electrical cable.

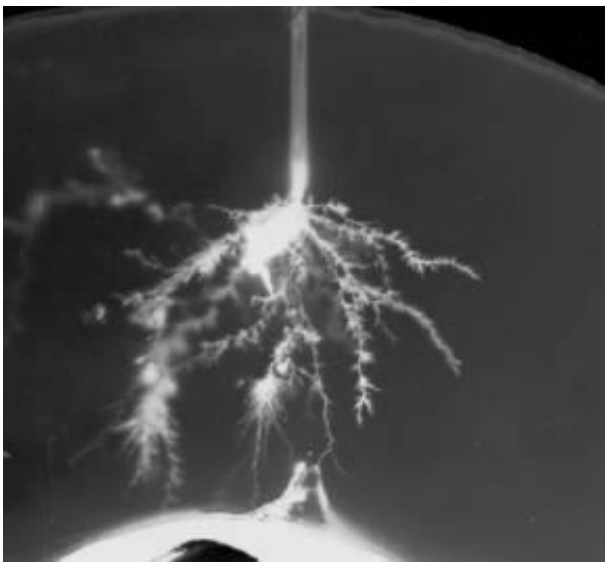

Figure 2-10: Typical illustration of electrical treeing [**20**]

Phase two of electrical treeing is known as the growth phase. The initial voids, created in phase one, become extended and form a defect in the cable. The defects are similar in shape to that of a tree, thus the name electrical treeing. The "branches" will continue to expand due to PD within these "branches" [**16**].

2.5. Cable condition monitoring techniques

2.5.1. Introduction

A cable condition monitoring (CM) technique is chosen according to a wide range of factors. These factors can include: the cable being tested, physical environment, affordability, ease of use as well as results obtained from tests. In order for a CM program to be effective, certain elements need to be considered. A list of the essential elements of a CM program is listed below [**2**]:

- Selection of cables to be monitored.
- Database development for monitored cables.
- The monitoring of the service environments
- The identifying of expected factors leading to aging and degradation.
- Selection of suitable condition monitoring techniques.
- Establish baseline condition of monitored cables.
- Perform regular test and inspection activities.
- Periodic review and incorporation of plant and industry experience.
- Periodic review and assessment of the condition of monitored cables.

2.5.2. Desired attributes of an effective CM technique

A CM program is based on the selection of appropriate CM techniques in order to be able to obtain certain results in a specific environment. The monitoring of the condition of an electrical cable involves the observation, measurement and trending of condition indicators. These indicators can be used to determine the physical condition of a cable [**2**]. An ideal CM technique can be described as a technique which adheres to the following desired attributes of a CM technique [**3**]:

- Non-intrusive and non-destructive
- Applicable to cable types and materials commonly used.
- Affordable and easy to perform.
- Provides trendable data.
- Capable of measuring property changes that are trendable and that can be correlated to functional performance during normal service.
- Able to identify the location of aging and degradation on the cable being tested.
- Able to predict a fault, due to aging and degradation, before cable failure.
- Allows a well-defined end condition to be established.

2.5.3. In-situ CM techniques

Visual inspection

Visual inspection is one of the most commonly used and most effective in situ CM techniques [**3**]. With this technique the cable is visually examined by the naked eye. Extra equipment can be used as aids to the inspection of the cable. This can include flashlights and/or a magnifying glass. Tactile information of the cable can also be gathered by touching the cable. This technique does not require any other special equipment. Due to the limitations of visual inspection, additional more intrusive testing is required, if degradation is identified. Visual inspection can be seen as an effective screening technique and therefore additional testing is required to successfully identify degradation of the insulation of electrical cables. Due to the simplicity of visual inspection, it cannot detect and quantify many types of cable degradation and aging mechanisms.

Visual inspection is often used for qualitative assessment of a cable's condition. The information gained can then be used to determine whether additional, more intrusive testing is required. For this technique to be successful, it is important to pay attention to some important cable attributes. These attributes include: colour, cracks and visible surface contamination. Colour can be a useful attribute in visual inspection and may include changes from the original colour as well as variations in colour along the length of the cable. The degree of sheen can also be used to detect aging and degradation of the cable. Any cracks on the surface of an electrical cable can be an indication of cable degradation. It is important to notice the lengths of cracks, direction, depth, location as well as the number per unit area. The last attribute that should be focused on is visual surface contamination. This is one of the attributes which can easily be detected by means of regular visual inspections. This should also include the identification of any foreign materials on the surface of the cable.

The main advantages of this technique are that it is an inexpensive technique, requires no additional equipment and can also be seen as a relatively easy technique to perform. Another important advantage of visual inspection is that it can reliably detect sections of the cable exhibiting the signs of unexpectedly severe degradation that can be produced by locally adverse environmental conditions [**2**]. A major disadvantage of visual inspection is that the cable must be accessible and visible. This then excludes cables in closed conduits, heavily loaded cable trays and also underground cables. The fact that this technique does not provide quantative data can also be regarded as a disadvantage. The results from a variety of inspections can be compared, however the results are subjective and may differ from different inspectors.

Compressive modulus (Indenter)

The compressive modulus of a material is defined as the ratio of compressive stress to compressive strain below the proportional limit [**2**]. Over a period of time the materials used for cable insulation will harden, thus increasing the compressive modulus. The degradation rate of insulation materials can thus be monitored by using the specific materials' change in compressive modulus over a period of time. Compressive modulus can be used for a number of insulation materials including: ethylene propylene rubber (EPR), silicone rubber (SR), Neoprene®, polyvinyl chloride (PVC), cross-linked polyethylene (XLPE) and chlorosulfonated polyethylene (CSPE) [**3**], [**21**], [**22**]. This technique is performed by using an Indenter Polymer Aging Monitor (Indenter) to measure the compressive modulus. A metallic probe is pressed into the insulation material, the indenter measures the force required for the resulting displacement. The compressive modulus is then calculated by using the measured values. These measurements are taken at a number of random points along the cable in order to get an estimate compressive modulus value for the complete cable. Compressive modulus as a condition monitoring technique is most successful on low-voltage cables [**2**].

The Brookhaven National Laboratory (BNL) found that compressive modulus measurements can be used as an effective condition monitoring technique for both in situ and laboratory conditions [**3**]. Compressive modulus is a non-destructive technique which provides trendable, repeatable results. These results can be correlated to other known cable properties, in order to indicate the condition of the insulation of the cable.

One disadvantage of compressive modulus is that the cable has to be accessible. Therefore this technique will not be useful on underground cables, cables in ducts or any other cables not directly accessible. Cables typically house a number of different layers. This causes another drawback to the compressive modulus technique. Although the outer jacket of the cable is accessible, it may be impossible to access inner layers of insulation materials for compressive modulus testing. Thus the compressive modulus will only give direct information on the brittleness of the outer jacket material. It will be impossible to indicate whether the insulation materials are weak or degraded.

Different insulation materials will react differently to various environmental conditions. This may cause certain materials to not produce a significant change in compressive modulus over a period of time. This then is another disadvantage of compressive modulus testing as the resulting small modulus changes might be difficult to correlate with the aging and degradation of an electrical cable [**2**].

Dielectric loss

The condition of electrical cables can be indicated by means of dielectric loss measurement. This technique includes two related tests: power factor test and dissipation factor test. This technique is based on the dielectric phase angle (θ) and the compliment of this angle, the dielectric loss angle (δ). These angles are determined by applying a steady-state ac test voltage (V) to the insulation of a cable. The test voltage will result in an apparent total current (I) flowing through the cable. The total apparent current (I) will have two components: a leakage current (I_R) and due to the capacitance of the cable, a charging current (I_C). Figure 2-11 illustrates the relationship among the applied voltage and the current components, as well as the dielectric phase angle (θ) and the dielectric loss angle (δ).

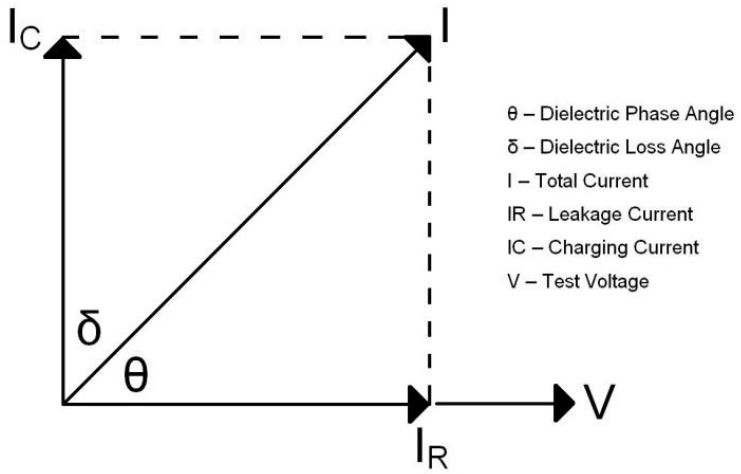

Figure 2-11: Dielectric Loss [**2**]

Various other components can also be calculated by means of the relationship graph illustrated in Figure 2-11. The components include: dielectric (insulation) power factor, dielectric (insulation) dissipation factor and the power factor tip-up. The formulas for these components are given below [**2**]:

Dielectric (insulation) power factor:

$$P_{(dielectric)} = \cos\theta \tag{2.1}$$

Dielectric (insulation) dissipation factor:

$$DF_{(dielectric)} = \tan\theta \tag{2.2}$$

Power factor tip-up:

$$P_{(tip-up)} = \Delta\tan\theta \tag{2.3}$$

Under normal circumstances the leakage current of electrical cable insulation will be smaller than the charging current. The leakage current will also be more sensitive to the condition of the insulation. Aging and degradation of the insulation of a cable will result in an increase in leakage current; the charging current will remain approximately constant. This then means that the ratio of leakage current (I_R) to charging current (I_C) will increase as the insulation of the cable degrades. This ratio (I_R/I_C) is the dielectric dissipation factor of the cable ($DF_{(dielectric)}$), given in (2.2). The dielectric dissipation factor is commonly used as a measure of the condition of cable insulation.

Insulation* r*esistance and polarization index

The condition of a cable's insulation can be determined by a standard industry technique called the insulation resistance technique. In this technique the resistance separating the cable conductor and the ground, is determined by applying a voltage between them. A small current will flow through the insulation to the ground of an insulated conductor, if a dc current is applied. This current consists of three components: the capacitive charging current, the leakage current as well as the dielectric absorption current [**2**]. The total current flowing through the insulation to the ground will be equal to the sum of these three components.

The three current components will change over a period of time. Both the capacitive charging current and the dielectric absorption current will have high initial values. The values of these two components will eventually decrease and approach zero, due to the fact that the insulation acts as a capacitor. The leakage current acts in an opposite way, as it will start at zero and gradually increase to a steady value, if the insulation is in a good condition. The total current will thus vary in different ways according to the condition of the electrical cable's insulation. The monitoring of this variation can be used as an effective CM technique. The ratio of two insulation measurements at different times is called the polarization index [**2**].

This technique is easy to perform and does not require any expensive equipment. The polarization index test is usually used as a simple pass/fail test. An advantage of this technique is that it provides quantitative data that can be trended as a measure of insulation condition. The polarization index test is also not a temperature dependant technique [**2**]. Although many factors may affect the insulation resistance, a test performed by Brookhaven National Laboratory (BNL) has found that the effect of other operating electrical equipment or energised cables close to the cable being tested is negligible [**3**]. A major disadvantage of the insulation resistance and polarization index technique is that the cable being tested must be disconnected [**2**], and can be seen as intrusive. This technique is also not as sensitive as other condition monitoring techniques.

AC Voltage withstand test

The ac voltage withstand test involves a high test voltage applied to the insulation of a cable. This demonstrates that the insulation can withstand a voltage potential higher than the normal operating voltage. The ac voltage withstand test is similar to the dc high potential test. This test is based on the principle that a cable with defects present, will fail under the high test voltage. If the test is performed without any failures, the cable's condition is considered to be good and without any defects. The test voltage for the ac voltage withstand test is usually applied at very low frequencies (< 1 Hz). This is to minimize the charging effect in the insulation of the cable. This test is performed by applying a high test voltage, typically two times the rated voltage, for a period of time, usually 10 – 20 minutes, to each conductor and ground of the cable. This technique can be seen as a pass/fail type technique, because if the cable passes the test it is assumed that there is no defects in the insulation and can continue to be used in operation. If not, it is assumed the cable's insulation has defects present and should be replaced.

In contrast with some of the other techniques, this test is relatively simple to perform and does not require specialised training. An advantage of this test is that if defects are found during testing, they can be repaired or replaced prior to failing. A major disadvantage of this technique is that the cable being tested must be disconnected in order to attach the test equipment. Another drawback is that regular ac voltage withstand tests may result in the degradation of the cable's insulation, as the applied high test voltage could cause a voltage breakdown and damage the insulation of the cable.

DC High potential test

The dc high potential test is a technique similar to that of the ac voltage withstand test. This test involves subjecting a cable's insulation to a high voltage potential. This is done to determine whether a cable can withstand a higher than expected potential for a specific period of time. Most materials used for the insulation of electrical cables can withstand the application of high dc potential for long periods of time, without any damage to the cable. A high ac potential however will have a significant effect on the insulation material of an electrical cable. Thus the dc high potential test is sometimes preferred to the ac withstand test.

The advantages and disadvantages of the dc high potential test are similar to that of the ac voltage withstand test. An advantage of this technique compared to the ac voltage withstand technique, is that the dc high potential test is less likely to affect the insulation of the cable. The equipment used for the dc high potential test is also smaller and more portable compared to equipment used for the ac voltage withstand test. This type of test is however no longer applicable on extruded AC power cables due to problems with space charge. Techniques including very low frequency (VLF) test techniques are generally used.

Step Voltage Test

In both the step voltage test and the dc high potential test a dc test voltage is applied to the electrical cable being tested. The only difference is that, in the step voltage test, a low voltage is used at the start of the test and then gradually increased in steps to reach the maximum test voltage. At each step the leakage current through the insulation is measured. Since these currents can be recorded and trended, this test can be seen as a diagnostic test. This test can also be used to provide insights into the condition of the insulation as a function of age and voltage potential.

The step voltage test has an advantage over the high potential test because damage to the insulation of the cable can be mitigated. This is done by monitoring the measured leakage currents. Except from this, the advantages as well as the disadvantages of these two techniques are similar. The step voltage test can potentially be a destructive test.

Time domain reflectometry

The condition of inaccessible cables is often tested by means of Time Domain Reflectometry (TDR). The technique of TDR works on the same principle as radar [**2**]. A pulse is transmitted down the length of the cable; usually this is a non-destructive pulse. The pulse will be reflected if it encounters a fault on the cable or if the end of the cable is reached. The pulse will also be reflected if the electrical impedance of the cable is changed by some sort of problem. The time required for the signal to travel to and from the point of reflection is recorded. The time can then be converted to a distance, which is used to locate the position of the fault [**3**]. In order for TDR to be used as a successful CM technique, the cable must first be tested to establish a baseline for the specific cable. Further TDR tests at later stages can then be used to trend the aging and degradation of the particular cable. TDR can be performed on low-voltage as well as medium-voltage cables.

The main advantage of this technique is that it can be performed in-situ and is also classified as a non-destructive technique. Another advantage of this technique is that it provides information which can be used to determine the location of a potential fault on the cable. The equipment required to perform TDR tests is affordable and also relatively easy to use [**2**]. Although the test equipment is easy to use, experienced personnel is required to successfully interpret the results obtained from the TDR testing.

Infrared thermography

Infrared thermography is a non-intrusive, non-destructive technique used for the monitoring of the condition of electrical equipment, by means of identifying elevated temperatures present in this equipment. This technique is performed by detecting, measuring and/or displaying the infrared or heat radiation emitted by an object, by means of thermal detection or imaging systems. Equipment used for infrared thermography is highly sophisticated and is capable of measurements as fine as one tenth of a degree Fahrenheit (°F). Spot meters and imagers are the two instruments typically used for infrared thermography. A Spot meter is a device used to measure infrared radiation at a specific area. The user points the device, with the help of a laser guided pointing device, to the spot to be measured. The device will then measure the infrared radiation at the specific spot. A spot meter converts infrared radiation into numeric temperature values [**2**]. An imager converts infrared radiation into a visual image or thermo-gram. Imagers are capable to perform highly sensitive measurements. The thermal images, captured by imagers, can be analysed over a period of time, with the help of computer software packages. These software packages can also be used to graph the associated temperature data. High operating temperatures or temperature hot-spots can lead to accelerated degradation of electrical cable insulation. Infrared thermography is therefore a useful CM technique, as it is possible to identify temperature hot-spots or elevated operating temperatures.

Illuminated borescope

The use of an illuminated borescope to inspect inaccessible cables has proven to be a useful screening technique for identifying stressors that can lead to cable degradation [**2**]. Visible damage to a cable can also be detected in inaccessible areas with the help of an illuminated borescope. The borescope allows the user to insert the instrument into conduits or other locations which would otherwise be inaccessible to inspect. Thus this technique can be used to detect mechanical damage to cables in inaccessible locations. A borescope can also be used as an aid for the visual inspection technique, to detect surface contamination on cables hidden from the naked eye. The use of an illuminated borescope will only act as a screening technique, as the results obtained can be used to determine whether additional, more intrusive testing is required.

Advantages of this technique are similar to that of visual inspection as it is: non-destructive, a simple operation to perform and requires little training. As with visual inspection the major disadvantage is that this technique does not provide quantitative data that can be trended. The illuminated borescope technique is therefore only used as a screening technique.

Line resonance analysis

The line resonance analysis (LIRA) test can be defined as the analysis of electrical test signals input to the cable under test using a waveform generator [**2**]. This test is a relatively new cable CM technique, information as well as test results regarding this technique are therefore limited. The LIRA test models a wire system using transmission line theory and uses narrow-band frequency domain analysis of high frequency resonance effects of unmatched transmission lines to detect changes in the insulation properties [**2**]. This technique can be used to detect both small and larger defects in the insulation of an electrical cable. The larger effects are indicated by amplitude change. The cumulative phase shift of the impedance is determined, in order to detect the small defects in the cable insulation. The change in permittivity in the insulation is responsible for the phase shift of the input impedance.

An advantage of the LIRA test is that it is possible to detect and localize meaningful property changes for various different insulation types and geometries for both aging and non-aging related effects [**23**]. This technique can be performed in situ without de-terminating the cable. By using this technique, the degradation of a cable's insulation can be detected prior to the cable failing. A disadvantage of this technique is that it is a complex test to perform and therefore specialized training is required. Another drawback of the LIRA test is that at the moment limited research regarding this technique is available.

2.5.4. Laboratory CM techniques

Elongation-at-break

Elongation-at-break (EAB) is an industry standard technique used for measuring the condition of a polymer. EAB can be described as the resistance to fracture of a material, when tensile stress is applied. This is often referred to as the "ductility" of a material. A number of stressors such as elevated temperature and radiation levels can lead to a polymer losing its ductility. The condition of cable insulation can thus be determined by monitoring the ductility of the material. EAB is a very accurate technique and is also a repeatable method for cable CM. Polymers are generally used for cable insulation as well as the jacket materials of electrical cables, thus EAB is a highly successful CM technique [**3**]. A calibrated tensile tester is often used to perform EAB tests, in accordance with ASTM standard D638 [**24**] and D412 [**25**]. A number of cable samples, usually several centimetres long, are used as test specimens. An ASTM-approved die is used to stamp the test specimens in the shape of a "dog bone". The tensile tester is then used to pull the specimens under precise loading conditions until they break. The test is therefore classified as destructive.

EAB is generally used as a benchmark for characterising the condition of cable materials. This is because EAB testing provides useful quantitative assessments. EAB measurements provide trendable data that can directly be correlated with material condition, and is seen as a reliable technique for the CM of electrical cables. If the EAB value of a specific cable decreases over a period of time, it may tend to form cracks in the insulation of the cable. As a result of the cracks it can lead to moisture intrusion and current leakage. A value of ≥ 50 % is often used as an acceptance criterion, as there is no standardised acceptance criterion for the minimum EAB value for an electrical cable. Tests have also been conducted to prove that a cable can have a useful lifetime, although this cable may have an EAB value less than 50% [**3**]. A major disadvantage of this technique is that it is destructive and also requires large portions of the cable for testing. Another drawback is that the test samples can only be obtained if the cable is removed from service.

Oxidation induction time/temperature

Antioxidants are generally added as an ingredient for the insulation materials used for electrical cables. Antioxidants are added due to the fact that electrical cables are exposed to oxidation for long periods of time [**2**]. The oxidation can cause the cable to degrade, thus the antioxidants are used to prevent the degradation of the insulation materials of electrical cables. The antioxidants however do not prevent the oxidation process on cables indefinitely. After a period of time the antioxidants will leak to the surface and the oxidation process will begin. Small samples of the cable can thus be taken to measure the time required before the inception of oxidation. This then indicates the remaining antioxidants within the material and can be used to estimate the remaining life of the insulation material.

Oxidation induction time (OITM) is a measure of the time at which rapid oxidation of a test material occurs when exposed to a predetermined constant test temperature in a flowing oxygen environment [**2**]. OITM are taken with a differential scanning calorimeter (DSC). This test can be seen as a non-destructive technique due to the fact that the test samples are very small. However, some consider it to be destructive from the standpoint of the test sample being used [**2**]. The oxidation induction temperature (OITP) test is a variation to the OITM test, and is also measured with a DSC.

Fourier transform infrared spectroscopy

The molecular structure of materials is often studied by means of Fourier transform infrared (FTIR) spectroscopy. A spectroscope is used to perform this technique, with a small material sample exposed to infrared radiation. The absorbance or transmittance of this radiation by the material at various wavelengths is then measured [**2**]. The atoms inside the polymer will absorb radiation and begin to vibrate when radiation passes through the insulation material. The atoms will reach a maximum value of vibration at a specific wavelength of radiation.

The presence of a carbonyl (C=O) peak can be indicated by studying the oxidation of insulation materials. This presence is shown by an important wave number in the FTIR spectrum at 1730 cm^{-1} [**2**]. If the presence of carbonyl is indicated it can be said that the material is undergoing oxidation, because of the fact that carbonyl bonds are being generated.

This technique can be seen as a non-destructive test, because of the fact that the test samples needed are very small. Another advantage of this technique is that it provides quantitative results. These results can be trended over a period of time and thus be used for the CM of an electrical cable. A disadvantage of the FTIR testing method is that the samples cannot be taken from areas of the cable which is inaccessible. Certain areas of the cable can therefore not be tested with the FTIR spectroscopy method.

Density

Another laboratory technique used for the CM of electrical cables is the measurement and trending of the cable insulation's density. The material structure of a polymer will change over a period of time due to oxidation. These changes may include: cross-linking, chain scission and the generation of oxidation products [**2**]. Thus over a period of time, a cable will shrink and cause an increase in density of the cable's insulation. Measuring and trending the density of a cable's insulating material can therefore be used as a cable CM technique [**26**]. A small piece of insulation material can be used for density measurements. The test specimens are usually smaller than 1 mg, therefore this technique can be seen as a non-destructive technique. The aging of insulation materials as determined by techniques such as EAB, have shown good correlation with density measurements. Density measurements can therefore be used as an effective cable CM technique. The major disadvantage of this technique is that the density tests will only provide information for the localised area from which the test sample was taken. Because of the fact that test samples must be obtained, certain problems can arise in the regard to inaccessible cables.

2.6. Partial Discharge

2.6.1. Introduction

If the conditions are suitable, localised gaseous breakdowns will occur, resulting in partial discharge (PD). PD can be classified as both a symptom of degradation as well as a stress mechanism of degradation. Although there are a number of different aging mechanisms, PD dominates as a degradation mechanism within electrical equipment [**27**].

The development of PD measurement techniques started in the 1950s and 1960s. During this time the main focus of the study of PD was focused on the physical principles of the degradation associated with PD. Many people refer to this era as the "golden age" of PD [**27**]. Various measuring techniques were introduced during the 1970s. These techniques include: electrical, acoustic and also chemical techniques for oil analysis [**27**]. Due to improved technology and also the availability of microprocessor technologies, the 1980s and 1990s focused on the ability to capture data obtained from PD measurements [**27**]. This data could then be analysed and the stored data could be compared to future results obtained from testing. Due to various economic reasons there is a constant need for the detection of degradation mechanisms within equipment to possibly prevent blackouts. At the moment the main focus of PD research is to refine and improve techniques for detecting discharge in electrical equipment.

2.6.2. The process of partial discharge

Erosion breakdown can affect the long term life of an insulator and can therefore be seen as a degradation mechanism. The main source of erosion breakdown is PD. If a discharge does not completely bridge the insulation between the terminals, it is classified as partial [**28**]. PD occurs in a small portion of the electrical path length. The magnitude of PD is often limited due to the fact that PD occurs in series with mostly good insulation, however constant PD can cause the insulation to degrade over a period of time.

A material with a small permittivity (e) will have a high Electric Field Intensity ($\mathcal{E}$). Opposite to this a dielectric with a high permittivity (e) will have a low value of Electric field intensity ($\mathcal{E}$). The flux density (D) is not affected by the medium. Air has a low relative permittivity (e_r) and thus will have a high value for electric field intensity ($\mathcal{E}$). The dielectric strength of air is relatively low in comparison to other materials. These two properties can be seen as the cause for PD. The reason for this is that, due to the low permittivity of air, if a dielectric material has voids filled with air, the electric field intensity ($\mathcal{E}$) in the voids will be higher than that of the rest of the dielectric. The air

filled voids will also have a lower dielectric strength. This then will cause sufficient ionization in the voids to cause an arc. The arc will short circuit the charges accumulating on opposite sides of the void. The process of slow charging and fast discharging will be repeated throughout operation. The void can thus be seen as a relaxation oscillator. This process is known as partial discharge.

Electric Flux Density "D"

A good understanding of electrical field theory best describes the occurrence of PD. According to Gauss's Theorem the Electric Flux Density at a distance r_1 from a concentrated charge Q on a small conductive sphere may be determined by enlarging the sphere until its radius is equal to r_2. The magnitude of the Electrical Flux Density at r_2 is the charge Q divided by the surface area of the enlarged sphere [**28**]. Gauss's Theorem is illustrated below in Figure 2-12. The Electric Flux Density is measured in charge per area and the unit used is Coulombs per square meter (C/m^2). As mentioned previously, the Electric Flux Density (D) is not affected by the medium.

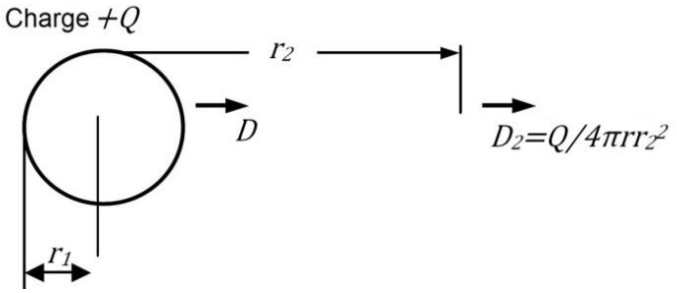

Figure 2-12: Gauss's theorem [**28**]

Electric Field Intensity (E)

The Electric Field Intensity may be defined as the force effectiveness of the electric field [**28**]. The strength and direction of the Electric Field Intensity ($\mathcal{E}$) is measured by the force and direction upon a test charge. Electric Field Intensity is measured in Newtons per Coulomb (N/C) and is dimensionally equivalent to Volts per meter (V/m) [**28**]. The process of measuring the Electric Field Intensity ($\mathcal{E}$) is shown in Figure 2-13. Electric Field Intensity ($\mathcal{E}$) is proportional to the Electric Flux Density (D) but inversely proportional to permittivity (e) of the medium [**28**].

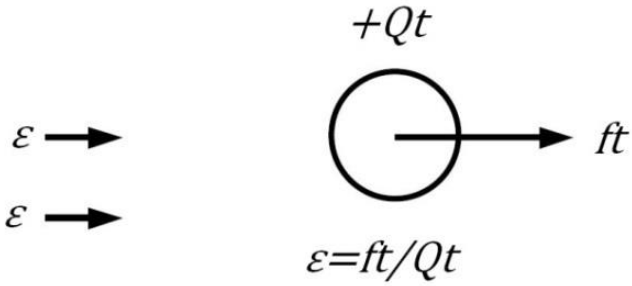

Figure 2-13: Electric Field Intensity [**28**]

The proportionality of electric field intensity and electric flux density is shown in equation (2.4). From this it can be concluded that the Electric Field Intensity ($\mathcal{E}$), unlike Electric Flux Density (D), is dependent on the medium.

$$\varepsilon = {}^{D}/_{e} \tag{2.4}$$

The permittivity (e) of a material is measured in Farads per meter (F/m). The permittivity of a vacuum is equal to 8.85×10^{-12} and is known as the electrical constant e_0 [**28**].The permittivity of a material is calculated by using equation (2.5) shown below.

$$e = e_r e_0 \tag{2.5}$$

Where e_r is the relative permittivity of the material. The relative permittivity values of some materials are given in Table 2-4.

Table 2-4: Relative permittivity of materials [**29**]

Material	**Permittivity (e_r)**	**Material**	**Permittivity (e_r)**	**Material**	**Permittivity (e_r)**
Vacuum	1	Sulphur	3.5	Cable Oil	2.2
Air	1.0006	Rubber	3	Water	4 - 88
Copper Catalyst	6.0 – 6.2	Transformer Oil	2.2	Paper	2.0

2.6.3. Partial Discharge Testing

A variety of techniques are available for the detection of PD within electrical equipment. These techniques include: electrical detection, acoustic detection, thermography and other camera techniques as well as chemical detection [**27**]. The various techniques, as well as the advantages and disadvantages of each will be discussed in this section.

Electrical detection

Electrical detection is a technique commonly used to detect PD. Although electrical detection can be seen as a successful technique, it is not always possible to use this technique on cables in specific environments. Electrical detection of partial discharge can be divided into three groups [**27**]: 1) measurement of each individual discharge pulse, 2) measurement of the total, integrated loss in the insulating system due to discharge activity and 3) measurement of electromagnetic field effects associated with discharge activity, using antennae and capacitor probes.

Individual discharge pulse measurement

Two methods are generally used to detect partial discharge by means of individual pulse measurement. The first method is to clamp a current transformer (CT) to the neutral of the electrical equipment being tested. The output of the CT is then measured with an oscilloscope or a similar recording instrument. The second approach is similar to that of the CT approach, as the measurements are also taken by an oscilloscope or similar device. Instead of using a CT this method makes use of a transducer connected to the high voltage terminals of the equipment being tested. The transducer is generally a capacitor divider type assembly [**27**]. Figure 2-14 illustrates both these techniques by showing the connection of the equipment of both to three phase equipment.

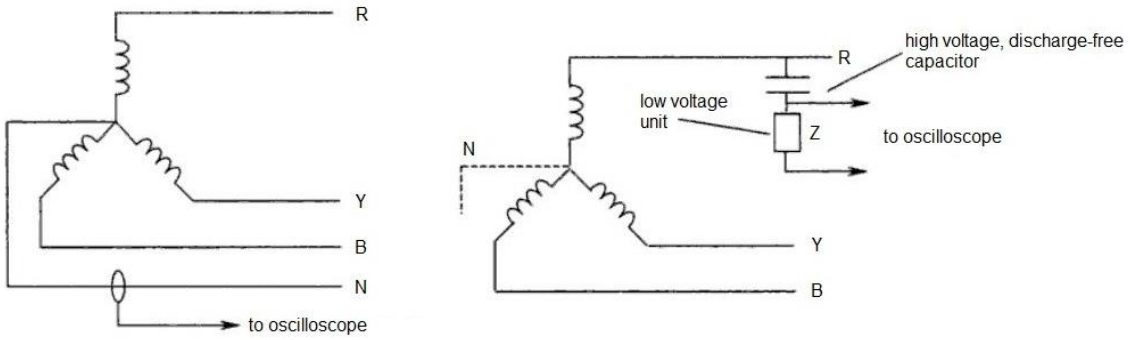

Figure 2-14: PD pulse measurement [**27**]

The first approach, where the CT is used as measurement instrument, is simple to use, affordable and also safe. This technique however can only be used if a neutral is available. Due to the fact that the CT can be clamped on, it will not be necessary to disconnect the electrical equipment being tested. This technique can therefore be seen as an online technique and can also be classified as non-intrusive. The CT technique has three major disadvantages. The first disadvantage is that the magnitude of the discharges can't be determined due to the fact that this technique cannot be effectively calibrated. The CT technique is also very sensitive to external interference from other sources. This disadvantage can be managed in some way by making reference measurements before connecting the CT to the neutral of the equipment. The last major disadvantage is that this technique does not provide effective phase information on the partial discharge. Thus the location of the discharges on the power cycle can't be determined [**27**].

The second technique commonly used for individual discharge pulse measurement is to connect a transducer to the high voltage terminals of the electrical equipment being tested. The transducer generally consists of a discharge-free high voltage capacitor and a low voltage impedance circuit [**27**]. The low voltage impedance circuit can either be a RC circuit or a RLC circuit. The transducer is then connected to a measuring instrument such as an oscilloscope. Instead of connecting the transducer to the high voltage terminals, a Rogowski coil can be used.

A Rogowski coil can be seen as a form of CT, but with certain distinct differences. The Rogowski coil is specifically designed to concentrate the magnetic flux more effectively than in a normal CT [**27**]. Ampere's law defines the principle of operation of the Rogowski coil. The Rogowski coil consists of a conductor with an air-cored coil connected around it. The current flowing through the conductor will result in an alternating magnetic field around the conductor. This magnetic field will induce a voltage in the coil connected around the conductor. The rate of change of current is proportional to the rate of change of the voltage induced in the coil [**27**]. It is easy to connect the Rogowski coil to the high voltage terminals of electrical equipment, as it is also a clamp on type of instrument, similar to a normal CT. Although the Rogowki coil may be less sensitive than the capacitive coupler approach, it has the advantage of being able to provide an indication of pulse direction. Due to the construction of the coil it can be used as both an online and a non-intrusive technique.

Loss measurement associated with discharge activity

PD will cause an increase in the current loss of an insulating system. The loss measurement technique focuses on this principle in order to be able to detect PD in electrical equipment. The presence of PD is detected by monitoring the tan δ of the system, where δ is the relative values of resistive to capacitive values [**27**]. The monitoring of tan δ is based on the fact that as the losses increase, the resistive current will also increase. As a result of the increased resistive current the value of tan δ will also increase. This technique is generally seen as an effective monitoring technique due to the fact that the electrical losses will increase enormously in the presence of PD. The losses due to PD will also dominate as the loss mechanism [**27**]. Figure 2-15 illustrates the monitoring of tan δ for a number of electrical motors. From the graph of tan δ versus applied voltage it is possible to derive certain characteristics.

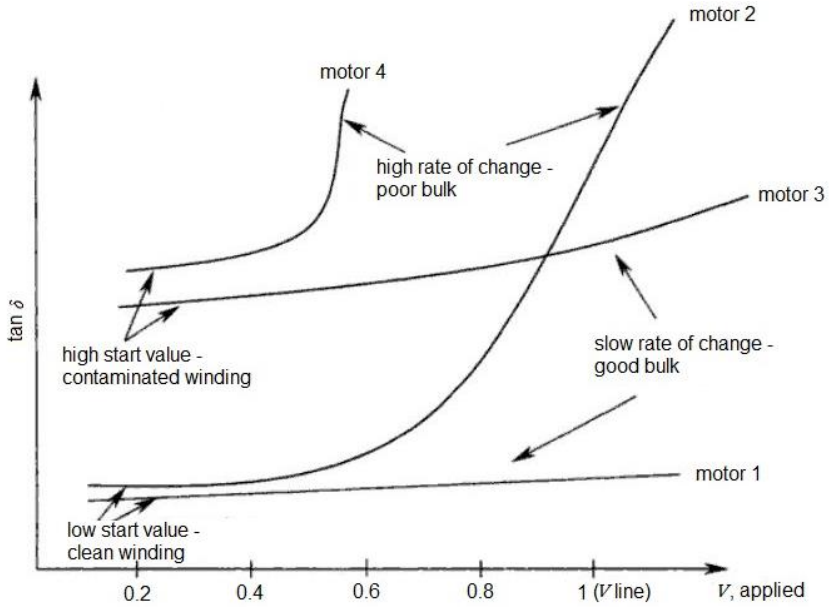

Figure 2-15: PD detection by means of monitoring tan δ [**27**]

This technique was generally performed by connecting a Schering Bridge to the high voltage terminals of the equipment. The technique has been improved over the past years to a point where instruments, available today, can make direct measurements of the different current components.

The main advantage of this technique is that it is simple to perform and it is also easy to interpret the obtained measurements. The main disadvantage is that this technique is only a measure of the degradation in the insulating system. This then means that the presence of PD may not be detected due to the ability of the equipment to sustain the discharges without damage to the insulating system. The present trend is to only use online measuring techniques, due to various economic reasons. The loss measurement technique however will not be a useful online technique as only a single value for tan δ can be obtained. This will then make it impossible to distinguish between the levels of PD. Figure 2-16 illustrates the typical design for a Schering Bridge type circuit.

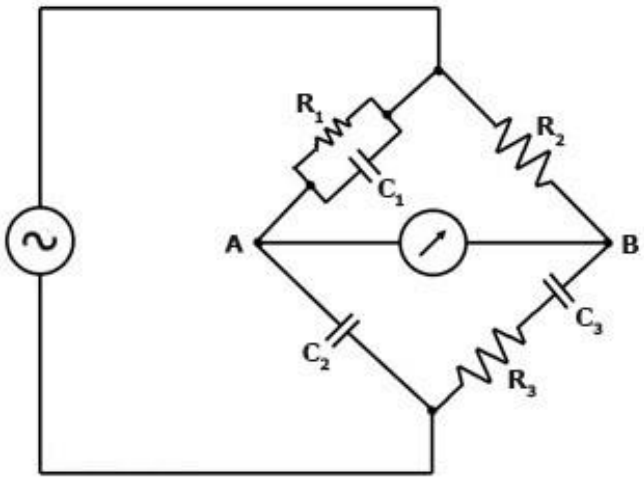

Figure 2-16: Typical design of a Schering bridge [**30**]

In Figure 2-16 the parameter C_3 is the unknown capacitor, whose value need to be calculated, R_3 is a series resistance, representing the loss in capacitor C_3, C_2 is a standard capacitor and R_2 a non-inductive resistance. C_1 in the diagram is generally depicted as a variable capacitor with R_1 a variable non-inductive resistance [**30**].

The purpose of the Schering Bridge is to measure the insulating properties of electrical cables and equipment. The Schering Bridge was developed by Harald Schering and has the advantage that the balance equation is independent of the frequency [**30**].

Antenna techniques

The phenomenon of radio interference noise being generated by PD has been recognised since the 1920s [**27**]. Since then various attempts have been made to accurately measure and quantify the presence of PD by means of a range of different antennae. The main focus of PD measurement by

means of antennae was the measurement of corona present on overhead lines and insulators [**27**]. This technique is performed by using specifically designed antennae to detect the discharge pulses. The antennae are coupled to a high bandwidth oscilloscope in order to be able to investigate the pulse shapes obtained from measurement. Due to the success as well as the relatively simple process of this technique it enjoys a large amount of research and could be a technique commonly used in the future.

Capacitive probe techniques

Capacitive probes can be used to detect the presence of a transient earth voltage (TEV). The transient earth voltages are produced by the electromagnetic waves generated due to the presence of PD. The generated electromagnetic waves will propagate away from the site of PD. The amplitude of the TEV is usually small and in the range of millivolts to volts, the value is however usually converted into dB for measurement [**27**]. The method of using capacitive probes in order to detect the presence of partial discharge is illustrated in Figure 2-17.

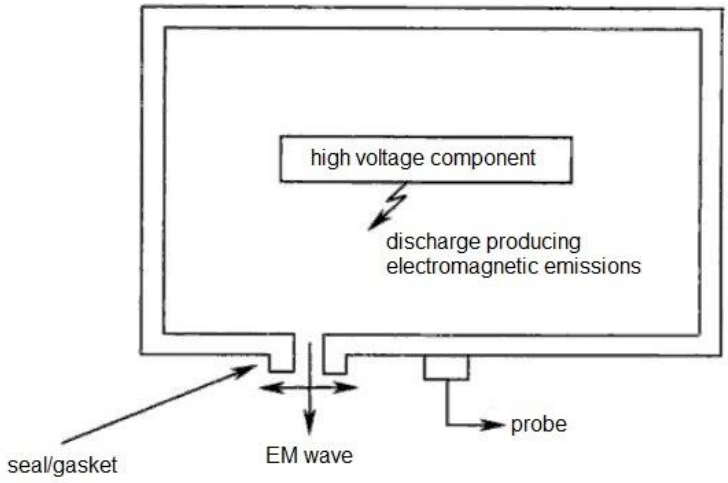

Figure 2-17: PD detection by means of capacitive probes [**27**]

When using only one capacitive probe, it is almost impossible to be able to indicate the exact location of the PD. By using a number of capacitive probes as well as the time of flight principle it can be possible to indicate a more accurate location of the discharge pulses. The method of using a number of capacitive probes is based on the theory that the probe closest to the source should detect the discharge first. As with many discharge monitoring techniques, noise can be a problem. It is therefore necessary to take a background reading in order to determine if a certain probe is suitable for monitoring the plant. The reading should be taken from a metallic surface not attached to any switchboard [**27**]. If the probe is not suitable for the plant, it will not be able to distinguish between noise and actual discharges being generated. A number of capacitive probe products are available and can range from handheld devices to systems with multiple probes connected to an event counter.

An advantage of this technique is the wide variety of components it can be used on, these include: circuit breakers, busbars, cable end joints as well as current and voltage transformers [**27**]. Due to the nature of the measurements the technique is also classified as non-intrusive and is used as an online technique. More details involving the advantages and disadvantages of the measurement of PD by means of capacitive probes is described in the work of [**31**]. This technique is often used in conjunction with a number of antennae. The antennae are used to detect noise which is then subtracted from the signals recorded by the capacitive probes. The antennae are thus used to be able to more accurately detect PD.

Acoustic detection

An acoustic signal is produced due to the effect of PD within electrical equipment. It is possible to use the acoustic signal in order to derive characteristics relating to PD. Piezoelectric sensors are often used to perform acoustic detection due to the high success rate of this type of sensor. If a force is applied to piezoelectric polymers, and the polymer is compressed, an external voltage proportional to the force will be produced. Due to this characteristic of piezoelectric polymers, they are often used in acoustic detection equipment. The energy released by the discharge will be proportional to the intensity of the acoustic waves being emitted [**27**]. It can therefore be said that the square root of the energy being released by the discharge is proportional to the amplitude of the wave. It is also known that energy can be given as the square of the charge, therefore the discharge magnitude should have a linear relationship with the acoustic signal [**27**]. Figure 2-18 (a) illustrates the typical setup for PD detection by means of acoustic detection.

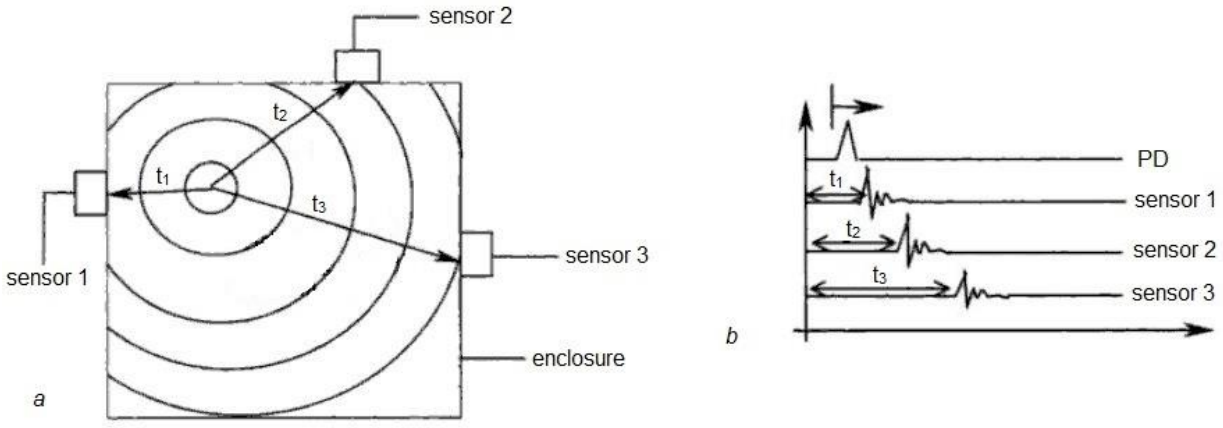

Figure 2-18: PD detection by means of acoustic methods [**27**]

In part (a) of Figure 2-18 it can be seen that the discharge is detected by means of three sensors. The PD activity is closest to sensor 1. Part (b) of the figure shows that the discharge will first be detected by the sensor closest to the discharge site and will continue to be detected until the last sensor, furthest

away, detects the discharge signal. Acoustic detection is an affordable technique for detecting PD and is also easy to perform. This technique can be used online. The major disadvantage of acoustic detection is that it is very sensitive to noise in the environment of testing.

Thermography and other camera techniques

PD within electrical equipment will cause an increase in temperature in the area of the discharge. Thermography can therefore be used to an extent to identify the presence of PD. Unfortunately this technique has limited success due to a number of reasons [**27**]. The main reason is that PD in some electrical equipment may be enclosed and thus difficult to measure with thermography equipment. Thermography is most successful when used where the discharges are external such as with overhead lines and busbars. However even with this, the results obtained are not quantitative. During the 1990s a daylight corona camera was developed to detect PD on overhead lines [**32**]. This camera uses independent UV video and visible cameras to detect the corona.

Chemical detection

If PD occurs, it produces certain by-products. Chemical techniques can be used to measure these by-products and thus indicate the presence of PD activity [**27**]. Although chemical techniques can be used to detect the presence of PD, it is most successful when applied on oil-filled equipment. The oil used in oil-filled equipment will degrade and in the degradation process, a number of specific gasses will form. Table 2-5 show a number of gasses typically absorbed in the oil when PD occurs.

Table 2-5: Gasses produced due to PD [**27**]

Name	**Symbol**	**Chemical bond**
Hydrogen	H_2	H - H
Methane	CH_4	CH_3 - H
Ethane	C_2H_6	CH_3 - CH_3
Ethylene	C_2H_4	$CH_2 = CH_2$
Acetylene	C_2H_2	CH ≡ CH

A small amount of oil is required to perform tests needed for the detection of PD by means of chemical detection. The techniques associated with chemical detection are affordable and also easy to perform [**27**]. Fault gas detectors are also commercially available to perform the tests under field conditions. Various interpretation strategies can be used to be able to obtain specific results from the measured samples.

2.6.4.PD testing on cables

Although various techniques can be used to detect PD within cables, the technique called cable mapping is most successful [**27**]. Cable mapping can be used to detect the magnitude and the location of PD within electrical cables. The process of CM of cables by means of cable mapping is described by means of the following statement: The cable with the highest PD activity can be seen as the cable likely to cause a failure. Once the cables with the highest PD are identified, the location of the discharge activity must be identified. These areas can then be monitored, repaired or even replaced [**33**]. On-line mapping can be a successful technique for the detection of PD activity in cables, as this technique is non-intrusive and therefore does not require the cable to be disconnected for testing.

On-line mapping

Two techniques generally used to detect PD by means of on-line mapping are: transponder and GPS synchronisation [**33**]. Both techniques are non-intrusive. If PD occurs within a cable, pulses travel outwards and in both directions from the site of discharge. One pulse travels directly to the point of measurement, while the other reflects from the far end and then travel to the measurement location [**33**]. The location of the PD activity can be determined by using these two pulses. The technique described above is depicted in Figure 2-19 (A). Figure 2-19 (B) shows an enlargement of the reflected pulse.

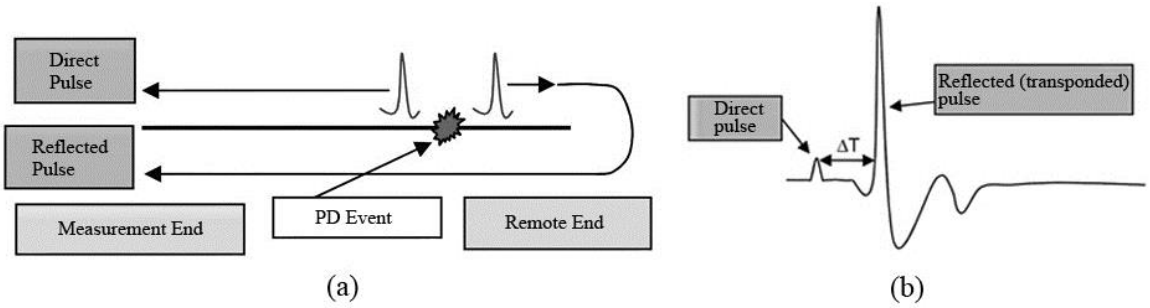

Figure 2-19: Single ended PD location method [**33**]

The location of the discharge activity can be determined if both signals can be identified at the location of the measurements being taken. The location of the discharge activity is determined by means of the time difference (ΔT) between the two pulses. As mentioned, two methods are generally used for on-line cable mapping. The transponder technique is usually used if the following situations occur [**33**]: when the attenuation is too large due to long cables, waveforms are too complex to interpret, in the case of teed or multiple jointed circuits, for circuits with a high number of switchgear and for cables with little change in impedance at the far end. The transponder will amplify the signal at the end of the cable in order for the return pulse to be identified at the measurement location. The advantage of this technique is that no waveform interpretation is needed and that the distance which can be monitored is doubled [**33**].

This technique used to determine the position of a PD defect from the measurement end of the cable is generally accompanied by the following equation [**33**]:

$$x = L - \frac{1}{2}.\mathrm{V}.\nabla T \tag{2.1}$$

where x is the position of the PD defect from the measurement end of the cable, V is the pulse speed in the cable and ∇T is the time of flight difference between the incident pulse and the reflected pulse.

If done correctly, on-line testing will yield similar results to that of off-line tests. Table 2-6 show the advantages as well as the disadvantages for both on-line and off-line techniques of partial discharge detection in cables.

Table 2-6: Advantages and disadvantages of on-line and off-line testing [**33**]

On-line		**Off-line**	
Advantages	**Disadvantages**	**Advantages**	**Disadvantages**
No need to switch circuit of and no MV power supply required	Data interpretation can be difficult	Proven technology	Circuit not loaded during testing
Circuit loaded when tested	Insulated earthing glands required	Calibrated sensitivity	Outage required
Economical			Equipment and outage costs
Teed circuits can be tested			Teed circuits cannot be tested easily

CM techniques for cables depend on the type of cable being tested, as well as the physical environment of the cable. CM techniques which use PD measurements can be seen as an effective technique to monitor the condition of electrical cables. The reason for this is that PD dominates as the degradation mechanism in electrical cables. It is important to note that a single technique is not sufficient to completely analyse the condition of an electrical cable. Multiple techniques must be utilized for the CM of cables in order to yield the best results.

2.6.5.High-voltage test techniques – Partial Discharge (IEC60270:200)

The purpose of the international standard on high-voltage test techniques (IEC60270) is to discuss the measurement of partial discharge in electrical apparatus, components or systems. The scope of the standard is focused on techniques using alternating voltages up to 400 Hz or direct voltages to perform the tests [**34**].

PD is described in this standard as the localised electrical discharge that only partially bridges the insulation between conductors and which can or cannot occur adjacent to a conductor [**34**]. PD generally occurs due to local electrical stress concentrations within the insulation of electrical equipment. PD is often accompanied by emission of sound, light, heat and chemical reactions.

Test Circuits

The essential tasks of the test circuit include energizing the test object as well as to provide the appropriate conditions for the detection of PD activity within the test object. There are four basic circuits from which all other test circuits for the detection and measurement of PD are derived [**34**]. The minimum magnitude of any PD quantity which can be measured is dependent on the ratio of the coupling capacitor to the test object of the test circuit. Test circuits used for measuring PD activity generally consist of the following:

- A test object, usually regarded as a capacitor
- A coupling capacitor, with low inductance
- A measuring system
- A high voltage supply
- Filter, to reduce background noise

Figure 2-20 illustrates the first basic test circuit. The coupling device in this circuit is placed on the earth side of the coupling capacitor.

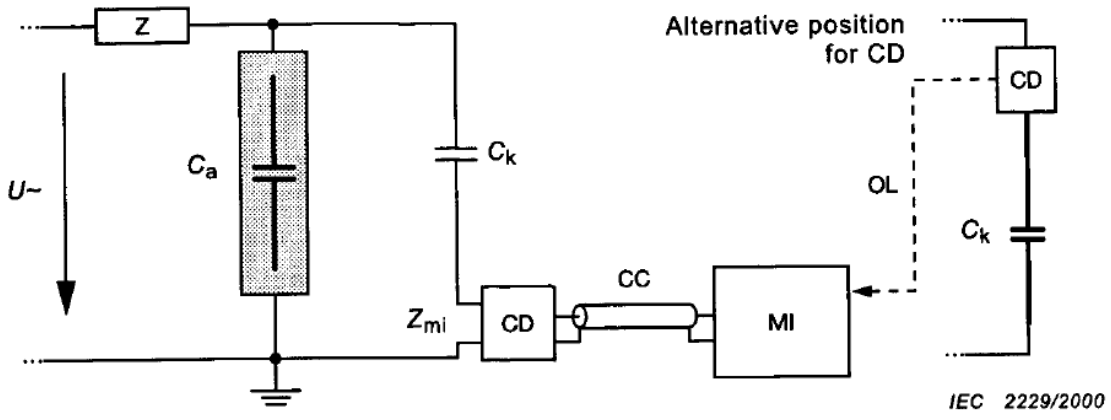

Figure 2-20: Test circuit – coupling device (CD) in series with the coupling capacitor [**34**]

The following represent the parameters in Figure 2-20:

U~ : high voltage supply
Z_{mi} : input impedance of measuring system
CC : connecting cable
OL : optical link
C_a : test object
C_k : coupling capacitor
CD : coupling device
MI : measuring instrument
Z : filter

This type of arrangement has the advantage of being suitable for test objects with only one earth terminal. The purpose of the filter, connected between the high voltage source and the test object, is to attenuate noise from the source.

Figure 2-21 illustrates the second basic test circuit. For this basic test circuit the coupling device is placed at the earth side of the test object. It is therefore important that the low-voltage side of the test object is isolated from earth.

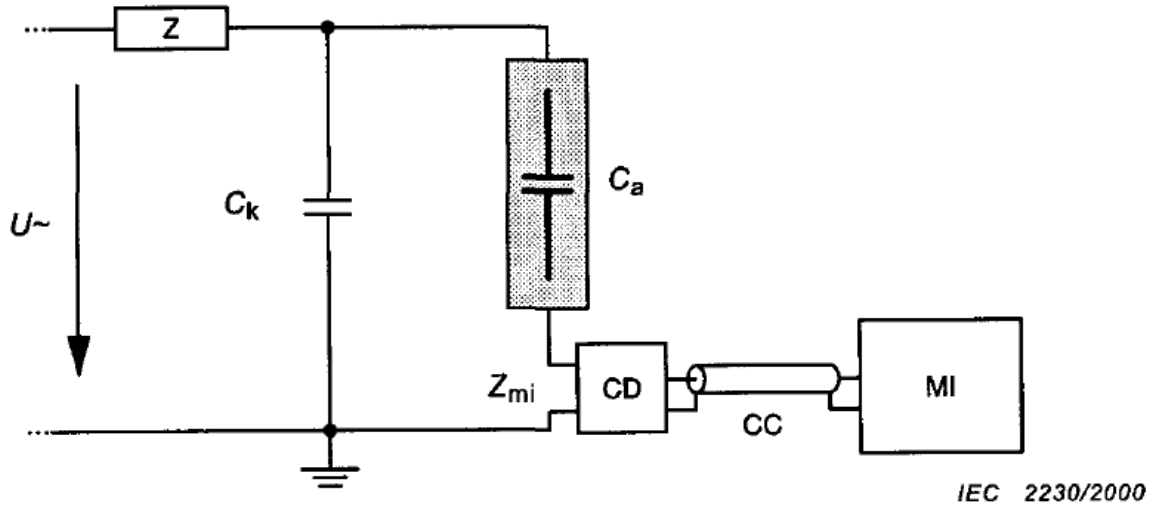

Figure 2-21: Test circuit – coupling device (CD) in series with test object [**34**]

It is essential to combine a protection circuit, designed to withstand the breakdown current in the test objects, with the coupling device [**34**]. The test circuit illustrated in Figure 2-21 can provide a better sensitivity than the circuit illustrated in Figure 2-20, especially for test circuits with low capacitance components.

Figure 2-22 shows the arrangement of the third basic test circuit which comprises a balanced circuit in which the instrument is connected between two coupling devices. The low voltage sides of both the test object and the coupling capacitor must be isolated from earth. The dielectric loss factors of the test object and the coupling capacitor, particularly in relation to their frequency dependence, should be similar [**34**]. This type of test circuit has the advantage of partially rejecting external disturbances and noise.

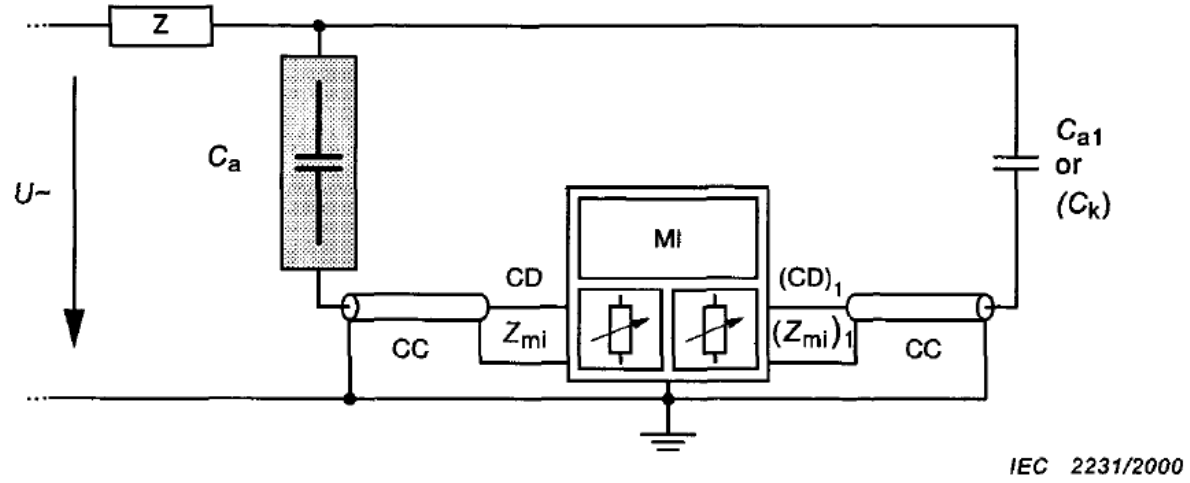

Figure 2-22: Test circuit – balanced circuit arrangement [**34**]

The final basic test circuit is shown in Figure 2-23. This type of test circuit is a combination of the first two basic test circuits, illustrated in Figure 2-20 and Figure 2-21. This circuit includes two capacitances, of which both may be test objects. The low-voltage side of both components is isolated from earth. The two capacitances need not be equal, but should preferably be of the same order. A gating system is generally used to discriminate between PD pulses originating in the test object and noise from other parts of the test circuit [**34**].

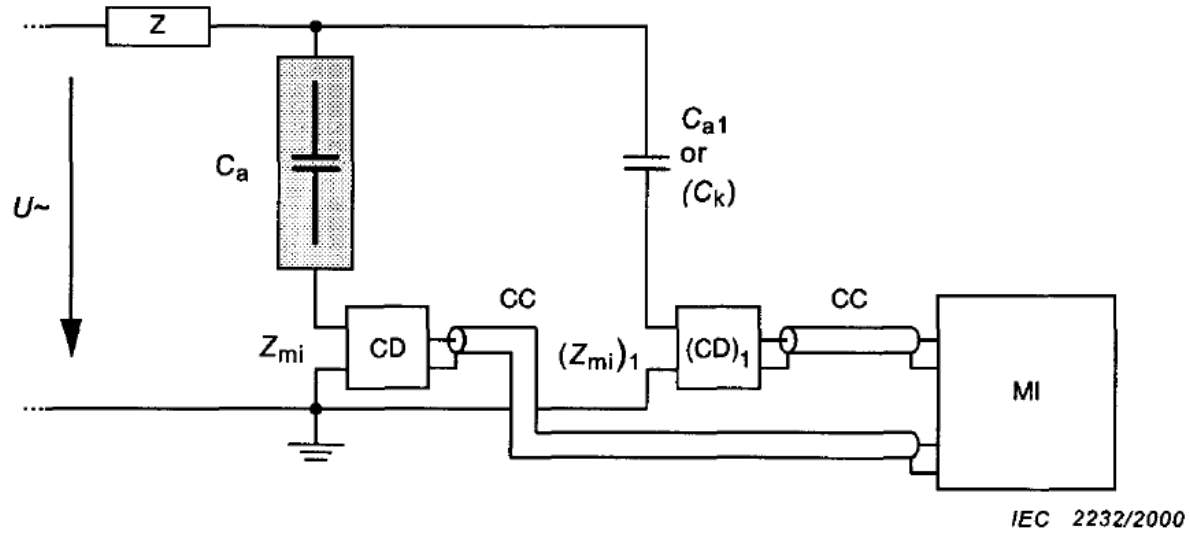

Figure 2-23: Test circuit – polarity discrimination circuit arrangement [**34**]

Measuring system

A measuring system for apparent charge can be divided into the following subsystems:

- Coupling device
- Transmission system
- Measuring instrument

The coupling device is used to convert the input currents to output voltage signals. These signals are then transmitted via the transmission system to the measuring instrument. The frequency response of the coupling device is defined as the ratio of the output voltage to the input current of the device. The frequency response is normally chosen to effectively prevent the test voltage frequency and its harmonics from reaching the measuring instrument [**34**].

The minimum requirement for a digital PD instrument is to be able to display the value of the largest occurring PD magnitude [**34**]. The PD instrument may also include the following additional quantities:

- The apparent charge
- Instantaneous value of the test voltage
- Phase angle.

It is possible to perform PD measurements by means of ultra-wide-band instruments [**34**]. PD is then usually detected by means of an oscilloscope together with an appropriate coupling device. It is a definite fact that background noise will always be recorded when PD measurements are taken. A sensitivity threshold may thus be introduced in order to prevent noise being recorded.

Tests

In order to obtain reproducible results in PD tests, careful control of all relevant factors is necessary. The surface of the external insulation must be clean and dry. This is due to the fact that moisture or contamination can cause partial discharges. It is also important to perform the tests with the test object at ambient temperature [**34**].

PD measurements can be taken without pre-stressing of the test object. The PD magnitude is measured at a specific voltage, which can be well above the expected PD inception voltage. The voltage is gradually increased during the process of measuring. The magnitude of the PD activity is measured and recorded while the voltage is being increased or reduced or throughout the entire test period [**34**].

The international standard on high-voltage test techniques (IEC60270) also includes non-electrical methods for the detection of PD activity. These methods include:

- Acoustical methods
- Optical methods
- Chemical methods

These methods are however not suitable for quantitative measurement of PD quantities as defined in the IEC60270 standard [**34**]. The non-electrical methods of PD detection are generally used to detect and/or locate the discharge activity.

The information provided within this section regarding the international standard on high-voltage test techniques (IEC60270) is vital to the outcome of the study as the simulations discussed within this dissertation is based on the test circuits and the developed monitoring technique is also based on the measurements and tests discussed within this standard.

The purpose of this chapter is to provide a thorough study of research topics related to the work presented in the rest of this dissertation. The literature study focused on CM techniques which make use of PD measurements to monitor the condition of medium voltage electrical cables. The knowledge gained from the work presented in this chapter was used as the basis for the work presented through Chapter 3 to Chapter 6 of this dissertation.

Chapter 3 Modelling

The purpose of this chapter is to discuss the process of deriving two models which will be used to simulate PD activity within medium voltage power cables. The derived models are both based on the well-known three-capacitor configuration. The validation process for both the models is also discussed within this chapter. The basic model will only include the fundamental parameters required for the simulation of PD. The comprehensive model will include parameters to accommodate the stochastic nature of PD. Both models will be used to simulate the occurrence of PD due to a single void within the insulation material of a power cable.

3.1. Background

According to David A. Nattrass the development of electrical models to study the behaviour of PD activity within the insulation of power cables started in 1932 when "Germant and Philippoff developed the simplest electrical representation of a defect within the insulation" [**35**]. This model has a macro approach to the analysis of partial discharge and is known as the capacitive model [**36**]. Over the years many improvements were added to this original model. The original model made use of a spark gap to simulate the occurrence of PD activity and was replaced by Whitehead in 1951 by an electronically controlled device. The main focus for the improvements on the original device was to be able to more accurately simulate PD activity within the insulation material of a power cable. This focus led to the introduction of the shunt conductance of the healthy part of the insulation and the void. The shunt conductance was introduced in 1999 by Paolleti and Golubev [**37**]. A number of research papers followed where a macro approach was used to study PD activity within power cables by means of different configurations of the capacitor model. Farad Haghjoo *et. al*. made further improvements on the basic three-capacitor model in 2012. The research in their paper did not only consider the geometric properties of the void and other internal parameters, but also the position of the void within the insulation material and the congestion of electric field lines while passing through the void [**36**].

For the purpose of this project the research will include the use of two derived models to study discharge activity within the insulation material of a power cable. Both these models will be based on the principles of the basic three-capacitor configuration. The first model will be referred to as the basic three-capacitor model and will only include fundamental parameters required for the simulation of PD activity within the insulation material of a power cable.

The second model will be an improved version of the first model with added parameters which will yield an increased accuracy when compared to actual results. The improved accuracy of the comprehensive model can be attributed to the fact that other than with the basic model: this model has a void with improved geometric properties, the model considers the position of the void within the insulation material and that the congestion of field lines while passing through a void is also taken into consideration.

3.2. Basic three-capacitor model

3.2.1. Introduction

The chosen void parameters are the most important factors for PD characterization. Different types of voids will each have a unique effect on the PD characteristics and therefore will be the main focus for the basic three-capacitor model. By only using the fundamental parameters for this model, a lack in accuracy can be expected. The basic model however still provides useful data for the study of discharge activity within power cables. The comprehensive model, which is also discussed in this chapter, will focus on adding a variety of parameters to the equations in order to improve the accuracy of the simulation model.

3.2.2. Modelling

As mentioned in the validation process, the simulation models will be modelled to accurately represent a typical medium voltage power cable. The basic model will only be modelled for a small section of the insulation material of the power cable. The dimensions of the model as well as the properties of the chosen materials are therefore identical to that of medium voltage power cables used in the industry. Figure 3-1 illustrates the test object that will be used for the simulation purposes of the basic model. The test object consists of a conducting layer on either ends of the insulation material. The occurrence of PD will be due to a single void within the insulation material. The permittivity of XLPE will be used as the permittivity of the insulation material in order to accurately model the insulation of a medium voltage power cable.

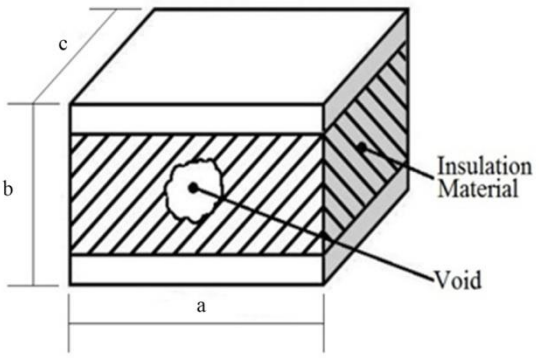

Figure 3-1: Test Object

A basic capacitor configuration can be derived from the test object to model the insulation material as well as the void. The capacitor configuration is shown in Figure 3-2. The insulation material of the test object is divided into three "zones" and each is associated with a specific capacitor. The "zones" are: the void, the insulation in the vicinity of the void and the rest of the healthy insulation.

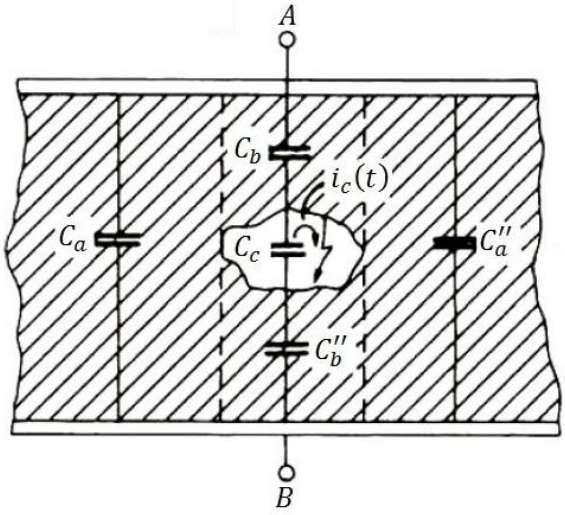

Figure 3-2: Capacitor Configuration [**38**]

The derived capacitor configuration forms a fundamental part of the circuit which will be used for the simulation of partial discharge activity. Figure 3-3 illustrates the complete circuit which will be used to design a MATLAB® Simulink® model for the simulation purposes of the basic three-capacitor model.

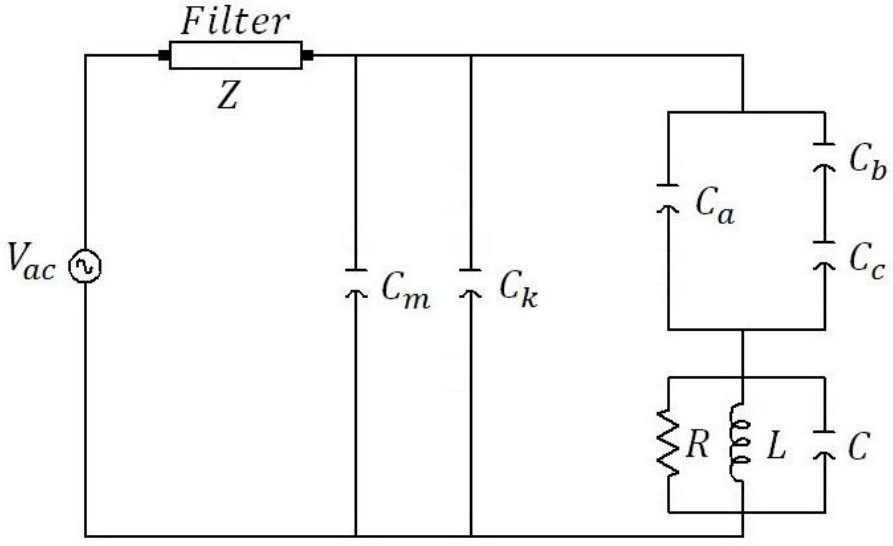

Figure 3-3: Derived circuit for basic model

The main component of this circuit is the test object consisting of the three capacitors, (C_c), (C_b) and (C_a). An equation for each of the three capacitors was derived; these equations are influenced by the permittivity of both free space and the insulation material, as well as the dimensions of the void. The void capacitor is denoted by (C_c), the capacitor associated with the insulation in the vicinity of the

void (C_b) and the capacitor for the rest of the healthy insulation is (C_a). The input impedance to which the measuring equipment will be connected is a parallel R-L-C branch. The wave shape of the PD pulse will be influenced by the input impedance of the circuit. The simulation model will also include a measuring (C_m) and coupling (C_k) capacitor. A high voltage filter (Z) is added to the circuit for the reduction of background noise, this will improve the accuracy of measurements obtained from this model.

3.2.3. Mathematical Model

The accuracy of both the simulation models will mainly depend on the derived equations for each. The equations will be derived by using basic principles of engineering and mathematics in order to ensure the validity of the derived models. The voltage across the capacitor associated with the void, (C_c), is given by:

$$V_c = \frac{V_a . C_b}{(C_a + C_b)} \tag{3.1}$$

An accurate measurement of the apparent charge for a test object is not possible and therefore it is important to be able to determine the apparent charge by means of an equation. The apparent charge can be calculated by means of the following equation:

$$q = C_b . V_{ac} \tag{3.2}$$

Pedersen developed a model which is based on the principle of induced charge. For the Pedersen model the apparent charge is given by [**39**]:

$$q = S \times V \times (E_i - E_l) \times \varepsilon_0 \times \varepsilon_r \times \Delta Z \tag{3.3}$$

where (S) is the void geometric factor and (V) the volume of the cylindrical void. The permittivity of free space and that of the insulation material is given by (ε_0) and (ε_r) respectively. The inception voltage for streamer inception is given by (E_i) and the limiting field for ionization by (E_l). The reciprocal of the distance between the two electrodes is denoted by: $\Delta Z(l/d)$, if:

$$E_l/p\ (air) = 24.2\ \text{v/pa. m} \tag{3.4}$$

By using equation (3.1) and the value for (E_l/p) calculated in equation (3.4), the value for ($E_i - E_l$) can be determined by means of the following equation:

$$\frac{E_i}{p} = \frac{E_l}{p}\left(1 + \frac{B}{\sqrt{2ap}}\right) \tag{3.5}$$

the constant characteristic of a gas in a void is given by (B) and the pressure of this gas is (p). The radius of the void is given by (a).

The most important equations for the basic three-capacitor model are the capacitor equations for the test object. For the basic three-capacitor model these equations will only be influenced by the permittivity of the insulation material, the permittivity of free space as well as the dimensions of the void. The capacitance value of the capacitor associated with the void is given by [**39**]:

$$C_c = \frac{\varepsilon_0 \times r^2 \times \pi}{h} \tag{3.6}$$

By making use of the dimensions of the void as well as the permittivity of free space and that of the chosen insulation material, the capacitance values for the insulation material close to the void and the rest of the healthy insulation can be calculated. The capacitance values for the two insulation "zones" are given by the following equations [**39**]:

$$C_a = \frac{\varepsilon_0 \times \varepsilon_r \times (a - 2b) \times b}{c} \tag{3.7}$$

$$C_b = \frac{\varepsilon_0 \times \varepsilon_r \times r^2 \times \pi}{h} \tag{3.8}$$

The equations discussed in this section of the dissertation will be used to determine the parameters of the basic-three capacitor model. The equations will also be used to analyse the simulation data in order to study the PD characteristics.

3.3. Comprehensive three-capacitor model

3.3.1. Introduction

As with the basic model, the simulations associated with the comprehensive model will also be based on the principle of deriving an electrical circuit from a cable model with a void within the insulation material. A number of parameters are added to the equations used for the basic model in order to achieve an improved accuracy for the comprehensive model. The comprehensive three-capacitor model has the advantage of improved accuracy, but also has some limitations in that it only simulates PD due to a single void within the insulation material and also does not consider the semiconducting layers of the power cable.

3.3.2. Modelling

Due to this being the comprehensive model a number of improvements are made in comparison with the basic model. Although both models have accurate dimensions, in regard to an actual power cable, the comprehensive model will more accurately resemble the physical cable. This is due to the fact that the model will consist of two cylindrical bodies resembling the cable conductor as well as the insulation material of the cable. The comprehensive model will also make use of a specific length of cable and not just a section of the insulation as with the basic model. Figure 3-4 shows the cross

sectional view of a power cable with a basic structure [**36**]. For the purpose of the simulations, only the cable conductor and insulation material will be considered. As with the basic simulation model, PD activity will be due to the single void within the insulation material of the power cable.

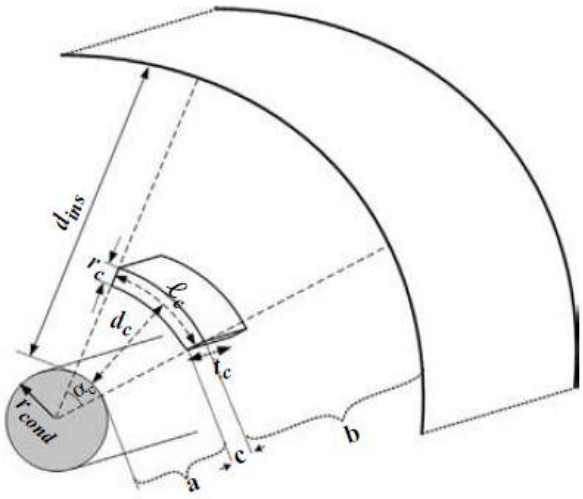

Figure 3-4: Cross sectional view of cable with void in insulation material [**36**]

The model illustrated in Figure 3-4 will be used to derive equations and an electrical circuit for the simulation of discharge activity. Due to the fact that the comprehensive model can be seen as an improved version of the basic model, the circuit will have a resemblance to the circuit used for the basic model. The derived circuit is shown in Figure 3-5; a voltage controlled switch will be used to initiate the occurrence of PD.

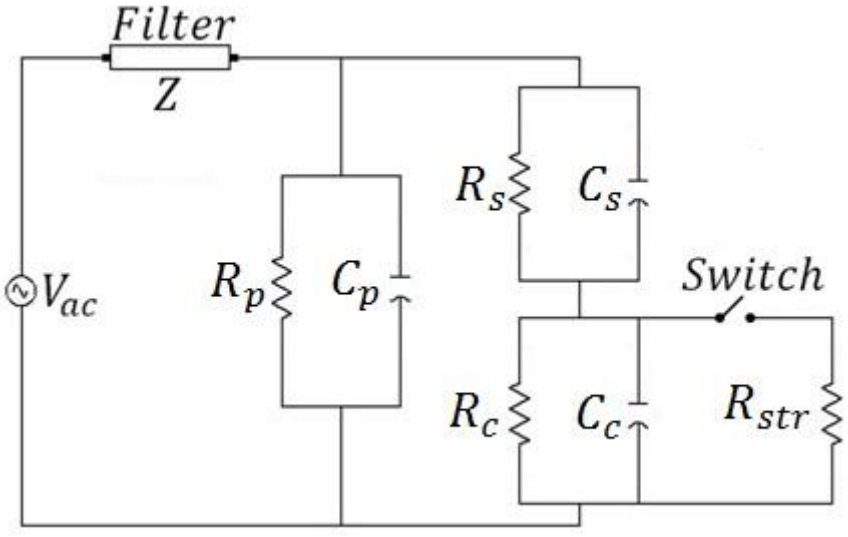

Figure 3-5: Derived circuit for comprehensive model

The circuit consists of nine basic elements. The capacitance value of the void capacitor (C_c) depends on the geometric parameters and the position of the void. The configuration of the electric field inside the void will also influence this capacitor, therefore it can be said that the permittivity of the enclosed gas will also affect the value of the void capacitor. The resistor associated with the void is (R_c) and

will represent properties of the void, including the internal surface condition. The capacitance value for the insulation close to the void is denoted by (C_s) and is affected by the same parameters as for the void capacitor (C_c). The resistance for the insulation close to the void is given by (R_s). This value is affected by the insulation loss factor $(\tan\delta)$ and will vary as the cable ages. For the rest of the healthy insulation, (C_p) is the equivalent capacitor and (R_p) the associated insulation resistor. The streamer resistance is denoted by (R_{str}) in the circuit and can be a linear time-invariant, linear time-varying or nonlinear resistor. The voltage-controlled switch will be closed as soon as the conditions for PD inception are met; this includes the voltage across the switch being equal or larger than the breakdown voltage. The switch will open if the voltage across it becomes lower than the residual voltage. The conditions for the switch to open or close will depend on the conditions of the void.

3.3.3. Mathematical Model

Gauss's law can be used to determine the voltage between surfaces of any two concentric cylinders [**40**]. Due to the physical structure of a power cable, as illustrated in Figure 3-4, this law can be applied to be able to determine various parameters of a power cable. If the two cylinders have radii of r_1 and r_2 respectively, the voltage can be determined by means of the following equation [**36**]:

$$\Delta V|_{r_1}^{r_2} = \int_{r_1}^{r_2} \frac{D(r)}{\varepsilon_{ins}} dr = \frac{q}{2\pi\varepsilon_{ins}} \ln\left(\frac{r_2}{r_1}\right) \tag{3.9}$$

the electric charge located on the surface of the conductor is given by (q). The capacitance per unit length for the insulation material between the two cylinders can be determined mathematically. This capacitance can also be determined for only a specific sector within the insulation material. If the arc of this sector is defined as (α_c), the capacitance can be determined by:

$$C_{sector} = \frac{q_{sector}}{\Delta V|_{r_1}^{r_2}} = \frac{q(\alpha_c/2\pi)}{\Delta V|_{r_1}^{r_2}} = \frac{\alpha_c \varepsilon_{ins}}{\ln(r_2/r_1)} \tag{3.10}$$

In order to determine the size of the angle (α_c), the length of the arc (l_c) is divided by the radius of the arc. The radius of the arc can be found by adding the radius of the conductor (r_{cond}) and the distance between the conductor and the centre of the void (d_c):

$$\alpha_c = \frac{l_c}{(r_{cond} + d_c)} \tag{3.11}$$

The insulation in the vicinity of the void can be divided into two zones: the zone between the void and the conductor, called zone "*a*" and the zone between the void and the outer layer of the insulation, called zone "*b*", as depicted in Figure 3-4.

The capacitances of these two regions can be determined for a length of (t_c), along the length of the cable, with the following two equations [**36**]:

$$C_a = \frac{\varepsilon_{ins}}{\ln\left(\left(r_{cond} + d_c - {}^{r_c}/_{2}\right)/r_{cond}\right)} \cdot \frac{l_c}{(r_{cond} + d_c)} \cdot t_c \tag{3.12}$$

$$C_b = \frac{\varepsilon_{ins}}{\ln\left((r_{cond} + d_{ins})/(r_{cond} + d_c + {}^{r_c}/_{2})\right)} \cdot \frac{l_c}{(r_{cond} + d_c)} \cdot t_c \tag{3.13}$$

The capacitance value of the insulation close to the void can thus be found as the equivalent series capacitance value of (C_a) and (C_b), therefore the equation can be written as:

$$C_s = \frac{C_a C_b}{C_a + C_b} \tag{3.14}$$

Based on equation (3.9) the capacitance value for the remaining healthy insulation (C_p) can be found as [**36**]:

$$C_p = \frac{2\pi\varepsilon_{ins}}{\ln\left((r_{cond} + d_{ins})/r_{cond}\right)} \cdot L \tag{3.15}$$

the length of the cable being used is given by (L). The capacitance value of the void (C_c) can be determined by using equation (3.10) and substituting the permittivity of the insulation material (ε_r) with the permittivity of free space (ε_0). Thus the capacitance of the void for a length of (t_c) can be written as [**36**]:

$$C_c = \frac{\varepsilon_0}{\ln\left(\left(r_{cond} + d_c + {}^{r_c}/_{2}\right)/\left(r_{cond} + d_c - {}^{r_c}/_{2}\right)\right)} \cdot \frac{l_c}{(r_{cond} + d_c)} \cdot t_c \tag{3.16}$$

Insulation resistance values are determined which are related to each of the three capacitor values. To be able to determine the insulation resistance of the volume, the relation between current density and associated electric field must be studied. The current density can be written as [**36**]:

$$J(r_2) = \frac{\sigma_{ins}}{e_{ins}} D(r_2) \tag{3.17}$$

the electric displacement field is given by (D) in equation (3.17). The related current, passing through the side surface of a cylinder with radius (r_2) can be determined. The current can also be determined for a sector with an arc of (α_c) and a length of (t_c) by means of:

$$I(r_2) = J(r_2).\alpha_c.r_2.t_c \tag{3.18}$$

This can then be used to determine the resistance value for the considered volume with the following equation:

$$R|_{r_1}^{r_2} = \frac{\Delta V|_{r_1}^{r_2}}{I(r_2)} = \frac{1}{\alpha_c}.\frac{1}{\sigma_{ins} t_c}.\ln\left(\frac{r_2}{r_1}\right) \tag{3.19}$$

Equation (3.19) can be used to derive equations for the resistance values of both zone "*a*" and zone "*b*". These equations can be written as [**36**]:

$$R_a = \frac{1}{\sigma_{ins}}.\frac{r_{cond} + d_c}{l_c t_c}.\ln\left(\frac{r_{cond} + d_c - r_c/2}{r_{cond}}\right) \tag{3.20}$$

$$R_b = \frac{1}{\sigma_{ins}}.\frac{r_{cond} + d_c}{l_c t_c}.\ln\left(\frac{r_{cond} + d_{ins}}{r_{cond} + d_c + r_c/2}\right) \tag{3.21}$$

A similar result is found when multiplying (C_a) from equation (3.12) to (R_a) and (R_b) from equation (3.13) to (R_b). This then confirms that (C_s) can be found by means of the equivalent series capacitance value of (C_a) and (C_b), as in equation (3.14). The resistance value of the insulation close to the void (R_s) can then also be found by the equivalent series resistance value of (R_a) and (R_b):

$$R_s = R_a + R_b \tag{3.22}$$

The resistance value of the healthy insulation (R_p) can be found by means of similar assumptions used to find the value of (C_p) [**36**]:

$$R_p = \frac{1}{2\pi L \sigma_{ins}}.ln\left(\frac{r_{cond} + d_{ins}}{r_{cond}}\right) \tag{3.23}$$

The resistance value associated with the void (R_c) can be found by using equation (3.19) and substituting the conductivity of the insulation (σ_{ins}) with the conductivity related to the void (σ_c). The equation can be written as [**36**]:

$$R_c = \frac{1}{\sigma_c}\frac{r_{cond} + d_c}{l_c t_c}\ln\left(\frac{r_{cond} + d_c + r_c/2}{r_{cond} + d_c - r_c/2}\right) \tag{3.24}$$

The electric field configuration due to the void has a significant influence on the model parameters and therefore some equations need to be corrected in order to compensate for the contribution of the electric field configuration. The determined value for the void capacitor by means of equation (3.16) is based on the assumption that the electric field, which is spread over the void and insulation, is homogeneous. Equation (3.16) further also only considers the permittivity of the void in order to be

able to model the contribution of the void [**36**]. Research conducted by Stratton [**41**] showed that the electric field inside a void will be amplified by a dimensionless factor (k_{ef}). According to Stratton this factor is determined by the following equation:

$$k_{ef} = \frac{\varepsilon_r}{\varepsilon_r + 2(1-\varepsilon_r) l_c . t_c . r_c . A} \tag{3.25}$$

If the void is considered to be spherical with a radius of (a), it can be determined that the area of this void will be:

$$A = \frac{1}{48a^3} \tag{3.26}$$

If the determined area of the void (A) is substituted into equation (3.25), the result is that the equation for (k_{ef}) becomes:

$$k_{ef} = \frac{3\varepsilon_r}{1 + 2\varepsilon_r} \tag{3.27}$$

This factor can then be used to improve the accuracy of the parameters associated with both the void as well as the insulation close to the void. The corrected capacitance value associated with the void can be written as [**36**]:

$$C_c^{cor} = k_{ef}^{-1} . \varepsilon_r . C_c \tag{3.28}$$

Due to the nature of equation (3.24), the contribution factor for the modified electric field will appear in both the nominator and denominator. For this reason there is no modification needed for (R_c). The presence of a void within the insulation material will cause the insulation material in the vicinity of the void to have a larger base surface. The enlarged base surface causes the complete volume to contain the same amount of field lines as inside the void. Thus the capacitance value for (C_s) as well as the resistance value (R_s), can be corrected by means of the following equations [**36**]:

$$C_s^{cor} = k_{ef} . C_s \tag{3.29}$$

$$R_s^{cor} = k_{ef}^{-1} . R_s \tag{3.30}$$

3.3.4. Switch Operation

The occurrence of PD will be regulated by means of a voltage-controlled switch, shown in Figure 3-5. The switch has an opening- and closing-mode, dependent on some parameters.

Closing mode

The voltage-controlled switch can be closed whenever the streamer can be started. Research from Niemeyer revealed that streamer inception is influenced by the possibility and/or probability of avalanche occurrence [**42**]. The breakdown voltage for a void filled with a non-attaching gas is given by:

$$V_b = \frac{\delta}{k_h}\left(2.1\sqrt{r_c} + 2.42 r_c\right) \tag{3.31}$$

where (k_h) is the correction factor related to humidity and (δ) the correction factor related to pressure and temperature [**34**]. The following equation can be used to determine (δ):

$$\delta = 295\frac{p}{T} \tag{3.32}$$

where (p) is the enclosed gas pressure and (T) the absolute cable temperature. The criterion for the switch to be closed can therefore be written as:

$$V_{C_C} \geq V_b \tag{3.33}$$

The above criterion is not the only necessary condition of the occurrence of PD. A probability function is used to model the presence of electrons with enough energy to activate the ionization process inside the void. The probability function is given by [**36**]:

$$P(t) = 1 - exp\left\{-\left[\frac{\ln\left(N_{surf}^{pu}\right).\Delta t^{pu}}{\alpha}\right]\right\} \tag{3.34}$$

where (N_{surf}^{pu}) is the value for the electron de-trapping rate and where the time delay after the voltage exceeds breakdown level is given by (Δt^{pu}). Both these variables are used as dimensionless per unit parameters.

The final step is to compare the probability value of equation (3.34) to a random number for stochastic time delays. If the random number is less than the probability function's value, the total PD inception condition is fulfilled and the switch will be closed.

Opening mode

Discharge extinction will occur once the voltage across the void falls below the threshold voltage [**43**]. The switch will be opened as soon as this happens. The threshold voltage is determined by means of [**36**]:

$$V_{res} = 2.42\frac{\gamma\delta}{kh}r_c \tag{3.35}$$

Research has shown that PD magnitude will increase when the temperature of the cable is elevated [**44**]. This is due to the fact that elevated temperatures will result in higher kinetic energy within the void, which allows for the streamer to be maintained during lower current values. The relation between PD magnitude and temperature can thus be investigated by a proper definition for the residual voltage dependency on temperature. This is possible by using (γ), given in equation (3.35), as a function of (T) in the following form [**36**]:

$$\gamma(T) = \gamma_0 - \frac{T}{T_0} \tag{3.36}$$

In this function the residual voltage will decrease more than the breakdown level if the temperature of the cable is elevated. The criterion for the switch to be opened can therefore be given by the following equation:

$$V_{C_C} \leq V_{res} \tag{3.37}$$

The equations used for the modelling of the comprehensive three-capacitor model are more complex than the equations used for the basic model. The complexity of the comprehensive models allows a variety of parameters to be altered and therefore the effect of each on PD activity can be studied.

3.4. Model Verification

The development of reliable and accurate simulation models is a critical component of the research project. The first step in assuring that the models are indeed accurate and reliable is to follow an effective verification procedure.

The main concern with verification of the simulation models is to determine whether the models were derived correctly. This is accomplished by determining if the input parameters and logical structure of the models are correctly represented. The verification process of the simulation models consists of four steps: 1) flow diagrams including each logically possible action, 2) model structure as self-documenting as possible, 3) print input parameters at end of simulations and 4) examine output parameters for reasonableness.

3.4.1. Flow Diagrams

The first step of the verification process was to create a flow diagram in order to explain the various components and logically possible actions of the simulation models, used to simulate PD activity in medium voltage XLPE cables.

The flow diagram shown in Figure 3-6 illustrates the various components of the basic simulation model. The flow diagram also indicates the logically possible actions of the basic model.

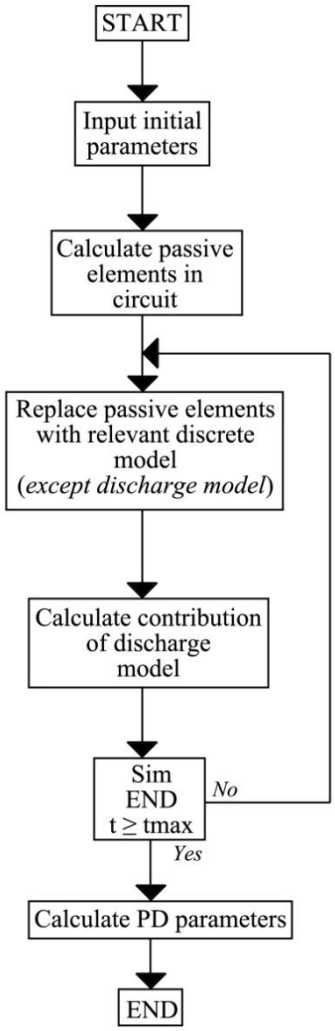

Figure 3-6: Flow diagram for the basic simulation model

The first step in the logical flow of the simulation program is to input the initial parameters. The simulation program then calculates the passive elements in the circuit. The simulation process is then started by replacing all the passive elements with relevant discrete models. The only exception is the discharge model which is not replaced with a discrete model. The contribution of the discharge model is then calculated and the simulation program determines if the simulation process has reached its end or not. The simulation program will return to step 3 if the simulation is still ongoing. The final logical step for the simulation program is to determine the PD parameters.

The flow diagram for the comprehensive model is shown in Figure 3-7. The Flow diagram of the comprehensive model shows similarities when compared to the flow diagram of the basic simulation model. The similarities are due to the fact that the comprehensive model is based on the basic simulation model.

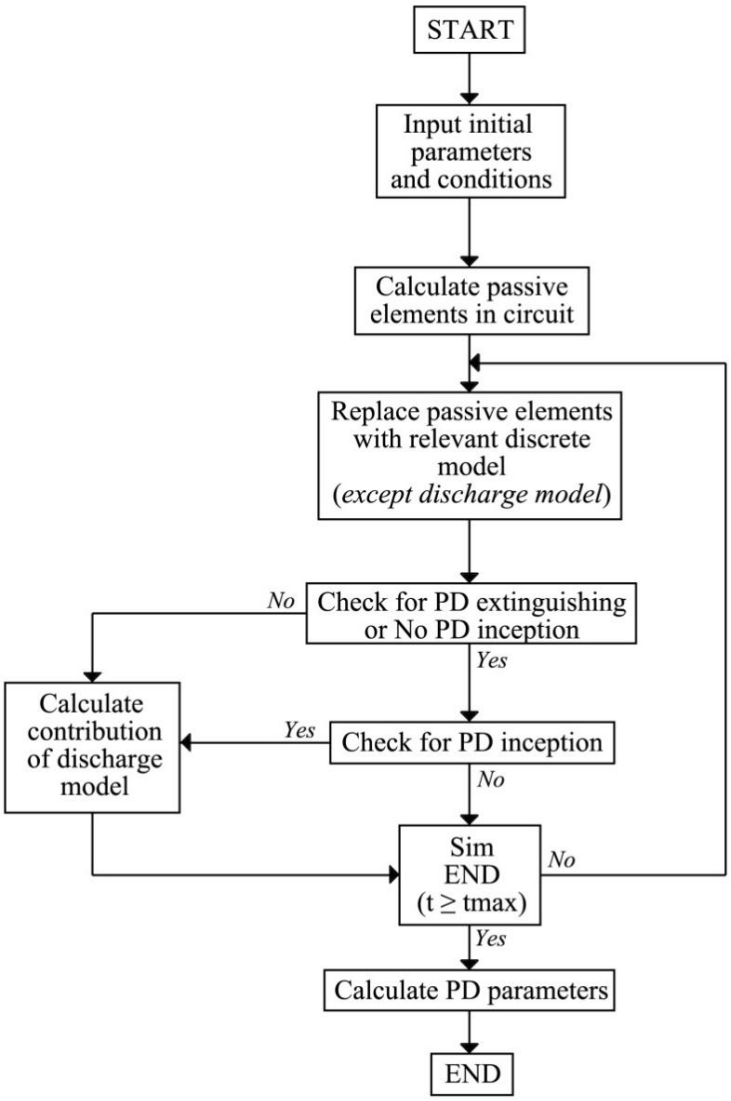

Figure 3-7: Flow diagram for comprehensive model

The first step of the simulation process is to input the initial parameters and conditions in the simulation model. The initial parameters were chosen to accurately represent a medium voltage XLPE cable. Datasheets of XLPE cables, included in the Data CD, were used to verify the accuracy of the chosen simulation parameters.

The next step of the simulation model is to calculate the values for all the passive elements in the circuit. The passive elements are then replaced with a relevant discrete model. The discharge model in the circuit is not replaced with a discrete model.

The simulation model then determines whether PD extinguishing or PD inception is present at this time of the simulation. If it is determined that PD extinguishing is present with no PD inception, the model determines the status of the simulation. If the end of the simulation is reached, the model calculates the PD parameters and terminates the simulation. In case of the simulation still in progress, the model returns to the step of replacing the passive elements in the circuit with a discrete model and continues with the simulation process.

In case no PD extinguishing is present and it is determined that PD inception is reached, the model calculates the contribution of the discharge model and proceed to determine the status of the simulation. The model continues with the process, if the simulation is still in progress, whereas the model calculates the PD parameters, if the end of the simulation is reached.

The flow diagram explains the process of simulating PD activity by means of the comprehensive simulation model and also discusses every possible logical action of the model. Examination of the flow diagram verifies that the model is correctly implemented for the specific purpose of simulating PD activity within the insulation material of a medium voltage XLPE cable.

3.4.2. Simulation model as self-documenting as possible

An important factor in the verification process of a simulation model is to create a model which is as self-documenting as possible. This includes a precise definition of each variable used and a general description of the functionality of each section of the simulation model.

The components and variables used for the basic and comprehensive simulation models are discussed in Section 4.2 and 4.3 respectively. The choice of initial parameters is defended by means of datasheets and engineering principles. The structure as well as parameters associated with the simulation models is based on fundamental theorems in physics and mathematics.

3.4.3. Print input parameters

Both the basic- and comprehensive simulation models were designed with a function to print the input parameters at the end of each simulation. This function is used to verify that all the chosen input parameters remains constant throughout each simulation. If the input parameters remain constant throughout a specific simulation it verifies that the simulation results are correct according to the initial setup of that specific simulation.

Three sets of simulations for each of the two simulation models were performed and the input parameters for the start and end of the simulations were printed out. The input and output parameters of the basic simulation model are given in Table 3-1 and that of the comprehensive simulation model in Table 3-2.

Table 3-1: Input and output parameters of basic model

	C_a		C_b		C_c		V_{ac} (kV)	
	Start	**End**	**Start**	**End**	**Start**	**End**	**Start**	**End**
Sim 1	3.04×10^{-12}	3.04×10^{-12}	9.80×10^{-14}	9.80×10^{-14}	3.70×10^{-14}	3.70×10^{-14}	6.6	6.6
Sim 2	2.81×10^{-12}	2.81×10^{-12}	2.20×10^{-13}	2.20×10^{-13}	8.34×10^{-14}	8.34×10^{-14}	6.6	6.6
Sim 3	2.34×10^{-12}	2.34×10^{-12}	6.13×10^{-13}	6.13×10^{-13}	2.31×10^{-13}	2.31×10^{-13}	6.6	6.6

Table 3-2: Input and output parameters of comprehensive model

	C_p		C_s		C_c		V_{in} (kV)	
	Start	**End**	**Start**	**End**	**Start**	**End**	**Start**	**End**
Sim 1	22.53	22.53	2.3×10^{-3}	2.3×10^{-3}	2.77×10^{-14}	2.77×10^{-14}	11	11
Sim 2	18.23	18.23	5.9×10^{-3}	5.9×10^{-3}	6.93×10^{-14}	6.93×10^{-14}	11	11
Sim 3	28.64	28.64	10.6×10^{-3}	10.6×10^{-3}	1.25×10^{-13}	1.25×10^{-13}	11	11

Examination of the Tables leads to the verification that the input parameters for both simulation models remained constant throughout the sets of simulations. This then verifies that the simulations are correctly performed, as implemented in the computer, for the entire simulation period.

3.4.4. Examine output for reasonableness

An important aspect of the verification process of a simulation model is to check the output for reasonableness. The reasonableness of the output from both simulation models were checked by means of comparing the simulation results to published research. Information from the literature study was also used to verify the reasonableness of the simulation results. For the purpose of verification only the output results were checked for reasonableness. For this reason the magnitudes of the output parameters were compared to other simulation models in order to investigate the deviation. A more in depth comparison to other simulation models as well as actual PD data was used for the validation of the simulation models.

The output parameters of the simulation models, discussed in Table 3-1 and Table 3-2, verify that the output parameters of both simulation models show minimum deviation from established PD knowledge. The conclusion can thus be made that the simulation models were correctly implemented for the simulation of PD activity within medium voltage XLPE cables.

3.4.5. Conclusion

The verification process of the simulation models were based on four steps. The outcome of these steps were used to verify that the models were correctly and accurately implemented for the simulation of PD activity within the insulation material of a medium voltage XLPE cable. The next important step is to analyse the simulation results in order to validate the simulation models. The verification and validation of the simulation models are two important steps in order to prove the accuracy and suitability of the derived models.

The models discussed in this chapter are used to simulate the occurrence of partial discharge within the insulation material of a medium voltage XLPE cable. For both derived models the discharge activity is due to a single void. The main objective was to be able to derive models which will accurately represent actual equipment. The simulations play a vital role in the understanding of the phenomenon known as PD. The simplicity of the basic model resulted in the model lacking the accuracy of the comprehensive model.

Chapter 4 Simulation Results

Simulations performed by means of the derived models are discussed within this chapter. The simulations were performed in order to study the effect of various parameters on the measured PD signal. The verification process of the simulation models is based on a three step procedure with the main focus on determining whether the model is an accurate representation of the actual system. Parameters for all the simulations were chosen in order to realistically represent an electrical cable as well as the surrounding environment of the cable.

4.1. Introduction

The simulations were performed in the MATLAB® Simulink® environment. The equations as well as the derived PD circuits discussed in Chapter 3 were used to construct the MATLAB® Simulink® models. Two models were constructed:

1) The basic three-capacitor simulation model and
2) The comprehensive three-capacitor simulation model.

Data from the simulations were exported to a number of MATLAB® workspaces in order to study the correlation between the measured PD signal and various parameters of the models. The results obtained from the two simulation models were compared to previous research in order to verify the accuracy of the output result of both models.

4.2. Basic three-capacitor model

4.2.1. Introduction

The MATLAB® Simulink® model for the basic three-capacitor configuration focuses mainly on the parameters of the void and the influence of these parameters on the discharge activity within the electrical cable. Results obtained from the various simulations were exported to a MATLAB® workspace in order to investigate the effect of specific individual parameters. The simulated data was also compared with experimental data, where possible.

4.2.2. MATLAB® Simulink® model

The MATLAB® Simulink® model for the basic three-capacitor simulations is shown in Figure 4-1. The PD signal is measured by means of a voltage measurement block (V_{pd}), connected across the RLC branch. The data obtained from this signal is exported to a workspace in order to analyse the PD data. The voltage across the test object is measured in order to be able to mathematically determine the value of the apparent charge. This is done by means of the voltage measurement block (V_C), of which the data is also exported to a workspace for analysis. The results obtained from the numerous simulations will be analysed in order to determine the correlation between the parameters of the simulation model and the effect of these parameters on the PD signal.

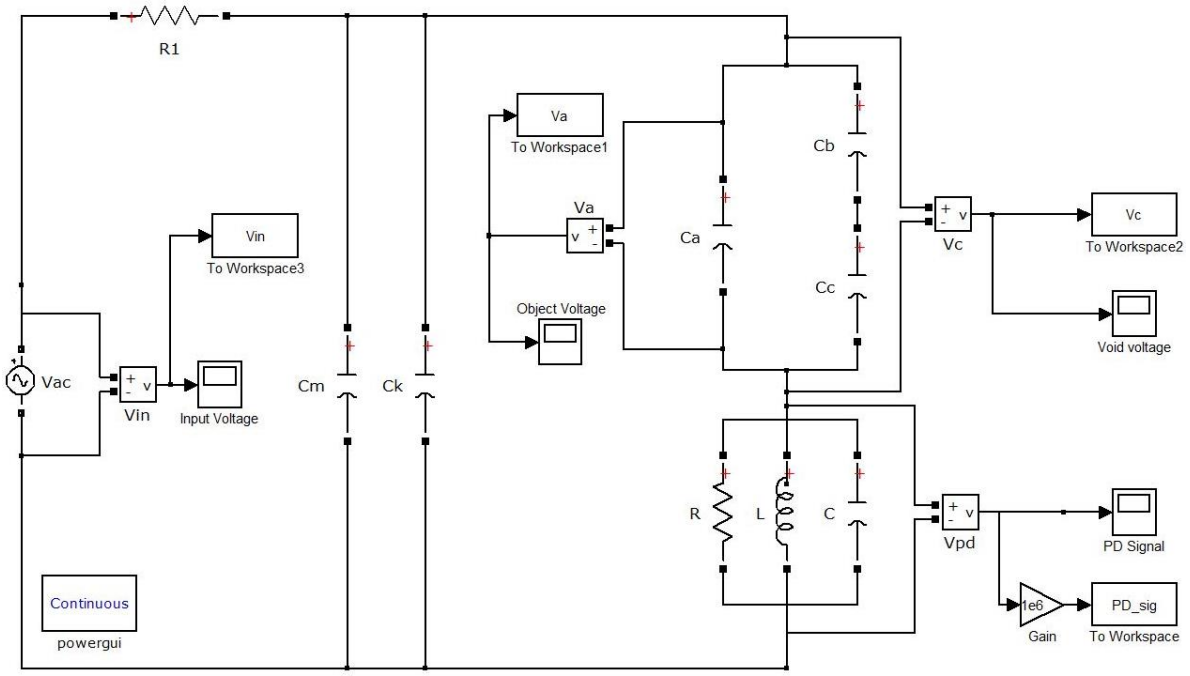

Figure 4-1: Basic three-capacitor simulation model

A set of standard parameters are used for all the simulations of the basic three-capacitor model. These parameters are given in Table 4-1. Specific parameters will be changed for certain simulations in order to be able to investigate their effect on the measured PD signal.

Table 4-1: Parameters used for the basic three-capacitor simulation model

Parameter	**Symbol**	**Value**
Test object length	a	30 mm
Test object width	b	30 mm
Test object height	c	6 mm
Relative permittivity of XLPE	ε_r	2.645 $F.m^{-1}$
Permittivity of free space	ε_0	$8.854x10^{-12}$ $F.m^{-1}$
Void radius	r	1 mm
Void height	h	3 mm

4.2.3. Simulations

The first simulation was performed with only the standard parameters given in Table 4-1. Figure 4-2 illustrates the measured PD signal.

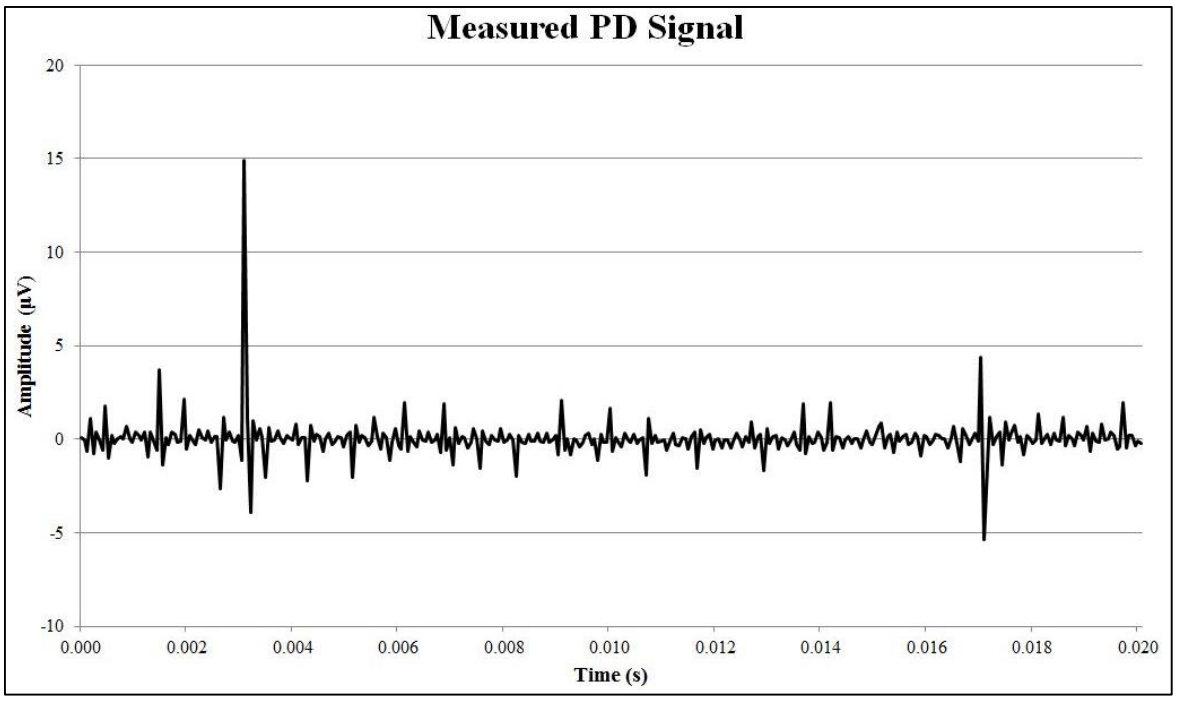

Figure 4-2: Simulated PD Signal

The input voltage was set to 6.6 kV and the PD signal was recorded for only one cycle (0.02 s) of the input signal. The signal shown in Figure 4-2 is a filtered signal and the removal of the 50 Hz component allows for only the PD data to be studied. The maximum amplitude of the simulated PD signal is 14.47 μV.

The simulated PD signal shown in Figure 4-2 was compared to a number of published research sources. The sources included PD signals obtained from practical as well as simulation data. The signal illustrated in Figure 4-3 was published in the work of Sabat and Karmakar [**39**].

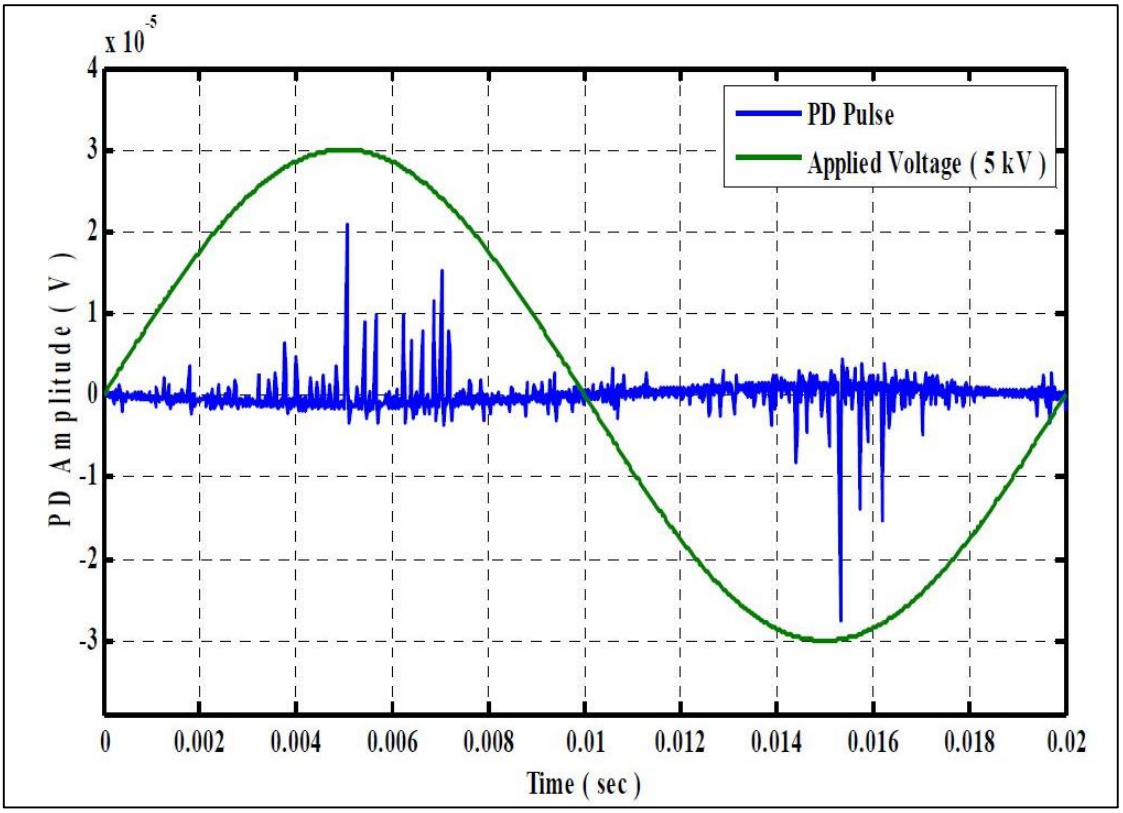

Figure 4-3: Simulated PD signal at 5 kV input voltage [**39**]

From Figure 4-3 it can be seen that the maximum amplitude for the PD signal is 20.9 µV. The maximum amplitude for the PD signal simulated by means of the basic simulation model is 14.47 µV. The two signals not only show similarities between the maximum amplitude of the PD signal, but also show similarities in waveform. The minor deviations between the two signals can be attributed to a difference in initial parameters.

A set of simulations was performed in order to study the effect of the input voltage on the maximum magnitude of the PD signal. For these simulations a constant void size was used and the input voltage varied between the values of 7 kV and 50 kV. The graph depicted in Figure 4-4 shows the results obtained from this set of simulations.

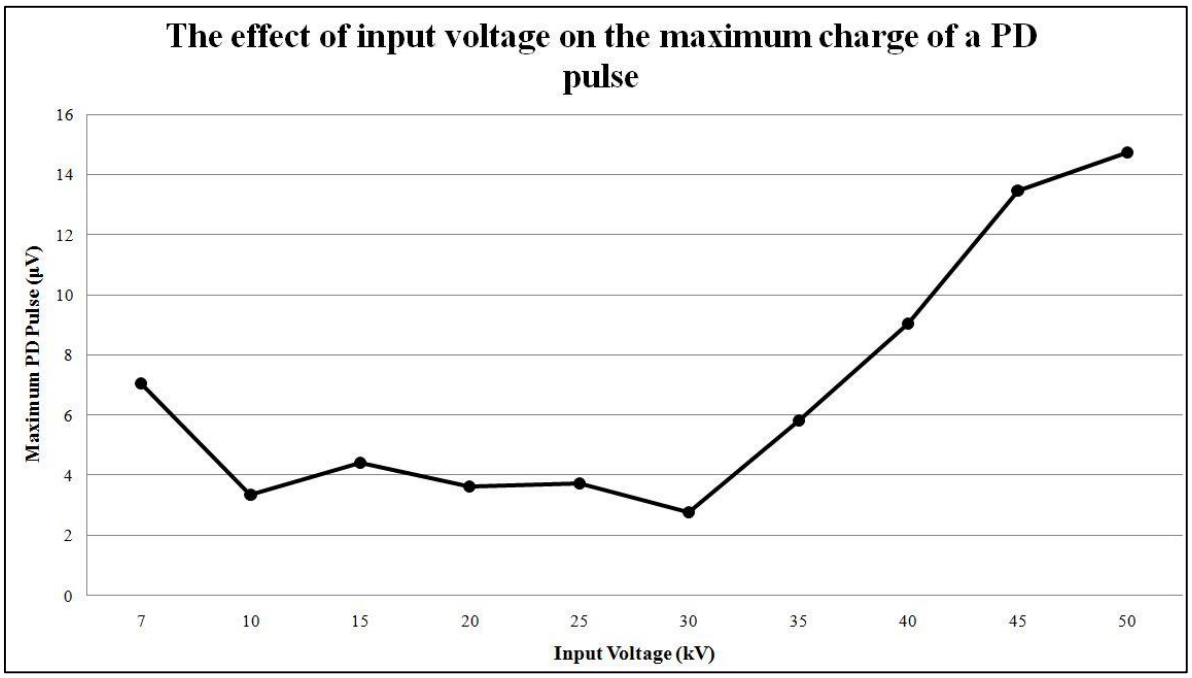

Figure 4-4: The effect of input voltage on the maximum PD pulse

From the graph it can be seen that an unusual high value of PD magnitude is present for the input voltage of 7 kV. For the values of the input voltage between 10 kV and 30 kV the resulting PD magnitude varies between 2 µV and 5 µV. As the input voltage increases beyond the 30 kV point, it is clear that the maximum amplitude for the PD signal also increases. From this the conclusion can be made that although the maximum PD magnitude will remain relatively constant over a range of input voltages, the overall effect of an increase in input voltage is increased values for the maximum amplitude of the PD signal.

The effect of the input frequency on the apparent charge of the PD signal was also studied by means of a set of simulations. Previous research showed that for input frequencies below the normal 50 Hz there was no trend in the resulting PD characteristics. This is due to the fact that at frequencies below 50 Hz, the PD characteristics were equally similar and different when compared to the PD characteristics at the standard 50 Hz operating frequency [**45**]. For this reason frequencies below the operating frequency of 50 Hz were ignored for these simulations.

For the simulations, used to study the effect of input frequency, a constant void size was used and the input voltage was also kept constant at 6.6 kV. The input frequency was increased by 50 Hz increments from the starting value of 50 Hz to the final value of 400 Hz. The simulation results are given by means of a graph shown in Figure 4-5.

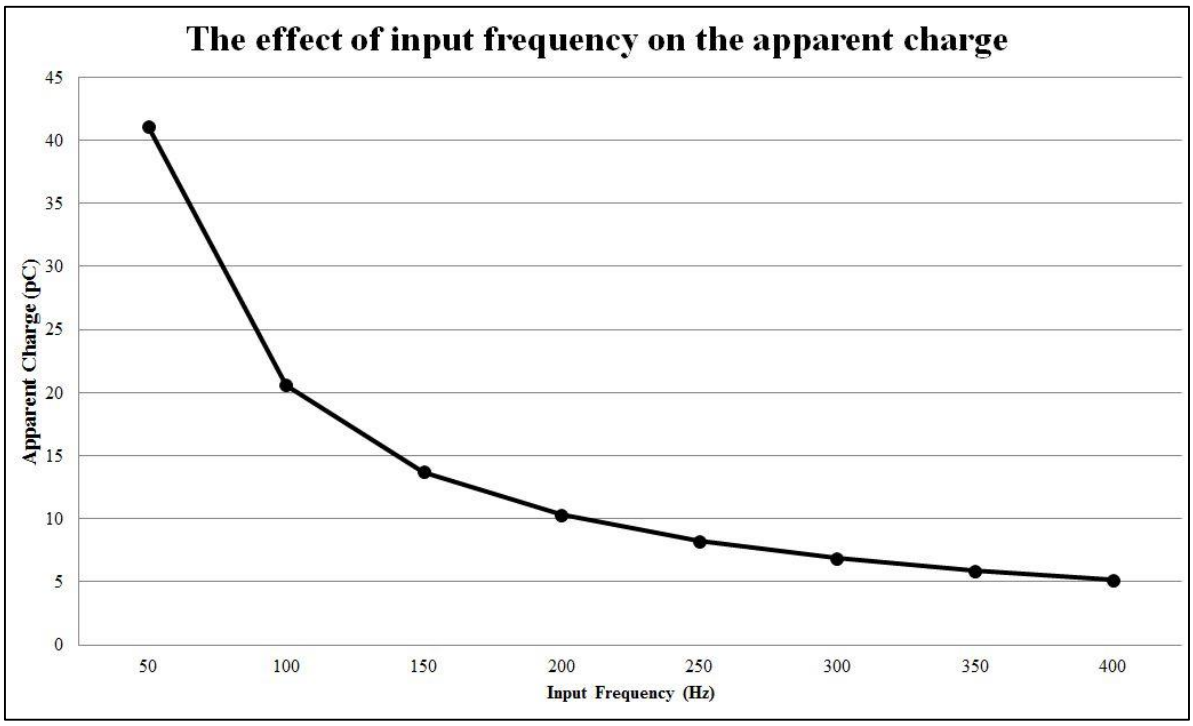

Figure 4-5: The effect of input frequency on the apparent charge

It can be seen that the input frequency has a definite effect on the resulting apparent charge of the PD signal. As the operating frequency is increased beyond the normal 50 Hz, the apparent charge, of the measured PD signal, decreases. The input frequency also affects other PD characteristics such as the PD inception voltage, the magnitude of the PD signal and the rise and fall times. Work done by C. Nyamupangedengu and I.R. Jandrell discuss the effect of the input frequency on PD characteristics in detail [**45**].

The final set of simulations was performed in order to study the correlation between the void size and the apparent charge of the PD signal. For this set of simulations the input voltage was kept constant and the volume of the void varied in size. The void dimensions included a constant height of 3 mm and the radius of the void was incremented in sizes of 0.5 mm from 1 mm to 5 mm. Due to the fact that for these simulations the void parameters varied for each individual simulation, the values for the three capacitors of the test object will also vary.

Table 4-2 shows the values for the void volume and the resulting values for the three capacitors for each simulation.

Table 4-2: Parameters for void volume and resulting capacitor values

Void Volume (mm^3)	**Ca (pF)**	**Cb (pF)**	**Cc (pF)**
9.425	3.2786	0.024524	0.0092719
21.206	3.1615	0.055179	0.020862
37.699	3.044	0.098097	0.037088
58.905	2.9274	0.15328	0.057949
84.823	2.8103	0.22072	0.083447
115.454	2.6932	0.30042	0.11358
150.796	2.5761	0.39239	0.14835
190.852	2.4590	0.49661	0.18776
235.619	2.3419	0.61310	0.23180

The values of the three capacitors shown in Table 4-2 were used for the simulations in order to study the effect of the void size on the apparent charge of the measured PD signal. Due to the fact that it is impossible to measure the apparent charge directly from the MATLAB® Simulink® model, equation (3.2) in Chapter 3 was used to mathematically determine the value of the apparent charge for each simulation.

Figure 4-6 illustrates the correlation between void size and apparent charge in the form of a line graph.

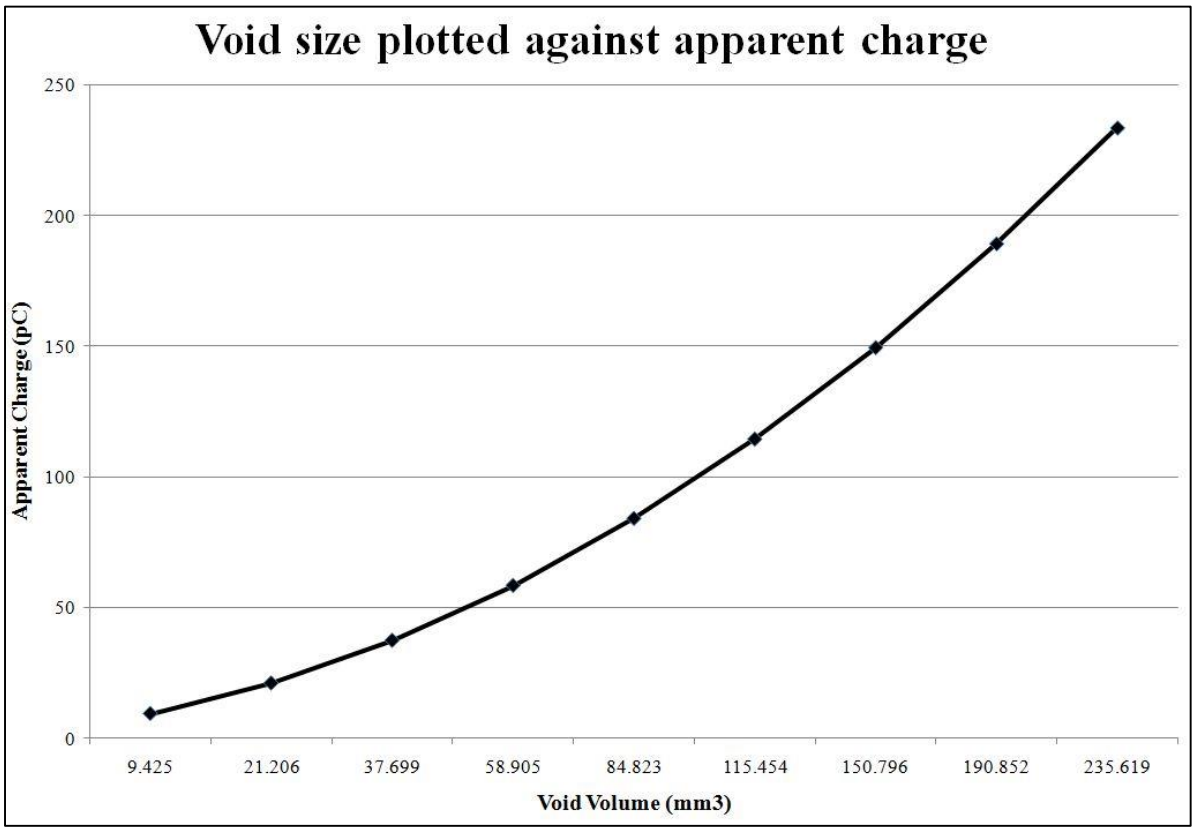

Figure 4-6: The influence of void volume on the value of the apparent charge

The values illustrated in Figure 4-5were used to determine the increments between the values of the void volume and the increments between the values of the apparent charge of the PD signal. The determined values are shown in Table 4-3.

Table 4-3: Increment values of void volume and apparent charge

Increments in void volume (mm^3)	**Increments in apparent charge (pC)**
11.781	11.684
16.493	16.361
21.206	21.032
25.918	25.711
30.631	30.383
35.343	35.060
40.055	39.730
44.768	44.400

The increments of the void volume and the apparent charge were used to graph the influence of the void size on the apparent charge of the PD signal. The results are shown in the graph depicted in Figure 4-7.

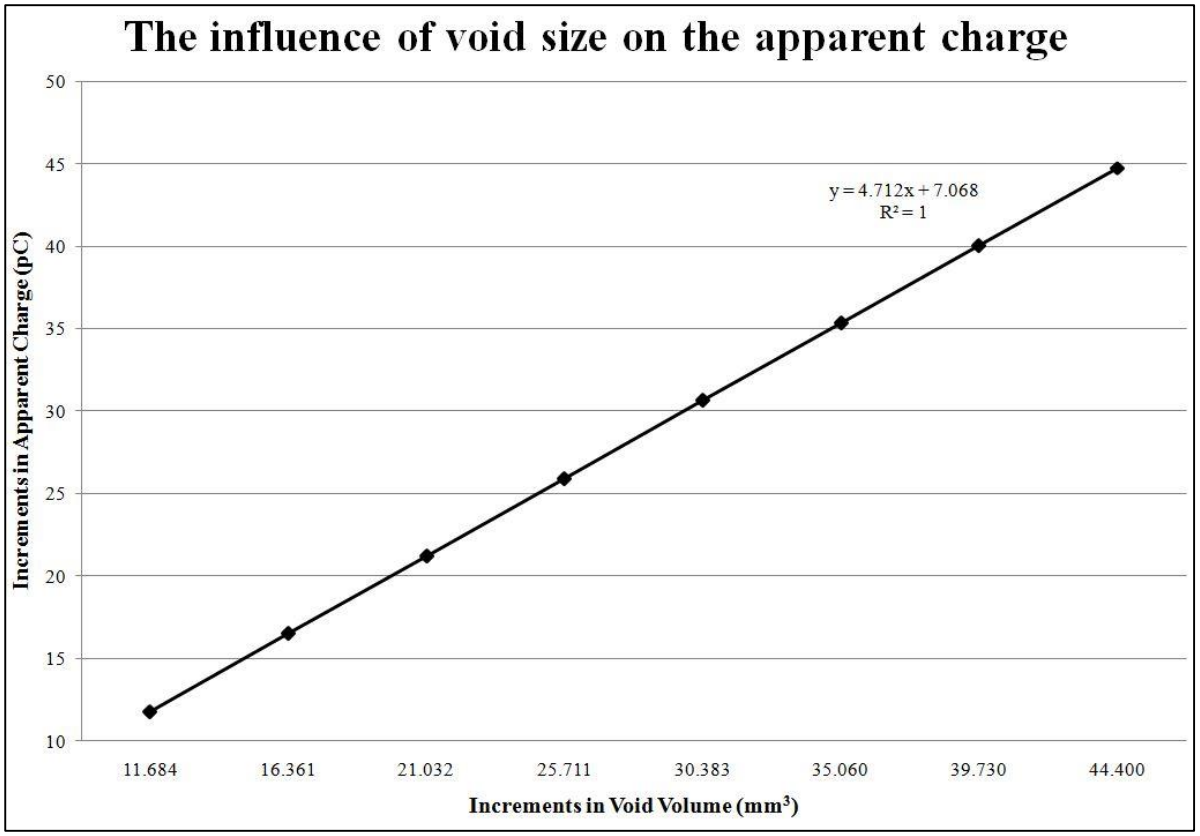

Figure 4-7: The influence of void size on the apparent charge

A study of the results shown in Figure 4-7 leads to the conclusion that the correlation between the volume of the void and the apparent charge of the measured PD signal is linear. From the figure it can be seen that the coefficient of determination, the R^2 value, of the trendline is equal to 1. Due to the fact that this value is equal to 1, it can be said that the assumed trendline or fitted trendline is an identical representation of the actual values. The conclusion can thus be made that a void with a larger volume will lead to an increase in apparent charge and in turn will cause more severe PD activity within the cable. The mathematical equation for the trendline, $y = 4.712x - 7.068$, can be used along with the determined value of the apparent charge to be able to determine an approximate value for the volume of the void within the insulation material of the cable.

4.3. Comprehensive three-capacitor model

4.3.1. Introduction

The MATLAB® Simulink® model for the comprehensive three-capacitor analysis of PD is, as with the basic model, also based on the well-known representation of a defect within the insulation material of a cable, developed by Germant and Philipoff in 1932 [**36**]. The comprehensive model can be seen as an improved version when compared to the basic model as it not only considers the geometric properties of the void. The comprehensive model is also capable of handling different positions of the void within the insulation material and also takes into consideration the congestion of electric field lines while passing through the void. The comprehensive MATLAB® Simulink® model was used to perform a number of simulations in order to study a variety of PD characteristics.

4.3.2. MATLAB® Simulink® model

The comprehensive three-capacitor model requires more initial parameters and results in a more complex MATLAB® Simulink® model. This model will also represent the occurrence of PD activity within electrical cables more accurately. Figure 4-8 illustrates the MATLAB® Simulink® model used for the comprehensive simulations.

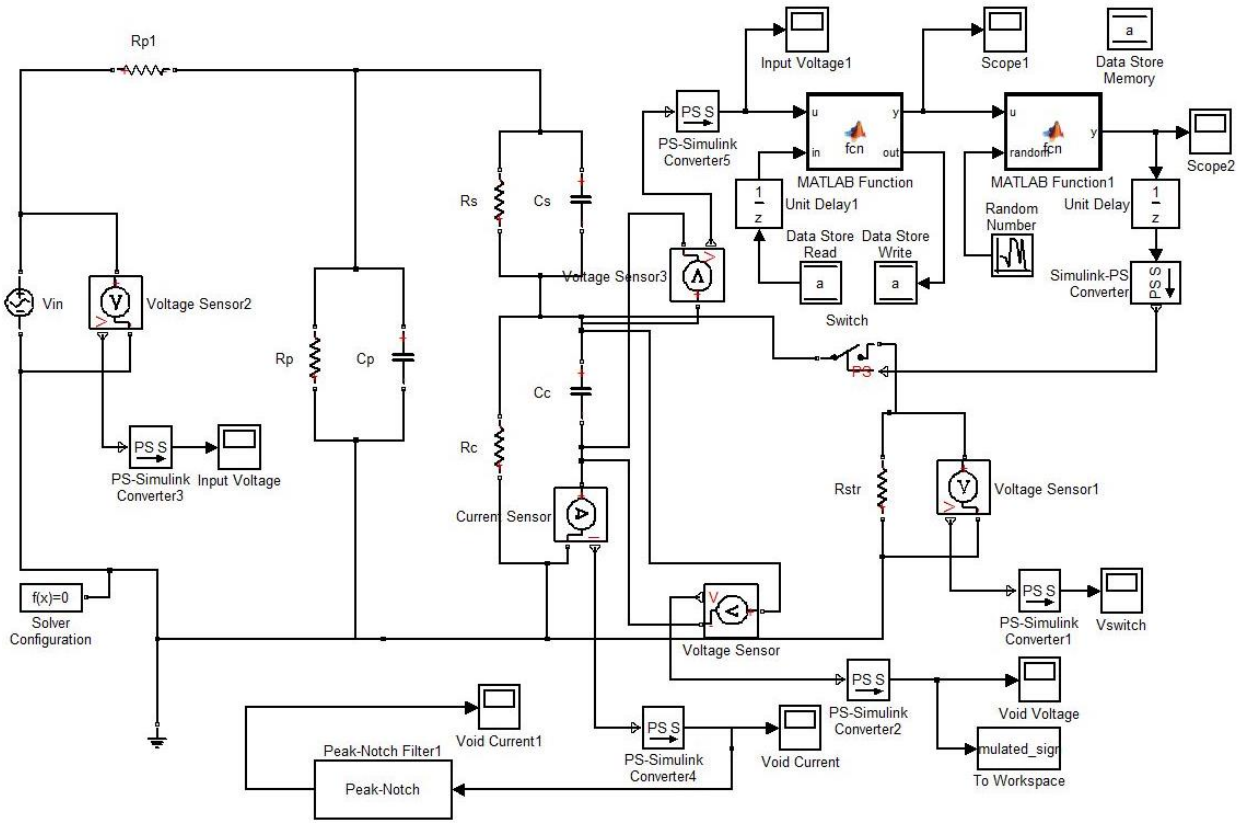

Figure 4-8: Comprehensive three-capacitor MATLAB® Simulink® model

From Figure 3-4 it is evident that the standard void shape is not cylindrical as with the simulations from the basic three-capacitor model. It is however possible to convert the dimensions of a non-cylindrical void to the basic cylindrical shape [**36**]. Consider the cylinder shown in Figure 4-9.

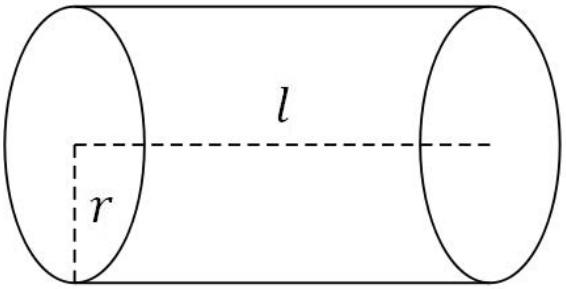

Figure 4-9: Representation of cylindrical void

If the assumption is made that the cylindrical void, with a radius (r) and length (l), has a uniform electric field (E_c), the surface area for $(d\theta)$ can be defined as [**36**]:

$$dA(\theta) = lrd\theta \tag{4.1}$$

Considering the fact that the cylindrical void will act as a capacitor, the effective area and the distance of the two plates of the capacitor are given by:

$$dA_{eff}(\theta) = dA(\theta).\cos\theta = \ lr\cos\theta\,.d\theta \tag{4.2}$$

$$d(\theta) = 2r\cos\theta \tag{4.3}$$

The electric charge of this capacitor can therefore be calculated by means of the following equation:

$$dQ(\theta) = dC(\theta).V(\theta) = dC(\theta).E_c.d(\theta) = \ \varepsilon E_c lr\cos\theta.d\theta \tag{4.4}$$

The total charge can then be obtained by integration of equation (4.4), as follows:

$$Q_{total} = \int_{-\pi/2}^{\pi/2} dQ(\theta) \tag{4.5}$$

The relation between the voltage across the void and the electric field can be expressed by means of the following equation:

$$E_c = \frac{V_d}{2r} \tag{4.6}$$

The capacitance of the void can thus be determined by making use of equations (4.5) and (4.6):

$$C_{total} = \varepsilon L = \ \varepsilon\frac{2rl}{2r} \tag{4.7}$$

From this the dimensions of a cylindrical void can be converted to that of the standard void shape by means of the following equations [**36**]:

$$t_c = l \tag{4.8}$$

$$l_c = r_c = 2r \tag{4.9}$$

This then allows for the exact same void dimensions to be used for both the basic and comprehensive simulation models. Table 4-4 shows the parameters and their values, which were used for the comprehensive three-capacitor MATLAB® Simulink® model.

Table 4-4: Parameters used for comprehensive model simulations

Parameter	**Symbol**	**Value**
Height of void	r_c	2 mm
Length of void	l_c	2 mm
Width of void	t_c	3 mm
Length of cable	L	1 m
Radius of conductor	r_{cond}	5.5 mm
Insulation thickness	d_{ins}	6 mm
Distance from conductor to centre of void	d_c	3 mm
Relative permittivity of insulation (XLPE)	ε_r	2.645 $F.m^{-1}$
Relative permittivity of free space	ε_0	8.854×10^{-12} $F.m^{-1}$
Conductivity of insulation	σ_{ins}	7×10^{-17} $mho.m^{-1}$
Conductivity of void (air)	σ_c	1×10^{-8} $mho.m^{-1}$
Correction factor related to humidity	k_h	1
Enclosed gas pressure	p	0.2 bar
Cable absolute temperature	T	315 K
Weibull parameters	$\alpha,\ \beta$	$\alpha = 120, \quad \beta = 0.63$

4.3.3. Simulations

The comprehensive three-capacitor MATLAB® Simulink® model allows the user to investigate various characteristics of the measured PD signal, such as: apparent charge, maximum amplitude as well as rise and fall times of the PD signal. The first simulation was performed with the parameters given in Table 4-4. The measured signal is illustrated in Figure 4-10.

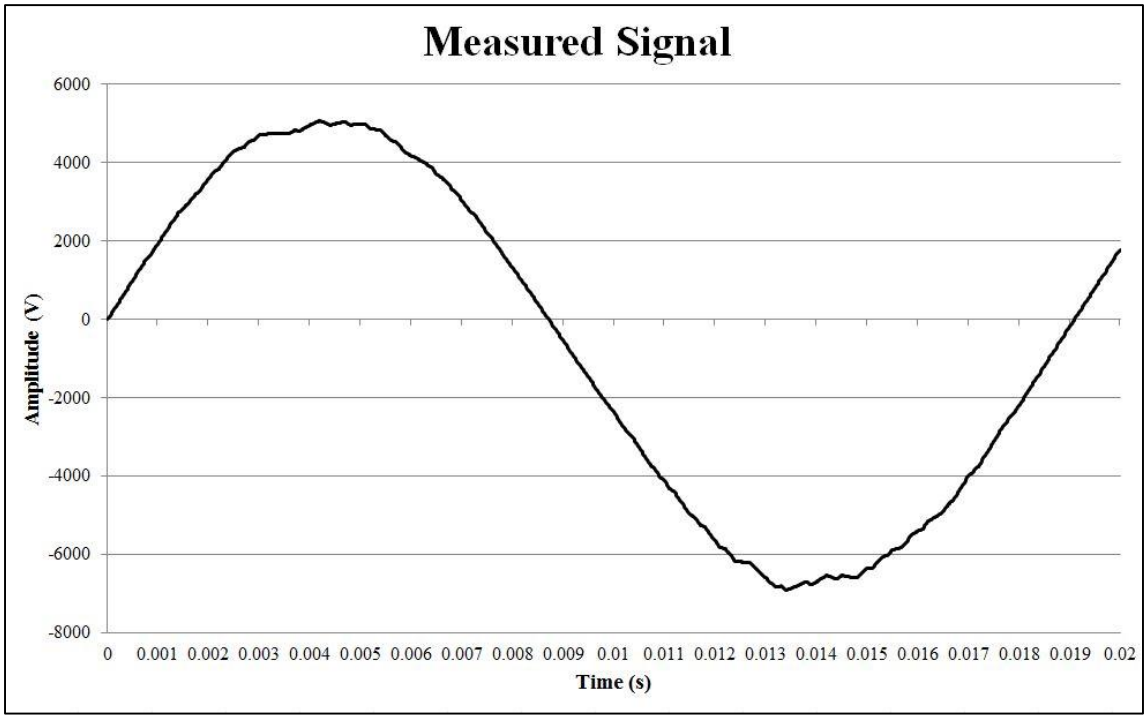

Figure 4-10: Simulated signal

Figure 4-11 shows enlarged areas of the measured signal given in Figure 4-10. The area surrounding the maximum values for both the positive and negative half cycles were enlarged. The enlarged figures offer a better view of the discharge activity.

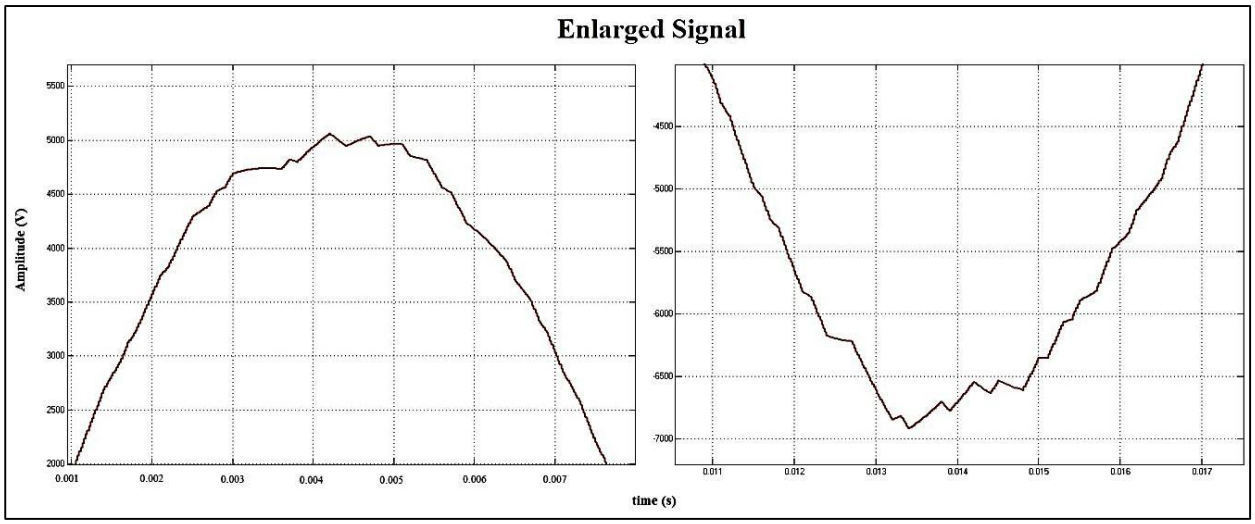

Figure 4-11: Enlarged regions of the measured signal

The basic three-capacitor model was used to investigate the effect of void size on the apparent charge of the PD signal. The comprehensive model allows for the position of the void, within the insulation material, to be altered and therefore will be used to study the effect of both the size of the void as well as the position of the void on the apparent charge of the PD signal. Three different void positions were used with the same set of values for the size of the void. The three positions included: a void close to the conductor of the cable, a void in the middle of the insulation material and also a void near the outer sheath of the cable. The positions of the void were calculated as follows [**36**]:

$$\text{Near the conductor:} \qquad d_c = 0.15 d_{ins} \tag{4.10}$$

$$\text{Middle of insulation:} \qquad d_c = 0.5 d_{ins} \tag{4.11}$$

$$\text{Near the sheath:} \qquad d_c = 0.85 d_{ins} \tag{4.12}$$

The length of the void (l_c) was incremented from 1 mm to 5 mm while both the height (r_c) and width (t_c) were kept constant. The first set of simulations was performed with a void in the middle of the insulation material of the cable. Table 4-5 shows the values for the volume of the void as well as the calculated values for the three capacitors.

Table 4-5: Parameters for void in the middle of the insulation

$\boldsymbol{d_c = 0.5 d_{ins}}$						
$\boldsymbol{r_c\ (mm)}$	$\boldsymbol{l_c\ (mm)}$	$\boldsymbol{t_c\ (mm)}$	$\boldsymbol{Volume\ (mm^3)}$	$\boldsymbol{C_c\ (pF)}$	$\boldsymbol{C_p\ (F)}$	$\boldsymbol{C_s\ (F)}$
2	1	3	2.36	0.0277	22.5312	0.0023
2	1.5	3	5.30	0.0416	22.5312	0.0035
2	2	3	9.42	0.0554	22.5312	0.0047
2	2.5	3	14.73	0.0693	22.5312	0.0059
2	3	3	21.21	0.0832	22.5312	0.007
2	3.5	3	28.86	0.0970	22.5312	0.0082
2	4	3	37.70	0.111	22.5312	0.0094
2	4.5	3	47.71	0.125	22.5312	0.0106
2	5	3	58.90	0.139	22.5312	0.0117

The second set of simulations was performed with the void close to the conductor of the cable. The simulation parameters are shown in Table 4-6.

Table 4-6: Parameters for void close to conductor

$d_c = 0.15d_{ins}$						
$r_c\ (mm)$	$l_c\ (mm)$	$t_c\ (mm)$	$Volume\ (mm^3)$	$C_c\ (pF)$	$C_p\ (F)$	$C_s\ (F)$
2	1	3	2.36	0.0276	22.5312	0.0037
2	1.5	3	5.30	0.0414	22.5312	0.0056
2	2	3	9.42	0.0552	22.5312	0.0074
2	2.5	3	14.73	0.0690	22.5312	0.0093
2	3	3	21.21	0.0829	22.5312	0.0111
2	3.5	3	28.86	0.0967	22.5312	0.013
2	4	3	37.70	0.110	22.5312	0.0148
2	4.5	3	47.71	0.124	22.5312	0.0167
2	5	3	58.90	0.138	22.5312	0.0185

The final position of the void was chosen to be near the outer sheath of the cable. Table 4-7 shows the parameters used for this set of simulations.

Table 4-7: Parameters for void near outer sheath

$d_c = 0.85d_{ins}$						
$r_c\ (mm)$	$l_c\ (mm)$	$t_c\ (mm)$	$Volume\ (mm^3)$	$C_c\ (pF)$	$C_p\ (F)$	$C_s\ (F)$
2	1	3	2.36	0.0278	22.5312	0.0017
2	1.5	3	5.30	0.0416	22.5312	0.0026
2	2	3	9.42	0.0555	22.5312	0.0034
2	2.5	3	14.73	0.0694	22.5312	0.0043
2	3	3	21.21	0.0833	22.5312	0.0052
2	3.5	3	28.86	0.0972	22.5312	0.0060
2	4	3	37.70	0.111	22.5312	0.0069
2	4.5	3	47.71	0.125	22.5312	0.0077
2	5	3	58.90	0.139	22.5312	0.0086

The values given in the three tables were used to perform the simulations required for the investigation of the effect of size and position of the void on the apparent charge of the PD signal. The results obtained from these simulations are shown in Figure 4-12.

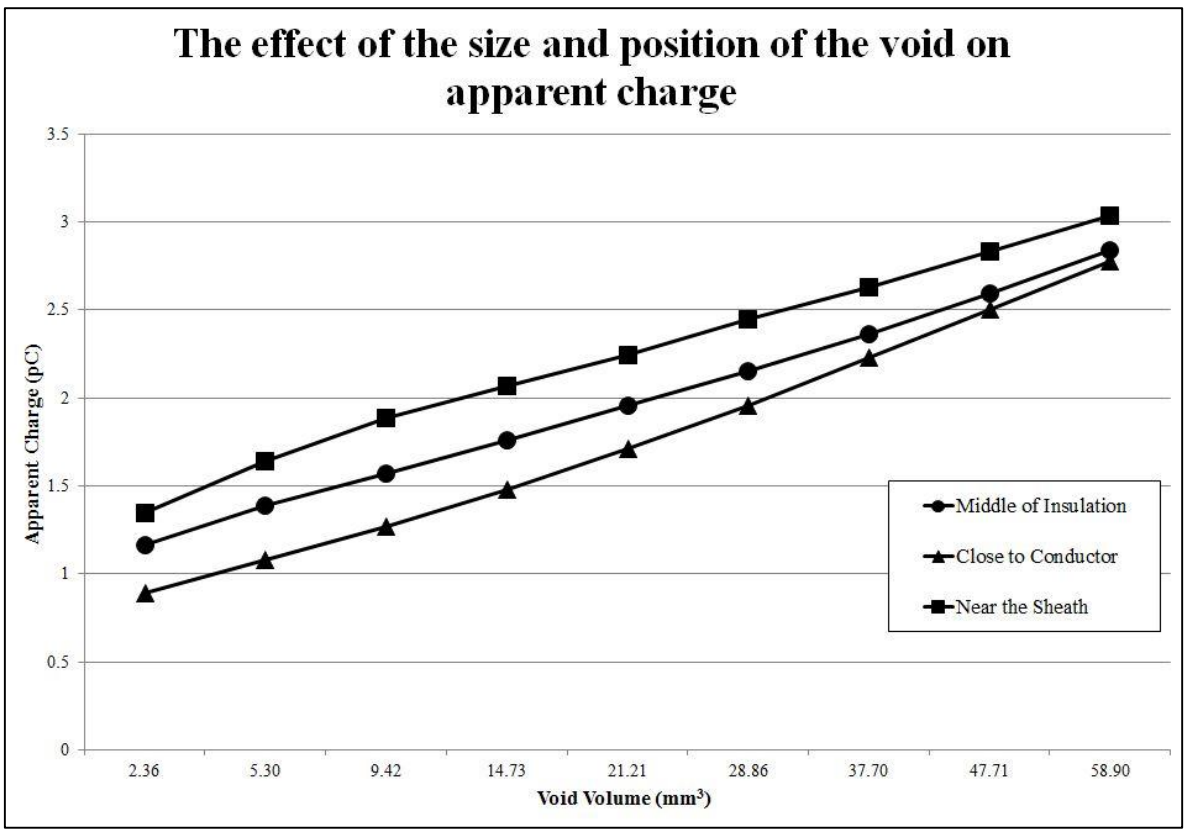

Figure 4-12: The effect of the size and position of the void on the apparent charge

The graphs in Figure 4-12 show that an increased void volume will result in an increased value for the calculated apparent charge of the PD signal. This was also the case with the results obtained from the basic three-capacitor model. The coefficients of determination for the three positions are: middle of the insulation $R^2 = 0.9983$, close to the conductor $R^2 = 0.9943$ and near the outer sheath of the cable $R^2 = 0.9958$. The coefficient of determination for all three positions is close to $R^2 = 1$. A linear trendline is therefore an accurate representation of the data of all three positions. From this the conclusion can be made that a void with larger dimensions will result in a higher apparent charge value. The position of the void influences the amplitude of the apparent charge. The position of the void will thus also have an influence on the calculated apparent charge of the PD signal. The influence of the position of the void will thus ultimately have an effect on the severity of the PD activity.

The final set of simulations, by means of the comprehensive three-capacitor MATLAB® Simulink® model, was performed in order to be able to investigate the effect of the input voltage on the apparent charge of the PD signal. The standard set of simulation parameters, given in Table 4-4, was used for these simulations. The input voltage was increased by 0.5 kV increments from 6.6 kV to the final value of 11 kV. The results obtained from this set of simulations are given in Figure 4-13.

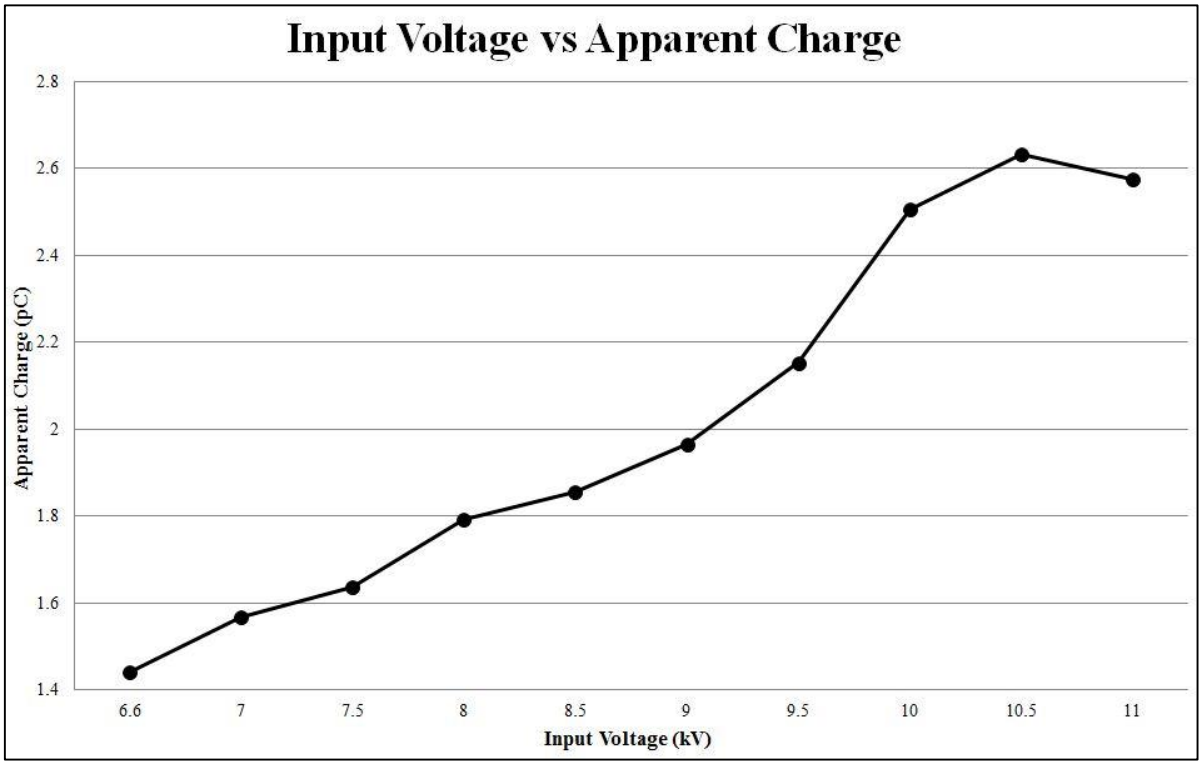

Figure 4-13: Correlation between input voltage and apparent charge

From Figure 4-13 it can be seen that an increase of the input voltage will result in increased values of the apparent charge of the measured PD signal. Although the overall effect is an increase in apparent charge, there is no trend or direct correlation between an increase in the input voltage and an increase in the apparent charge value. The basic three-capacitor simulation model yielded similar results when the effect of input voltage on apparent charge where studied. Results from published research also indicate that increased input voltage values will result in an increase of the calculated apparent charge of the measured PD signal.

4.4. Validation of the Simulation Models

4.4.1. Introduction

Validation of a simulation model is one of the most important steps, as the objective of the validation procedure is to determine whether the model is an accurate representation of the actual system. The process used to prove the validity of the simulation models in this dissertation is based on the following three steps:

1. Develop model with high face value.
2. Test assumptions of the model empirically.
3. Determine how representative the simulation output data are.

The three steps listed above were used to determine whether both the basic simulation model and the comprehensive simulation model were "built right".

4.4.2. Develop model with high face value

The main objective for this step of the validation procedure is to determine whether the models seem reasonable to people who are familiar with the system under study. A number of credible research sources were investigated during the literature study phase of this dissertation. The work presented in these research sources will be used to determine the face value of the basic and comprehensive simulation models, due to the similarities of the work presented in these sources and the work presented in this dissertation.

Basic Simulation Model

The basic simulation model was created by making use of only the fundamental parameters of PD activity. The modelling of the basic simulation model is based on the well-known three capacitor model for PD. The fact that the three capacitor model is the basis for the basic simulation model already testifies to the high face value of the model, as it is common practise to use the three capacitor model when analysing PD within medium voltage power cables [**38**].

The basic simulation model was modelled to accurately represent a typical medium voltage cable. The parameters given in Table 4-1 were therefore derived from actual medium voltage power cable data. The data used to derive the parameters of the simulation model is given in the data sheets included in the attached data CD. The void parameters of the basic simulation model are the most important factors for PD characterization of this model. Research indicated that the typical size of voids within the insulation material of a medium voltage cable has a height of 2-3 mm and radius of 1-2 mm [**46**].

The typical volume of voids within the insulation material of a medium voltage cable is 10 mm^3 [**46**]. The void parameters shown in Table 4-1 indicate that the chosen parameters used for simulation purposes are accurate when compared to credible PD research.

It is also important to note that the parameters of the basic simulation model were derived from mathematical and engineering principles, discussed in Chapter 3. A Simulink model was created, for the simulation purposes, which identically represents the derived mathematical model.

Comprehensive model

The comprehensive model, as suggested by the name, was modelled to be a more comprehensive version of the basic simulation model. The fact that the comprehensive model was created by using the same principles used to model the basic simulation model, leads to the conclusion that all the assumptions made in this section, in regard to the basic simulation model, will be applicable to the comprehensive simulation model.

The comprehensive simulation model is also based on the well-known three capacitor model [**38**]. The main difference between the basic and comprehensive simulation models is that the comprehensive model makes use of more initial parameters in order to more accurately simulate PD activity. The mathematical equations, discussed in Chapter 3, used to derive the comprehensive model are therefore more complex when compared to the equations used to derive the basic simulation model. The added complexity of the comprehensive model is warranted by means of mathematical and engineering principles. Similar to the basic simulation model, the input parameters of the comprehensive model were derived from actual medium voltage cable data, as well as typical void parameters.

Conclusion

The fact that both the simulation models were based on the well-known three capacitor model, as well as the fact that parameters used for simulation purposes can be validated by means of actual data and credible research, testifies to the validity of both the simulation models. Both simulation models were derived from mathematical and engineering principles, thus minimizing or completely eliminating the assumption element for both simulation models. Simulink models were created to identically represent the derived models for both the basic and comprehensive simulation models.

By analysing the above mentioned statements, the conclusion can be made that both the basic and comprehensive simulation models were modelled with a high face value. This statement contributes to the validity of the simulation models used for the purposes of this dissertation.

4.4.3. Test assumptions of the models empirically

The purpose of this step is to quantitatively test the initial assumptions made in the development stage of the simulation models. A sensitivity analysis was used to empirically test the assumptions of both simulation models. The purpose of a sensitivity analysis is to determine if the output of a specific simulation model significantly changes when the value of an input parameter is changed. Some aspects of the model will however be sensitive to changes in initial parameters. These aspects will be discussed in order to understand the sensitivity to change of input parameters.

The best way to perform a sensitivity analysis is to analyse specific output parameters for a range of input parameters. The values shown in Table 4-8 are output parameters obtained from the basic simulation model. The range of input parameters for the same simulations is also shown in this table.

Table 4-8: Sensitivity analysis parameters

Void Volume		**Apparent Charge**	
Input Value (mm^3)	**Difference (mm^3)**	**Output Result (µC)**	**Difference (µC)**
9.425	11.781	9.349	11.684
21.206	16.493	21.033	16.361
37.699	21.206	37.394	21.032
58.905	25.918	58.426	25.711
84.823	30.631	84.137	30.383
115.454	35.343	114.520	35.060
150.796	40.055	149.580	39.730
190.852	44.768	189.310	44.400
235.619		233.710	

It is a well-known fact that the volume of the void has a linear effect on the apparent charge of the PD signal. The void volume was incremented from 9.425 to 235.619 mm^3. The resulting apparent charge ranged between 9.349 and 233.710 µC. The difference between two iterations for both parameters was determined and is shown in Table 4-8.

The difference between two iterations was used to determine the percentage deviation for the two iterations. The results are shown in Table 4-9.

Table 4-9: Sensitivity analysis

Percentage Deviation (%)	**Sensitivity**
0.820	-0.018
0.802	0.017
0.820	-0.021
0.799	0.009
0.808	-0.008
0.800	0.012
0.812	0.009

The percentage deviation was then used in order to determine the sensitivity of the output parameter in terms of variation of the input parameter. From the results shown in the table it can be seen that the sensitivity between two iterations is between -0.021 and 0.017. This proves that the output of the simulation models do not significantly change when the value of an input parameter is changed.

The sensitivity analysis played a vital role in proving the validity of the simulation models in terms of an empirical analysis.

Conclusion

It was shown that the output of both the basic and comprehensive models is not sensitive to variations of input parameters. The sensitivity analysis was performed for both simulation models, in order to empirically analyse the assumptions of both simulation models. The fact that the sensitivity analysis for both models yielded positive results, further testifies to the validity of the simulation models discussed in this dissertation.

4.4.4. Representativeness of the simulation output data

The most definite test of a model's validity is determining how closely the simulation output resembles the output from the real system. Both models simulate PD activity due to a single void within the insulation material of a medium voltage power cable. This however is not always the case with practical models. Although actual cables may have multiple voids within the insulation material, trends as well as PD characteristics can still be studied by making use of a single void.

Asima Sabat and S. Karmakar also studied the effect of the input voltage and the void volume on the apparent charge in their work: “Simulation of Partial Discharge in High Voltage Power Equipment” [**39**]. The basic three-capacitor model discussed in this dissertation is similar to the simulation model used by Sabat and Karmakar.

Sabat and Karmakar studied the effect of the applied voltage on the maximum amplitude of the PD signal. Their work states that the maximum amplitude of a PD signal is a function of the applied voltage. They also suggested that the effect of the applied voltage on the maximum amplitude will not follow a specific trend, due to the fact that PD is a random phenomenon[**39**]. This correlates directly with the work presented in this dissertation. Figure 4-4 shows that the input voltage has a definite effect on the maximum amplitude of the PD signal, but with no specific trend. According to Sabat and Karmakar: “It is clear that with the increase of the high voltage the PD is also increased” [**39**]. This is almost identical to the statement: “From this the conclusion can be made that although the maximum PD magnitude will remain relatively constant over a range of input voltages, the overall effect of an increase in input voltage is increased values for the maximum amplitude of the PD signal” made in this dissertation.

From the above statement it is evident that the work presented in this dissertation and the work of Sabat and Karmakar resulted in similar conclusions with regard to the effect of input voltage on the maximum amplitude of a PD signal. It is also noticeable that the values obtained from the simulations presented in these works are similar. The table below indicates the values for maximum PD amplitude and input voltage.

Table 4-10: Representativeness of simulation output data

Work presented in this dissertation				**Sabat and Karmakar**			
Applied Voltage (kV)		**PD Amplitude (µV)**		**Applied Voltage (kV)**		**PD Amplitude (µV)**	
6.6		2.88 – 14.47		6		2.09 – 8.15	
Range				**Range**			
Applied Voltage (kV)		**PD Amplitude (µV)**		**Applied Voltage (kV)**		**PD Amplitude (µV)**	
Min:	**Max:**	**Min:**	**Max:**	**Min:**	**Max:**	**Min:**	**Max:**
6.6	50	2.78	14.75	5	30	2.09	150

From Table 4-10 it is clear that the results from both sources, with regard to the effect of applied voltage on the maximum amplitude if the PD signal, show a clear correlation. The minor deviations between results can be attributed to the fact that certain initial parameters of the simulations of the individual work are not identical, for example the void size.

The relation between void size and the apparent charge of a PD signal was also investigated in the work of Sabat and Karmakar. According to Sabat and Karmakar: "It is observed from simulation results that the relation between void volume and apparent charge is a linear one" [**39**]. This coincides with the results shown in Figure 4-6 and the conclusion made in the work presented within this dissertation.

The table below indicates the apparent charge values as well as the void volumes used for the simulation purposes of the work presented in Sabat and Karmakar [**39**] and this dissertation.

Table 4-11: Validation of simulation output

Work presented in this dissertation		**Sabat and Karmakar**	
Void Volume (mm^3)		**Void Volume (mm^3)**	
Min	**Max**	**Min**	**Max**
9.43	235.62	0.5	4
Apparent Charge (pC)		**Apparent Charge (pC)**	
Min	**Max**	**Min**	**Max**
9.35	233.71	0.014	3.478

The conclusion can therefore be made that the simulation output of the work presented in this dissertation closely resembles the output from the work presented in Sabat and Karmakar.

The comprehensive three-capacitor model is based on the work of Farhad Haghjoo, Esmaeel Khanahmadloo and S. Mohammad Shahrtash [**36**]. The results obtained from the comprehensive MATLAB® Simulink® model, again shows similarities to trends of the results presented by Haghjoo *et al*.

The figure below indicates the simulated PD waveform obtained from the simulation model presented in comprehensive 3-capacitors model for partial discharge in power cables [**36**].

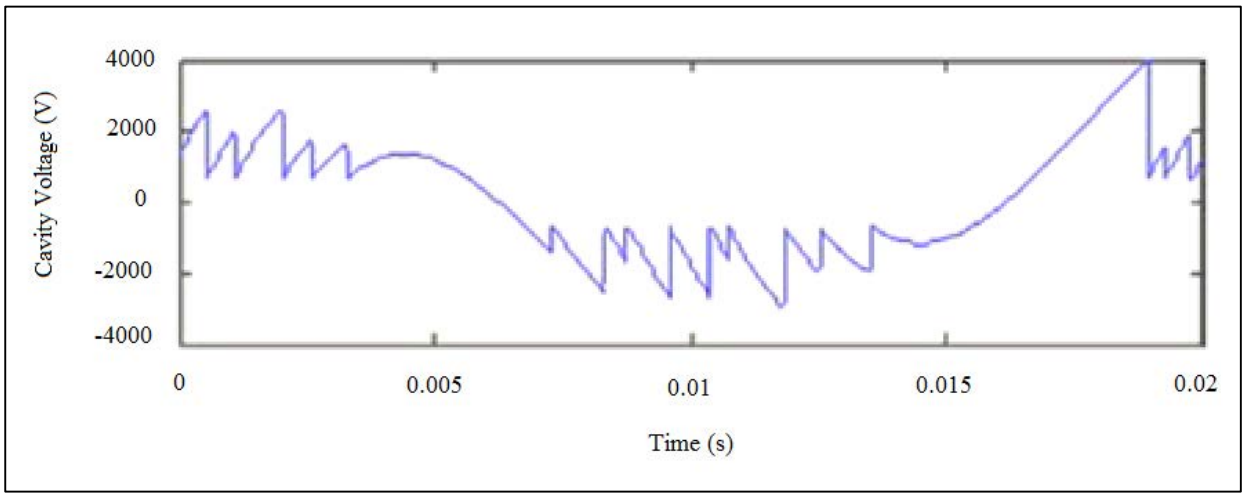

Figure 4-14: Simulated PD Signal [**36**]

By examining the PD signal in Figure 4-14 it can be seen that the PD signal shown in Figure 4-10 and Figure 4-11 of this dissertation exhibits similar characteristics. It is also worth noting that the amplitudes of the signals are both similar in magnitude. The deviations between the output signals of the two simulation models are due to the initial input parameters being different for each individual simulation.

Figure 4-12 shows that the volume of the void has a definite effect on the apparent charge of the PD signal. As the volume is increased the magnitude of the apparent charge will also increase. According to Farad *et al.*: "The charge of PD signals increases when the void size becomes larger" [**36**]. Relevant published experimental results have shown similar conclusions [**47**].

The effect of the input voltage on the apparent charge of the PD signal was also investigated and discussed within this dissertation. Figure 4-13 shows that the trend is that the apparent charge will increase as the magnitude of the input voltage is increase. This conclusion is comparable to results of the work of Farad *et al*. [**36**].

The effect of the input frequency on the apparent charge of the PD signal was also investigated and the conclusion was made that an increase in input frequency will result in decreased values for the apparent charge of the PD signal. The research presented in [**45**] lists various other sources of published research which all came to the same conclusion.

The effect of the input frequency on the apparent charge of the PD signal was investigated by means of both the basic and comprehensive simulation models. The results are shown in Figure 4-5. The output results of the simulation models coincide with the conclusion made by C. Nyamupangedengu and I.R. Jandrell [**45**].

Both models showed similarities to the results of published research and therefore substantiate the validity of the proposed models. Some results obtained from the simulations of both models were not compared to results obtained from practical PD measurements. This is mainly due to the fact that laboratory experiments of the simulation setups were not performed. Considering all the elements of the simulation models, it would be almost impossible to find an identical environment suited for the comparison with practical measurements. Both models have shown similarities when compared with qualitative features and/or trends and the lack of the comparison to practical data therefore do not render the validity of the proposed models as inadequate.

4.4.5. Conclusion

The purpose of the procedure described in this section of the dissertation is to prove the validity of both the basic and the comprehensive simulation models. The validation of the models was performed by conducting three steps. These steps include:

1) Develop model with high face value,

2) Test assumptions of the model empirically and

3) Determine how representative the simulation output data are.

The validation of the two proposed models was mainly based on the fact that both models are based on fundamental theorems in physics and mathematics and the fact that the output results of both models show similarities when compared to the results of published research. The positive outcome of the three steps of the validation procedure proves the validation of the simulation models.

The purpose of this chapter was to discuss the various simulations performed by means of the two MATLAB® Simulink® models. The results obtained from both the basic- and the comprehensive three-capacitor models showed similarities when compared to published research. This verifies that both models can simulate the occurrence of PD activity correct and accurately. The fact that results obtained from both the models show similarities when compared also validates both the simulation models discussed in this chapter.

Chapter 5 The PD Measurement System

The purpose of this chapter is to provide a detailed discussion of the design process for the condition monitoring (CM) system. An overview of the system is provided and each component discussed in detail. The IEEE std 400™ -2001, which is a guide for field testing of power cables, is used as the basis for the design of a PD condition monitoring system. MATLAB® programs are used for the analysis of the measured data in both the time- and frequency-domain.

5.1. Introduction

In this chapter a CM technique is proposed for the on-line detection of PD activity within medium voltage power cables. The measurement of PD signals is an important part of a CM technique. Extensive PD research allowed measurement techniques to evolve over the past few years. Initial measuring techniques focused mainly on the quantification of the apparent charge, whereas improved techniques focus on the analysis of statistical distribution of the charge amplitude and phase angle as well as on the frequency spectrum analysis of each individual PD pulse. Phase Resolved Partial Discharge (PRPD) and Time Resolved Partial Discharge (TRPD) are two methods commonly used for the identification and classification of PD. Commercial PD measuring equipment generally make use of a data acquisition (DAQ) card with a fixed sample rate; it is however to the user's advantage if the measurement method can be altered, without any hardware modifications. The proposed CM technique is based on the use of a digital oscilloscope and designed MATLAB® programs, which allow the user to change various parameters without any hardware modifications.

The IEEE Guide for Field Testing and Evaluation of the Insulation of Shielded Power Cable Systems [**48**] is considered when designing this particular CM system. The purpose of this guide is to discuss the various methods available for CM of the insulation material of shielded power cables. The guide also includes PD testing, with the focus on the measurement of discharge activity, fundamentals of PD and the characterization of PD. According to this guide discharge activity can be measured by means of special sensors connected to a splice or termination of a cable system. These measurements are taken at the system voltage, with the frequency spectrum used to identify the discharges. This statement forms the basis of the design of the CM technique discussed in this chapter.

5.2. Measurement system

5.2.1. Overview

This section provides an overview of the complete measurement system. Each component of the system is discussed in detail at the applicable section of this chapter. A high frequency current transformer (HFCT) is used as the sensor for on-line PD detection. Due to the physical structure of this device, it can easily be connected for PD measurements along the length of the cable. This type of sensor has the advantage that it does not have to be connected to the earth strap of the cable, but can be connected directly to the cable.

The measured signal is recorded by means of a digital oscilloscope. The oscilloscope is an important part of the measurement system as the quality of the oscilloscope will influence a variety of parameters of the measured data. The sensitivity of the oscilloscope is also very important due to the fact that the amplitude of measured PD signals can be very small. In the case that the digital oscilloscope may lack the sensitivity to capture the small PD signals, a pre-amplifier can be used to amplify the signal prior to digitization.

A personal computer (PC) is connected to the system in order to control the digital oscilloscope as well as to store the recorded data. MATLAB® programs, equipped with a graphical user interface (GUI) are used to analyse the recorded data in both the time- and frequency domain. Figure 5-1 shows the basic setup of the equipment of the CM technique. The pre-amplifier is not shown in the figure, due to the fact that it is optional and only necessary if the scope lacks the required sensitivity.

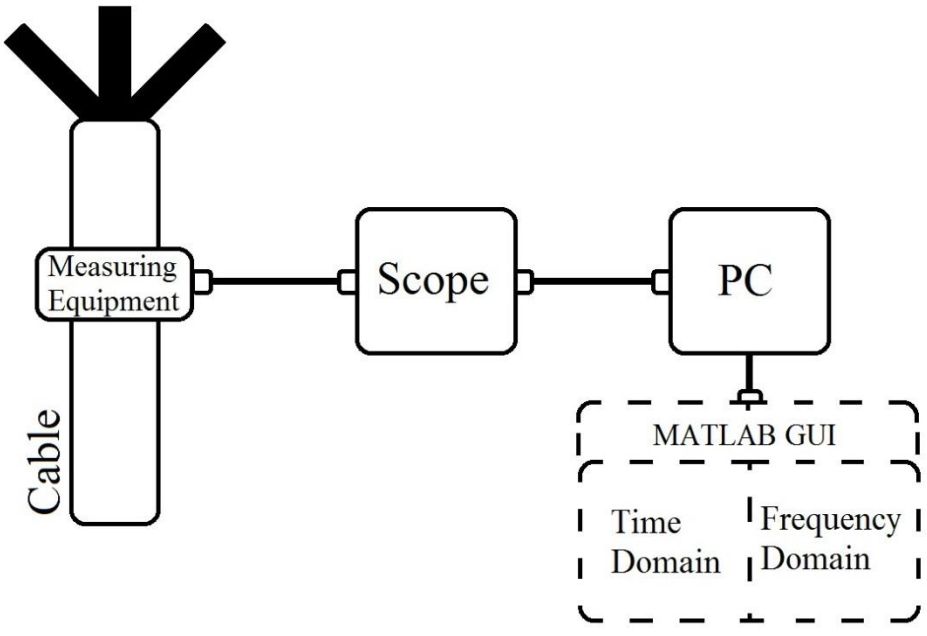

Figure 5-1: Designed PD measurement technique

5.2.2. Measuring Equipment

PD pulses are generally wide-band pulses with small amplitudes and for this reason the sensors used for PD detection need to be sensitive enough to detect the small amplitudes and also be able to measure signals with very high frequencies. A variety of equipment is available for the detection of PD within electrical cables, these include: Rogowski coils, HFCTs and also ultra-high frequency (UHF) antennas.

A HFCT is used to perform the measurements, due to its availability and advantages when used with cables. The construction of a HFCT is identical to that of any other transformer and includes: a primary winding, a magnetic core and a secondary winding. By using a CT for PD measurements the user is given the advantage that the measuring equipment is galvanic isolated from the generally high operating voltages. A HFCT is capable of measuring signals with high frequencies and is specifically designed to be able to detect PD signals. The HFCT used for the measurements are in the shape of a horseshoe, hence the name: horseshoe clamp. An illustration of a split-core CT and a typical horseshoe clamp is shown in Figure 5-2. The physical differences of these two types of HFCT are evident in this figure.

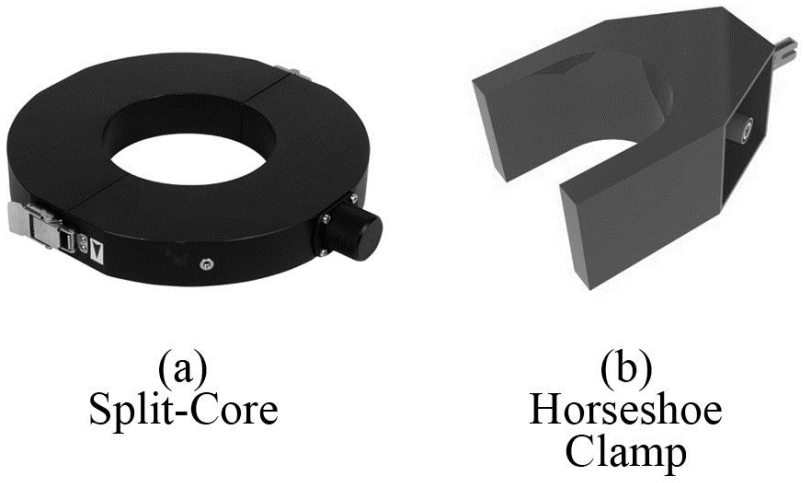

Figure 5-2: Horseshoe clamp

The main advantage of this type of sensor is that the physical structure allows the user to connect and disconnect the sensor around the cable with ease. With the horseshoe clamp, measurements can be taken by placing the sensor directly around the cable. This then eliminates the inconvenience of using a measuring device which can only be connected to the earth strap. For the purpose of this CM technique the horseshoe clamp is connected directly to the digital oscilloscope, due to the oscilloscope's sufficient sensitivity.

5.2.3. Digital Oscilloscope

It is important to be able to store and analyse the measured data. For this system, measurements are taken on-line and then stored on a PC. The data is analysed by means of a number of designed MATLAB® programs. The Handyscope HS5, a product of TiePie Engineering [**49**], is used to record and store the measured data. The HS5 digital scope is shown in Figure 5-3.

Figure 5-3: Handyscope HS5 by TiePie Engineering [**49**]

The choice of scope was mainly influenced by: the sampling rate, bandwidth and resolution of the digital scope. The small size of the HS5 was also a determining factor why this particular scope was chosen as it makes it easier to transport to areas where the measurements are taken. The key specifications of the HS5 are shown in Table 5-1; a complete data sheet of the HS5 is available on the Data CD attached to this dissertation.

Table 5-1: Key specifications of the HS5

Product Code	HS5-220
Max. Sampling Speed	200 Ms/s
Bandwidth	250 MHz
Resolution	14bit (0.006%), (16bit enhanced resolution)
Memory	32 M Samples per channel
Accuracy	0.25% DC vertical, 0.1% typical

The software provided by TiePie Engineering is used to control the device during measurements. The software allows the user to store the measured data in .mat files, which can easily be accessed by MATLAB®, for the analysis of the data. The provided software includes an interface which allows the user to observe the measured signal in both the time- and frequency-domain simultaneously. A number of tools are also included which can be used to manipulate and observe the measured signal.

5.2.4. Personal Computer (PC)

The main function of the PC is to act as the device which enables the user to control the CM system. The digital scope is therefore connected to a PC. The PC is also used as a storage device where the recorded data can be stored for analysis. The stored data can be analysed in both the time- and frequency domain by means of MATLAB® programs equipped with GUIs. For the purposes of the study presented in this dissertation an off-line analysis system is used. This implies that data is measured and then analysed at a later time. It is however possible to use the MATLAB® programs for on-line analysis with some alterations to the source code. An on-line system is preferred to an off-line system when implemented in the industry.

Time domain analysis

The First designed MATLAB® GUI is used to analyse the measured data in the time domain. The data is analysed for three cycles (0.06 s) of the measured signal. The time domain analysis yields important results regarding the discharge activity within the electrical cable. Figure 5-4 shows the user interface of the MATLAB® GUI for time domain analysis. The GUIDE® environment of MATLAB® was used to be able to create the GUIs for both the time- and frequency-domain programs.

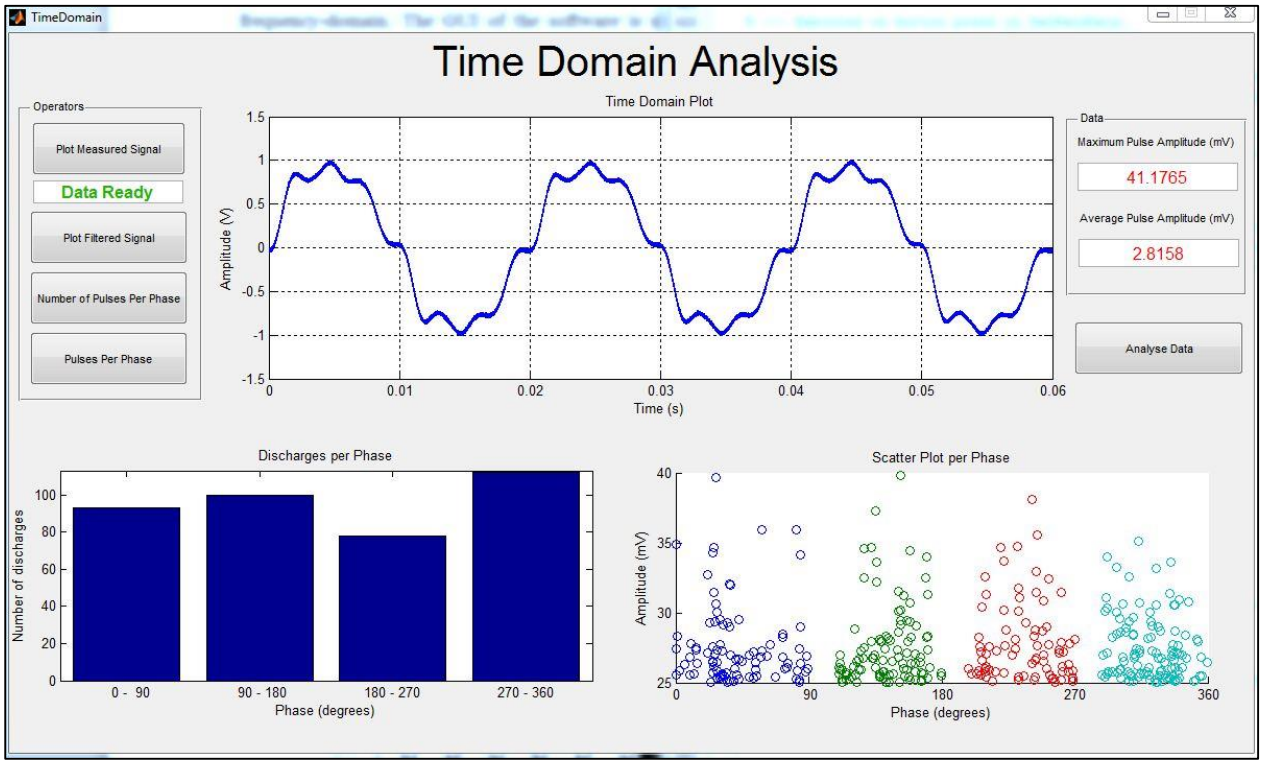

Figure 5-4: Time domain MATLAB® GUI

The first function of the time domain GUI is to plot the measured data. The plotted signal can be compared to the signal displayed by the digital scope. This then can act as a failsafe to ensure that the correct data is being analysed. The data can then be filtered to remove the 50 Hz component and

ensure that only PD data is analysed. The 50 Hz component is removed by using a standard notch filter. The filtered signal is then displayed in the main window at the top of the GUI.

An important aspect of a PD monitoring system is to be able to determine in which phase the discharges occur. The GUI has two functions to determine the number of PD pulses for each phase and also the position of each individual pulse in the four phases. Figure 5-5 shows the functional flow for these functions.

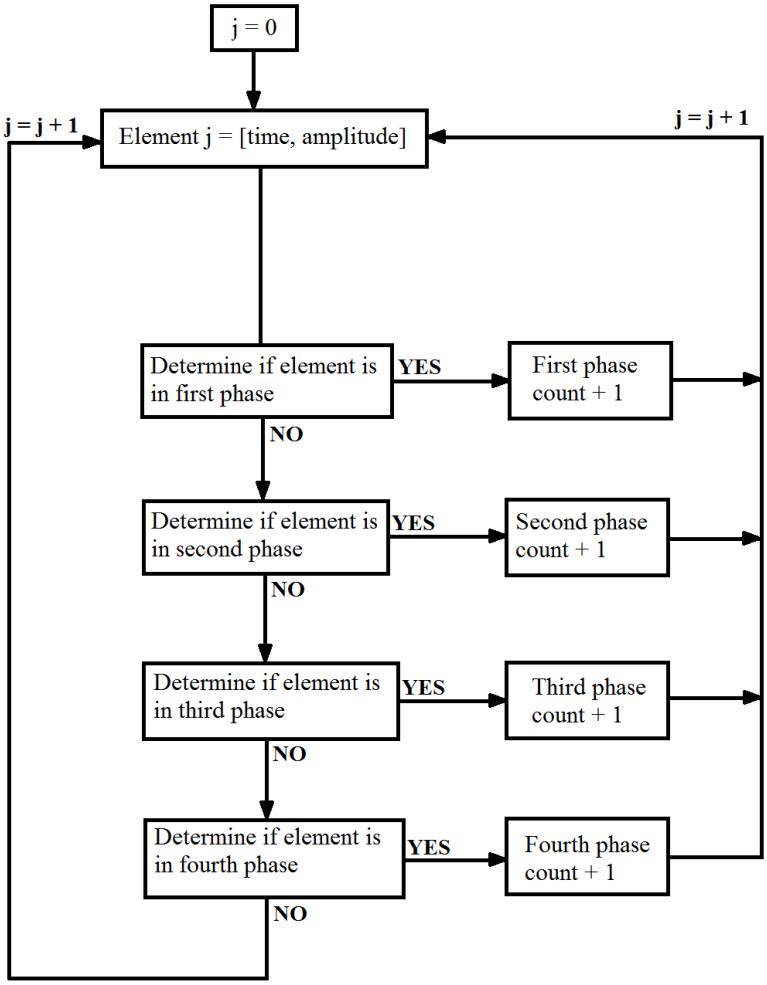

Figure 5-5: Functional flow of source code

The functional flow illustrates that the function will analyse each data point individually. The data is in matrix form and each data point has two elements: time and amplitude. The function uses the time of each data point to determine the specific phase angle of the data. Once the phase angle of the data point is determined the function will return to the top of the code and analyse the next data point. This process is repeated until all data points are arranged according to their specific phase angle positions.

The first function is used to create a scatter plot of the measured data according to the specific phases of the individual pulses. The data obtained from this function is used for phase resolved partial discharge (PRPD) analysis of the measured signal. A section of the source code for this function is given in Figure 5-6.

```
%Scatter plot of discharges within each phase
%-------------------------------------------------------------------------
p1=0;
p2=0;
p3=0;
p4=0;

l = length(mat1);

for j=2:l;
    if mat1(j,2)>=0.03 %0.03 minimum cutoff for PD spike(below-no, above-yes)
    %First phase scatter
    %-----------------------------------------------------------------------
      if mat1(j,1) <= 5
          p1=p1+1;

          first_phase_scatter(p1,1) = [mat1(j,1)];
          first_phase_scatter(p1,2) = [mat1(j,2)];
      end

      if (mat1(j,1)>=21)&(mat1(j,1)<=25)
          p1=p1+1;

          first_phase_scatter(p1,1) = [mat1((j-20),1)];
          first_phase_scatter(p1,2) = [mat1(j,2)];
      end

      if (mat1(j,1)>=41)&(mat1(j,1)<=45)
          p1=p1+1;

          first_phase_scatter(p1,1) = [mat1((j-40),1)];
          first_phase_scatter(p1,2) = [mat1(j,2)];
      end
    %-----------------------------------------------------------------------
```

Figure 5-6: Source code for scatter plot of discharges

PRPD analysis is an essential part of a CM technique, as it is used to identify the source of the discharges. It is important to be able to identify the source of the discharges, as different sources will not affect the degradation of the cable's insulation material at the same rate. The identification process is based on the comparison of measured PRPD patterns with characteristic PD patterns. The shape of the patterns, their symmetry, the magnitude of the discharges and the frequency at which the discharges occur will be used to identify the PRPD patterns.

The GUI also has a function to determine the number of discharges per phase. The data from this function is used to aid the PRPD analysis of the measured signal. The data will be displayed in the form of a histogram. A section of the source code for this function is given in Figure 5-7.

```
%Count discharges per phase
%-------------------------------------------------------------------------
mat1 = [time1, data1]; %Combine data and time into one matrix
l = length(mat1);

firstphase=0;
secondphase=0;
thirdphase=0;
fourthphase=0;

for j=2:l;
    if mat1(j,2)>=0.03 %0.03 minimum cutoff for PD spike(below-no, above-yes)
    %Count first phase
    %-----------------------------------------------------------------------
      if mat1(j,1) <= 5
          firstphase=firstphase+1;
      end

      if (mat1(j,1)>=21)&(mat1(j,1)<=25)
          firstphase=firstphase+1;
      end

      if (mat1(j,1)>=41)&(mat1(j,1)<=45)
          firstphase=firstphase+1;
      end
    %-----------------------------------------------------------------------
```

Figure 5-7: Source code for computing amount of discharges

The functional flow of the function used for calculating the number of discharges per phase is similar to that of the function used to scatter plot the measured signal, shown in Figure 5-5. The only difference is that the specific position within a phase is not required for this function, as it only needs to determine whether the data point is in a specific phase or not.

Frequency domain analysis

A MATLAB® program was designed to be able to analyse the measured data in the frequency domain. The difference between time- and frequency-domain analysis is, as the names suggest, that time domain analysis gives the behaviour of the signal over time and frequency domain analysis provides information regarding the signal's magnitude and phase at each frequency. The transformation of the signal can be seen as the most important concept of frequency domain analysis. The transformation is used to convert the signal from the time domain to the frequency domain and vice versa. Fourier transforms are used for the transformation purposes of the MATLAB® program.

The frequency domain analysis is used to complement the PRPD analysis of the measured data. The frequency domain analysis is also used to determine the location of the fault as well as the severity of the discharge activity. The interface for the frequency domain GUI is shown in Figure 5-8.

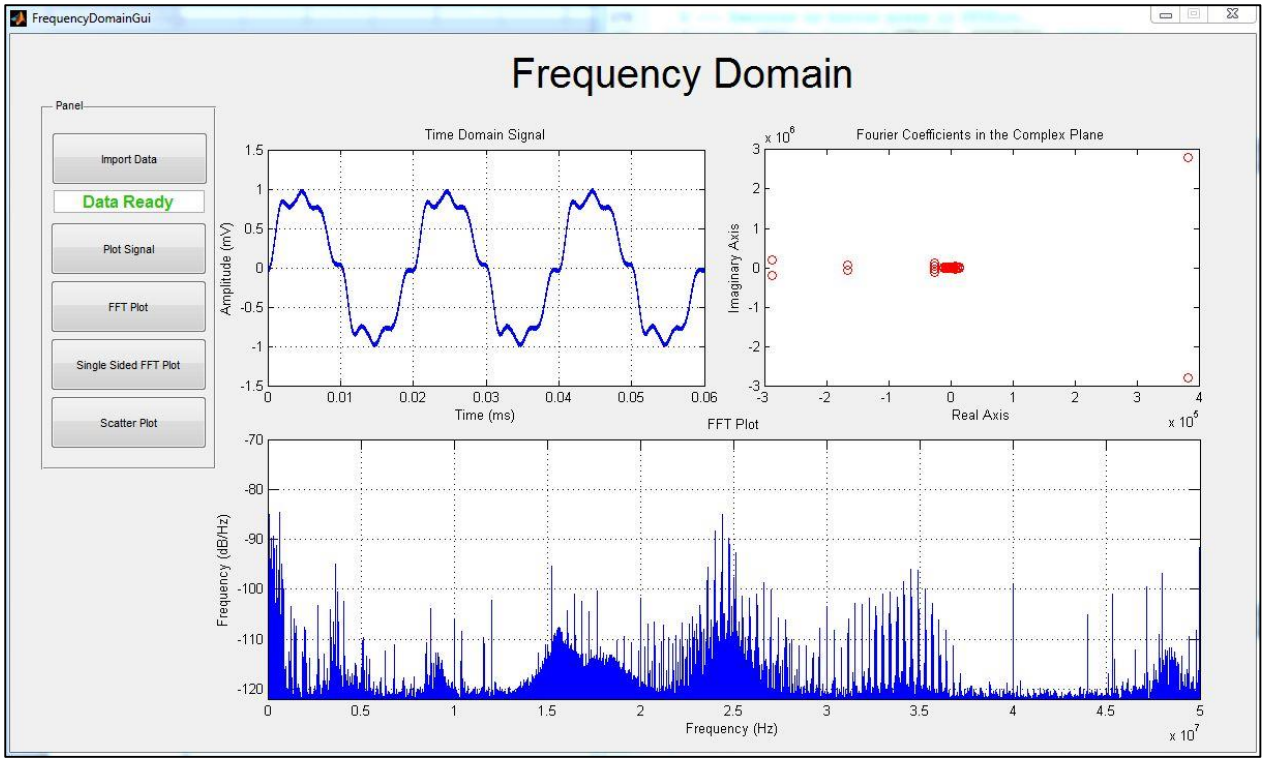

Figure 5-8: GUI used for frequency domain analysis

A built-in fast Fourier transform (FFT) of MATLAB® is used to compute the discrete Fourier transform (DFT) of the measured signal. Fourier transforms are used to convert time to frequency and allows the user to see at which frequencies the discharges are more prolific. The FFT of the measured signal is shown in the main window, at the bottom, of the frequency domain GUI. The FFT is a method commonly used for the purpose of converting data from the time-domain to the frequency domain. The first step to perform a FFT analysis of the time domain data is to decompose an N point time domain signal into N single point signals. The spectrum of each individual point is then determined. The final step in a FFT analysis is to synthesize the N frequency spectra into a single frequency spectrum. The functional flow diagram of a FFT function is shown in Figure 5-9

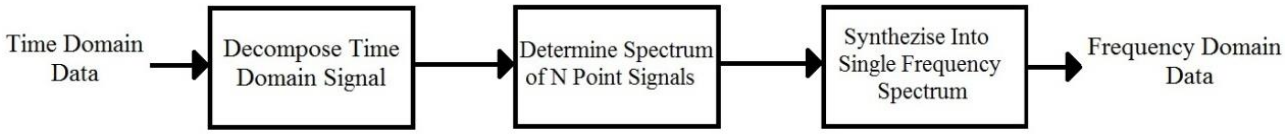

Figure 5-9: Functional flow of FFT function

The source code for computing the FFT of the measured time domain data is shown in Figure 5-10. The source code also includes a function which is used to plot the FFT data in the frequency domain GUI. The FFT function of this specific frequency domain program was designed to plot the data in dB/Hz versus frequency.

```
%FFT Plot
%--------------------------------------------------------------------------
%--------------------------------------------------------------------------
global data1
global Fs
global x


Fs = 100000000;

A = load('C:\Users\Heino\Desktop\MARTEC Data\Data3_1.mat');

x = A.src1.Data(50000:6049999);

N = length(x);
xdft = fft(x);
xdft = xdft(1:N/2+1);
psdx = (1/(Fs*N)).*abs(xdft).^2;
psdx(2:end-1) = 2*psdx(2:end-1);
freq = 0:Fs/length(x):Fs/2;
plot(handles.axes1,freq,10*log10(psdx));
title(handles.axes1,'FFT Plot');
xlabel(handles.axes1,'Frequency (Hz)');
ylabel(handles.axes1,'Frequency (dB/Hz)');
ylim(handles.axes1,[-122 -70]);
grid(handles.axes1, 'on')
%--------------------------------------------------------------------------
%--------------------------------------------------------------------------
```

Figure 5-10: Source code for FFT function

5.3. Conclusion

The design of a CM technique is very important as adequate monitoring of cables enables the engineer to act before cable faults can cause outages. The designed system is used to take practical measurements while the cable is under normal operating conditions. Apart from being non-intrusive, the system is also non-destructive as no over-voltages are required for the measurements. The technique will therefore not affect the life of the cable being measured. The safety of a CM technique is a very important aspect. The safety of this system is guaranteed due to the fact that no disconnections are required when taking the measurements and the physical construction of the measuring equipment also safeguards the operator from being exposed to hot parts.

The detection of PD activity can be seen as an easy technique to perform, it is however much more difficult to analyse the measured data. For the successful analysis of the condition of the insulation material of a cable, it is necessary to use PD measurements in combination with a detail analysis performed by a specialist. The expertise of a specialist is vital to any CM technique, as any automated PD monitoring system is, at this time, still dependent on the analysis provided by these specialists.

The detailed design of the monitoring system which was used to perform the measurement and analysis of practical PD data was discussed in this chapter. The numerous components of the system, along with the purpose of each, were also discussed. It is also important to note that the measuring of PD data is only a small component of a complete CM technique. The most important aspect is the analysis of obtained data. The expertise of PD specialists therefore plays a vital part in the success of such a system. The discussed system was used to measure PD data in a practical environment and the analysis of the data is discussed in the chapter 6.

Chapter 6 Experimental Results

The purpose of this chapter is to discuss the results obtained from the measurement system discussed in the previous chapters. The setup of equipment as well as the purpose of each component of the measuring system is discussed; photos of the practical setup are also included to aid the discussion of the system. The validation process of the results includes the comparison of the chosen system to systems used in the industry and also systems commonly discussed in research papers. MATLAB® was used to implement programs for the analysis of the signals in both the time- and frequency-domain. The results obtained from both these programs are discussed in detail within this chapter.

6.1. Introduction

The purpose of chapter 5 was to discuss the detail design of a cable CM technique, which was used to measure and analyse practical PD data. The practical measurements as well as the analysis of the measured data are discussed in this chapter. The designed system will only be used as an instrument to detect the presence of discharge activity within electrical cables. It can therefore be seen as the engineer's first line of defence and more in depth studies as well as the technical expertise of a specialist is required for a complete analysis of the PD activity within the cable.

The measurements were made possible with the help of MARTEC which allowed the use of their equipment as well as test specimens for the PD measurements.

A number of steps must be completed in order to successfully measure and analyse practical PD data. These steps are influenced by the type of CM technique being used as well as the practical data obtained from the measurements. As mentioned before, the interpretation of analysed PD data is the single most important step of any CM technique. This step requires the expertise of a specialist in order to correctly interpret the results and formulate accurate assumptions as to the condition of the electrical equipment being monitored.

Figure 6-1 illustrates the flow diagram required to use the CM technique to measure and interpret practical PD data. The first step of the flow diagram is the experimental setup of the measuring equipment. The next step is to accurately measure practical PD data. The measured data is stored on an external device. The stored data is then analysed in both the time- and frequency-domain by means of MATLAB® programs. The analysed data is interpreted in order to determine the electrical condition of the cable being monitored.

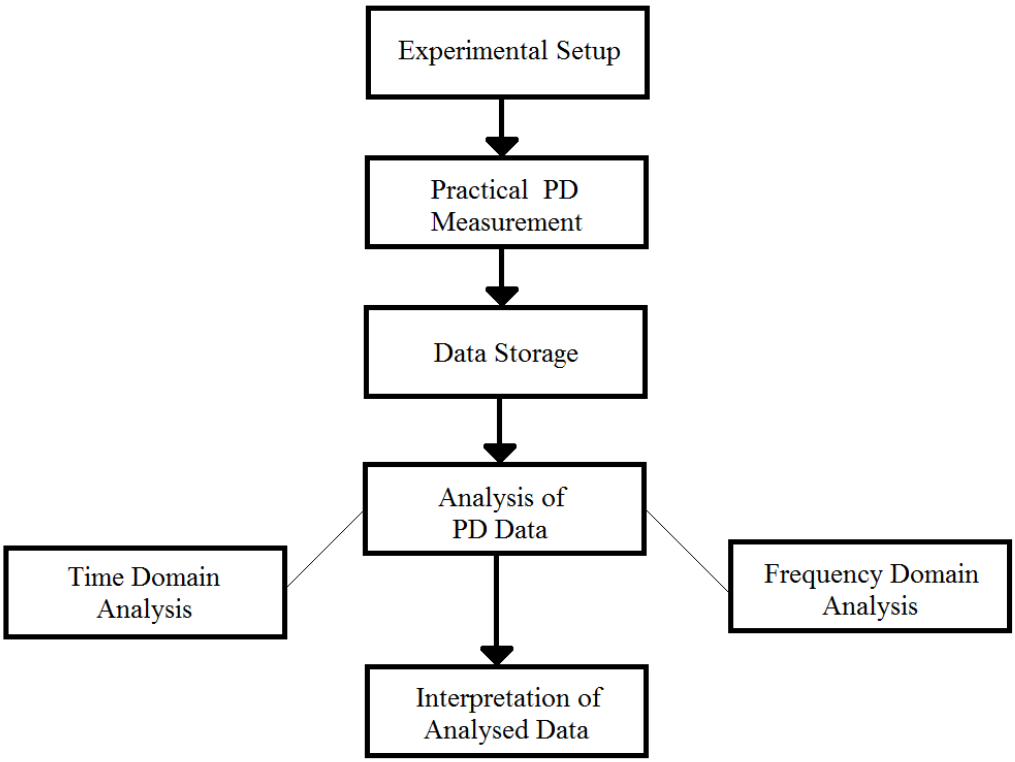

Figure 6-1: Flow diagram illustration of the practical CM process

The components of the flow diagram that illustrates the CM process of measuring and analysing practical PD data is discussed in the following sections. It is important that each of the steps, shown in Figure 6-1, are completed correctly and accurately in order to be able to successfully interpret the analysed PD data. The interpretation of analysed data is the most important step of the entire procedure.

6.2. Experimental setup

6.2.1. Introduction

The experimental setup of the CM technique includes the combination of measuring equipment and test specimen required for the measuring of practical PD data. The experimental setup of the CM technique is based on the designed system illustrated in Figure 5-1

The complete experimental setup is shown in Figure 6-2. The setup includes: the PC used to control the system and store the data, the scope which is used to record the PD data and the cable termination which is used as the test specimen.

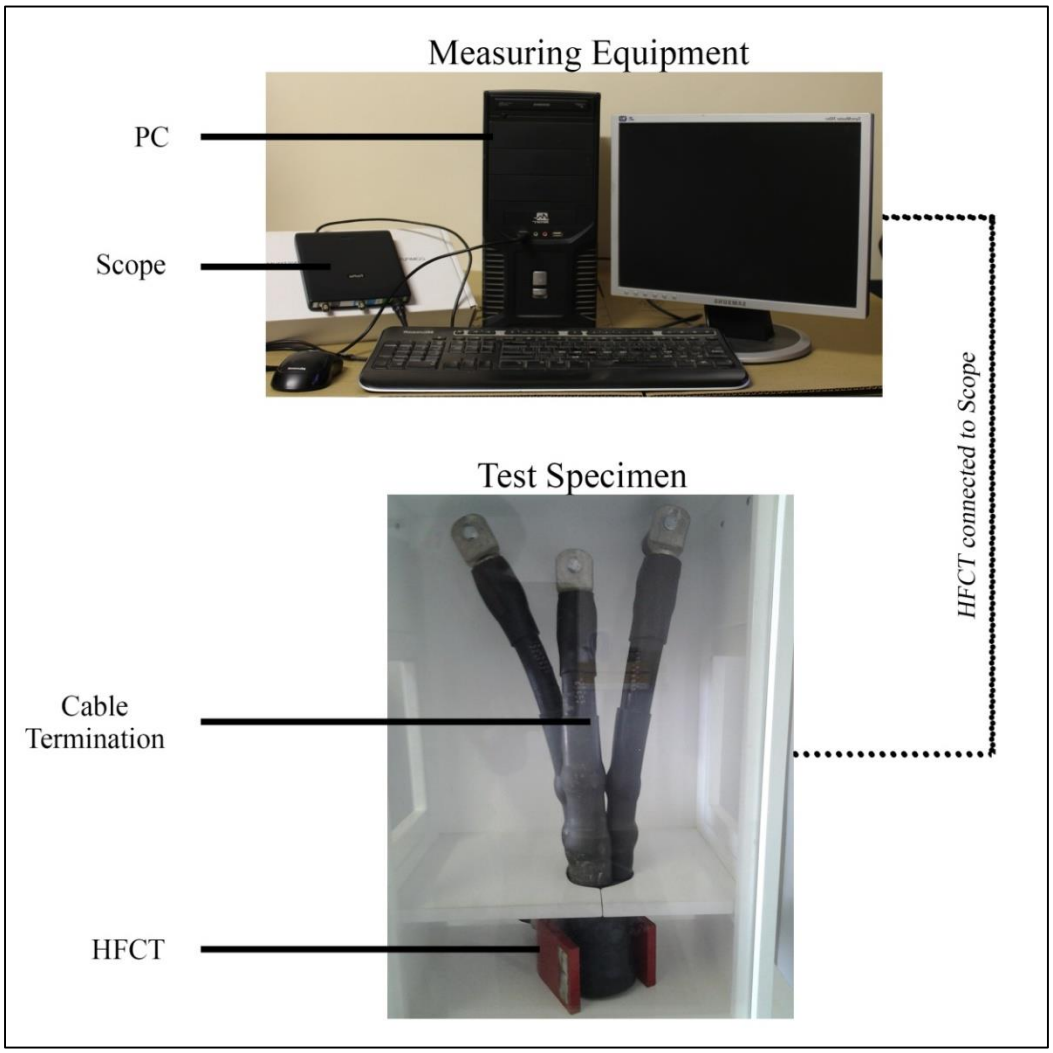

Figure 6-2: Experimental setup of equipment

The experimental setup shown in Figure 6-2 was used to perform all the practical measurements of PD data. Each component of the experimental setup is discussed in detail in the sections to follow. The test environment made it impossible to capture the complete experimental setup in a single figure.

6.2.2. Instruments

The test specimen used for the PD measurements is a cable termination which was taken out of operation due to the fact that discharge activity was detected within this section of the cable. The cable termination is connected to a high voltage variable autotransformer, commonly known as a variac. Figure 6-3 shows the variac which was used for the variable input voltage required for the PD measurements.

An autotransformer differs from a traditional transformer due to the autotransformer only having one winding instead of the traditional two. Portions of the same winding act as both the primary and secondary sides of the auto transformer. The physical construction of the variable autotransformer allows the user to adjust the input voltage to different levels. This is a useful application of the variac, as it makes it possible to study the effect of the input voltage on the discharge activity within the cable.

Figure 6-3: High voltage variable autotransformer

An HFCT in the shape of a horseshoe, supplied by MARTEC, was connected around the cable in order to detect and record the PD signals. Figure 6-4 shows the horseshoe clamp connected around the cable. The horseshoe clamp was connected directly to the Handyscope HS5, which was used to record the measured signals. From this the deduction can be made that the practical setup used for the PD measurements is an exact representation of the detail design for the measurement system depicted in Figure 5-1.

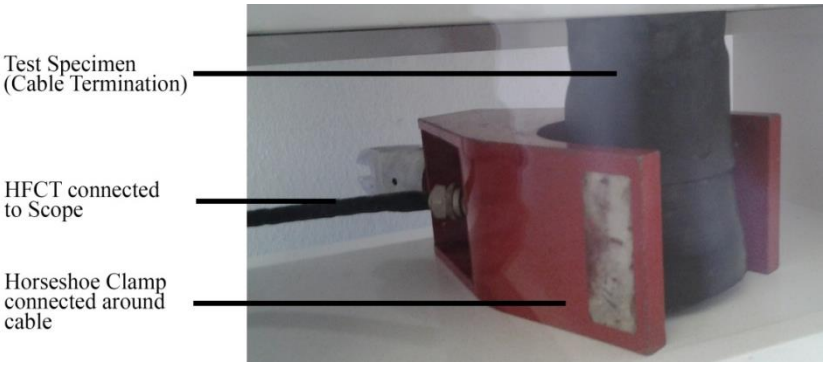

Figure 6-4: Horseshoe clamp connected around cable

The cable termination with the horseshoe clamp, at the bottom, connected around the cable can be seen in Figure 6-5.

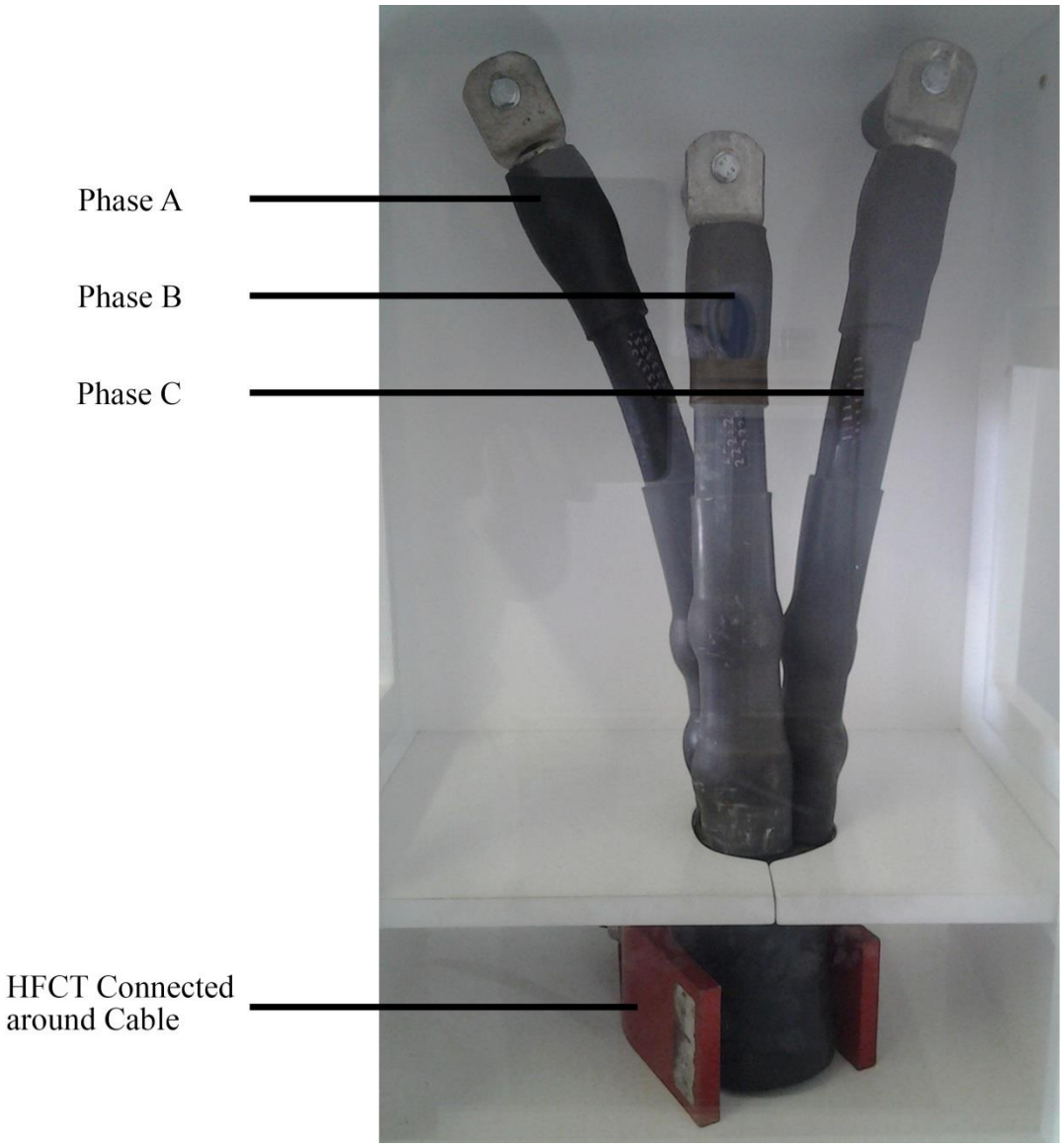

Figure 6-5: Experimental setup of cable termination and HFCT

The setup of equipment and the test specimen remained constant for all the PD measurements, with the only variable being the input voltage supplied by the variac. The data for each of the measurements were individually stored to be analysed at a later time.

At the time the tests were performed it was possible to witness small discharges between the three cables at the top in the form of an arc. It was however not possible to capture this on image due to the speed and random nature of the discharges.

6.2.3. Recorded data

The Handyscope HS5 was used to record the measured PD data. TiePie Engineering included software, with the digital scope, which can be used to control the scope directly from the PC connected to it. The measured data was taken on the same test specimen at input voltages of: 1.6 kV, 3.2 kV and 5 kV. A number of samples were taken at each input voltage in order to improve the accuracy of the measurements. The TiePie software can be used to view the measured signal in both the time- and frequency-domain. The GUI of the software is shown in Figure 6-6. The time domain view of the measured signal is shown at the top of Figure 6-6, whereas the bottom of Figure 6-6 illustrates a side-by-side view of both the time- and frequency-domain views of the measured signal.

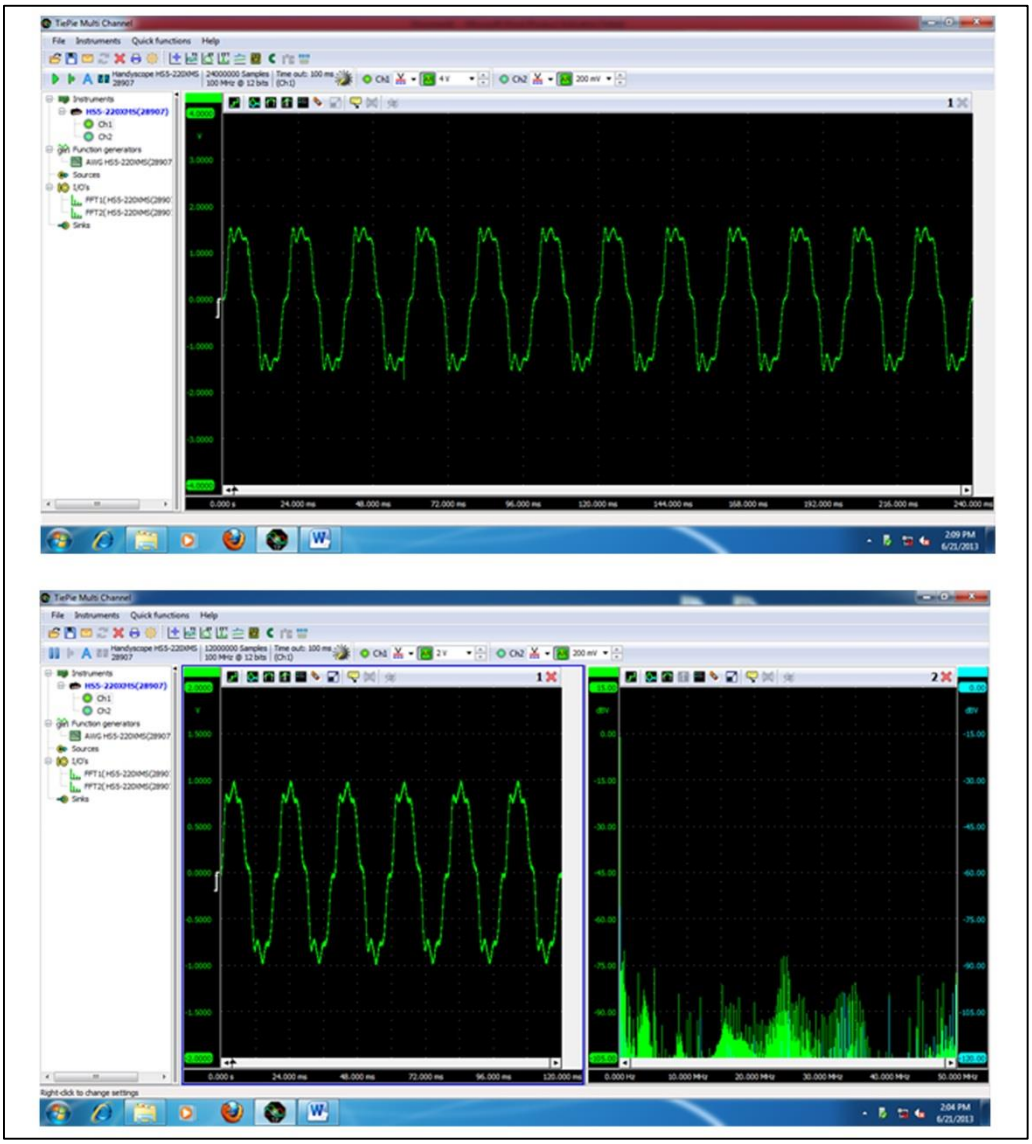

Figure 6-6: Handyscope HS5 measurement software

The digital scope was used to store the data in .mat files, due to the accessibility of the MATLAB® programs used for the analyses of the data. Only the time domain data of the measured signal was stored. The MATLAB® programs, designed for the analysis, were then used to convert the time domain data of the recorded signal to the frequency domain. The data is stored in the form of a matrix,

with each element containing a value for time and amplitude. This makes it easy to manipulate the data in the MATLAB® environment and also allows the user to individually work with either the time elements or the amplitude elements of the recorded data. The chosen system is a non-intrusive CM system due to the fact that no disconnections, resulting in down time, are required in order to take the measurements. The HFCT is also isolated from the power network and no over-voltages are required during the measurement phase, resulting in the system to be non-destructive as well. At the moment the measuring system is set up to perform offline PD analysis. The system can however be converted for online PD monitoring. The only requirement for the system to be used as an online system will be alterations to both the MATLAB® programs. The setup of the measuring equipment can remain exactly the same as for the offline application.

6.3. Validation of results

Although validation is generally associated with the design of simulation models, it is also important to validate the accuracy of the measured data and data analysis. The validation process of the results is based on the comparison of the measurement technique to techniques used in the industry. The measurement technique used to capture the PD data is the main concern for the validation of the results. It's a common fact that the measurement of PD signals is not a difficult task to perform; still it has to be executed correctly and with precision.

The technique used to capture the PD data includes the use of a HFCT connected around the cable; the data obtained from the HFCT is then stored by means of a digital oscilloscope with the required accuracy as well as sampling rate. This technique is commonly used to capture PD data [**34**]. It is also previously mentioned that MARTEC supplied assistance in a way that they supplied much needed practical knowledge regarding the measurement of PD signals. MARTEC then also use the technique discussed in this chapter as one of the many techniques they use to measure PD signals.

The fact that the chosen technique is commonly used in the industry and is also often discussed in research regarding PD, attributes to the validity of the results gained from this measuring technique.

6.4. Measurement results analysis

6.4.1. Introduction

The analysis of the measured PD data can be seen as the most important part of the CM system. It was previously mentioned that PD signals can be measured with ease, but the analysis of the data requires comprehensive knowledge of the phenomenon known as partial discharge. The measured data was analysed for both the time- and frequency-domain. It is important to note that the main purpose of the monitoring system is to detect discharge activity within medium voltage power cables. Due to the simplistic approach of this system, detail may be lacking in the analysis of the data. The system will however include important aspects regarding PD analysis. The analysis of a specialist is still vital to the success of any monitoring technique and the analyses, discussed in this chapter, are tools to aid the specialist in the interpretation of the measured data.

6.4.2. Time domain analysis

The MATLAB® program designed for the time domain analysis was used to analyse the recorded signals over time. The time domain analysis is used to study: the PD signal over time, maximum and average amplitudes of the PD signal, the amount of discharges per phase as well as the PD patterns of the measured signal.

The MATLAB® GUI, designed for the analysis of PD data in the time domain, is a fully functional tool, which allows the engineer to investigate various aspects of a measured PD signal. Each function of the GUI is designed to automatically perform the mathematical functions needed to determine the specific characteristic of the PD signal. This is useful as it will ensure accuracy and will also save the engineer time in doing the various operations by hand. The GUI was programmed so that the source code is easy to understand and also allows room for alterations to the original code. Future work can include source code, added to the original GUI, in order for it to perform online analysis of measured data.

The PD measurements were taken at: 1.6 kV, 3.2 kV and 5 kV. Figure 6-7 shows the signals generated by means of the time domain GUI, at each of the three chosen input voltages. The time domain GUI was programmed to analyse the measured data for three cycles (0.06 s) of the measured signal. The signals shown in Figure 6-7 are the original measured signals. For the analysis of the PD data it is necessary to filter the 50 Hz component of each signal, this will ensure that only the PD data is considered for the analysis.

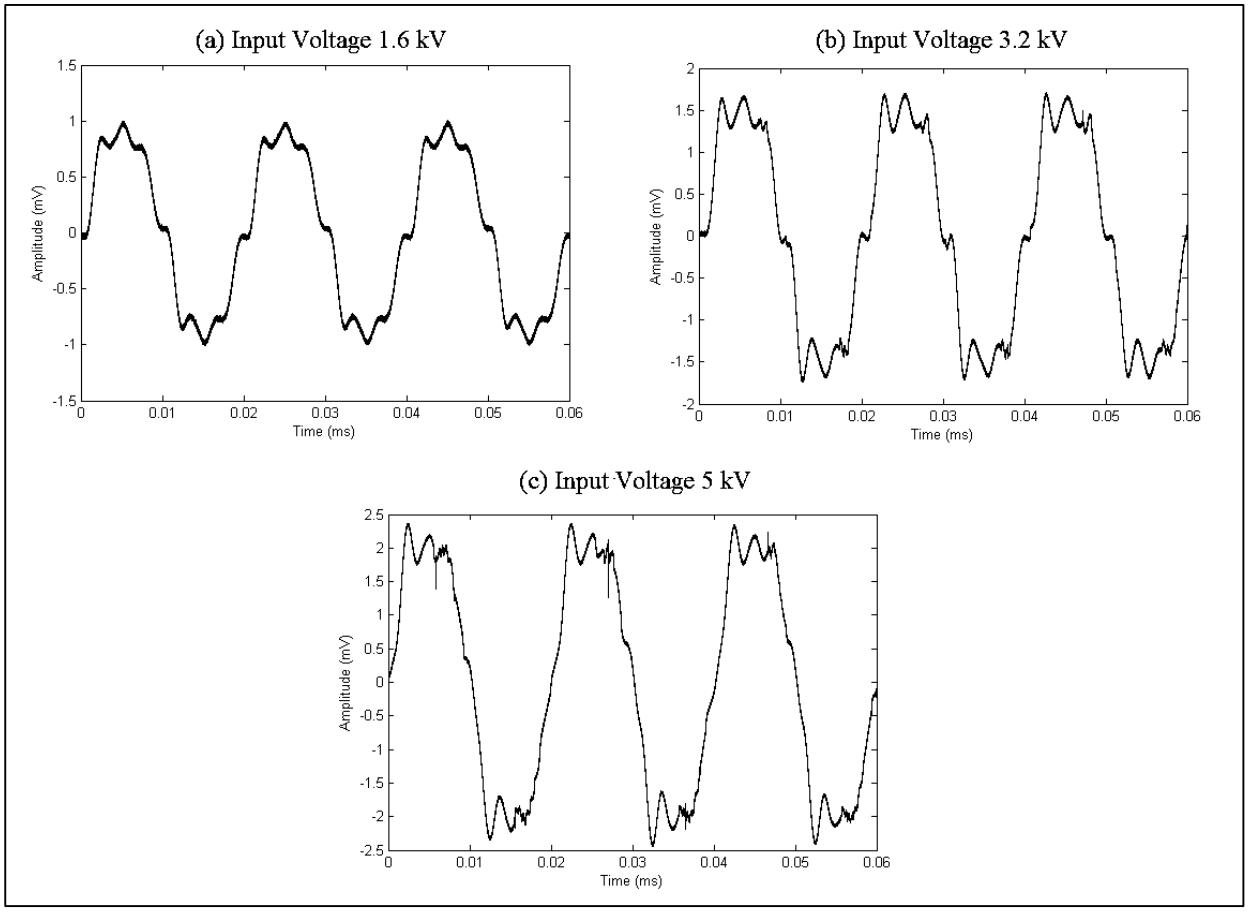

Figure 6-7: Measured signals at: (a) 1.6 kV, (b) 3.2 kV and (c) 5 kV

The MATLAB® GUI houses a function which can determine the number of discharges for each phase of the measured signal. A section of the source code for this function is shown in Figure 5-7. The function was used to determine the amount of discharges for the measured signals at: 1.6 kV, 3.2 kV and 5 kV. Numerical values for the analysis of PD pulses per phase are shown in Table 6-1.

Table 6-1: PD pulses per phase

Input voltage (kV)	First Quadrant	Second Quadrant	Third Quadrant	Fourth Quadrant
1.6	93	100	78	112
3.2	140	189	137	214
5	274	356	218	365

The values for the amount of discharges per phase were used to construct a histogram in order to determine if a trend could be found between the number of discharges per phase and the input voltage. The histogram is shown in the graph illustrated in Figure 6-8.

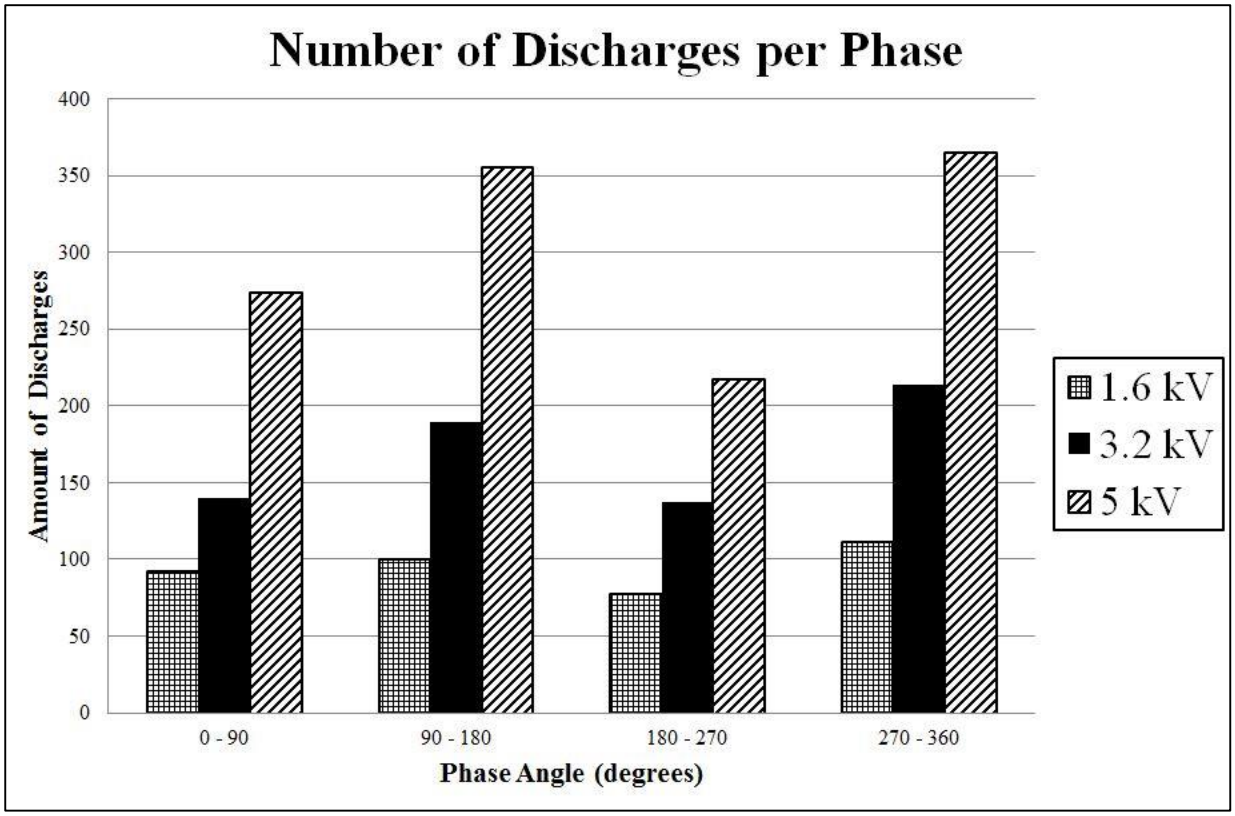

Figure 6-8: Amount of discharges per phase

From the graph it can be seen that a common trend for all of the three input voltages are present. The simulations discussed in Chapter 5 were used to investigate the effect of the input voltage on the characteristics of the PD signal. The conclusion was made that an increase in the input voltage will cause higher values for discharge amplitude as well as the apparent charge of the PD signal. Published research also investigated the effect of input voltage on the amount of discharges in each phase window. The common conclusion was that an increase in input voltage will also cause the amount of discharges in each phase window to increase. A similar conclusion can be made when studying the results shown in Figure 6-8. There is however no fixed trend between input voltage and the increase in number of discharges per phase.

From the graph it can be seen that there is a significant increase in the number of discharges at 5 kV, when compared to that of the other input voltages. This can be due to the state of degradation of the cable being tested. When the 5 kV level is reached the input voltage is at such a level that PD activity, within the insulation material of the cable, is at a more severe level and will thus cause a significant increase in various PD characteristics.

A function was also added to the GUI to plot the position of the discharges in each phase. This is a very important tool as it is used to perform PRPD analysis of the measured data. The PD pattern portrayed by this function can be compared to characteristic PD patterns in order to determine the type and origin of the discharge activity. The PD patterns for the three signals are shown in Figure 6-9.

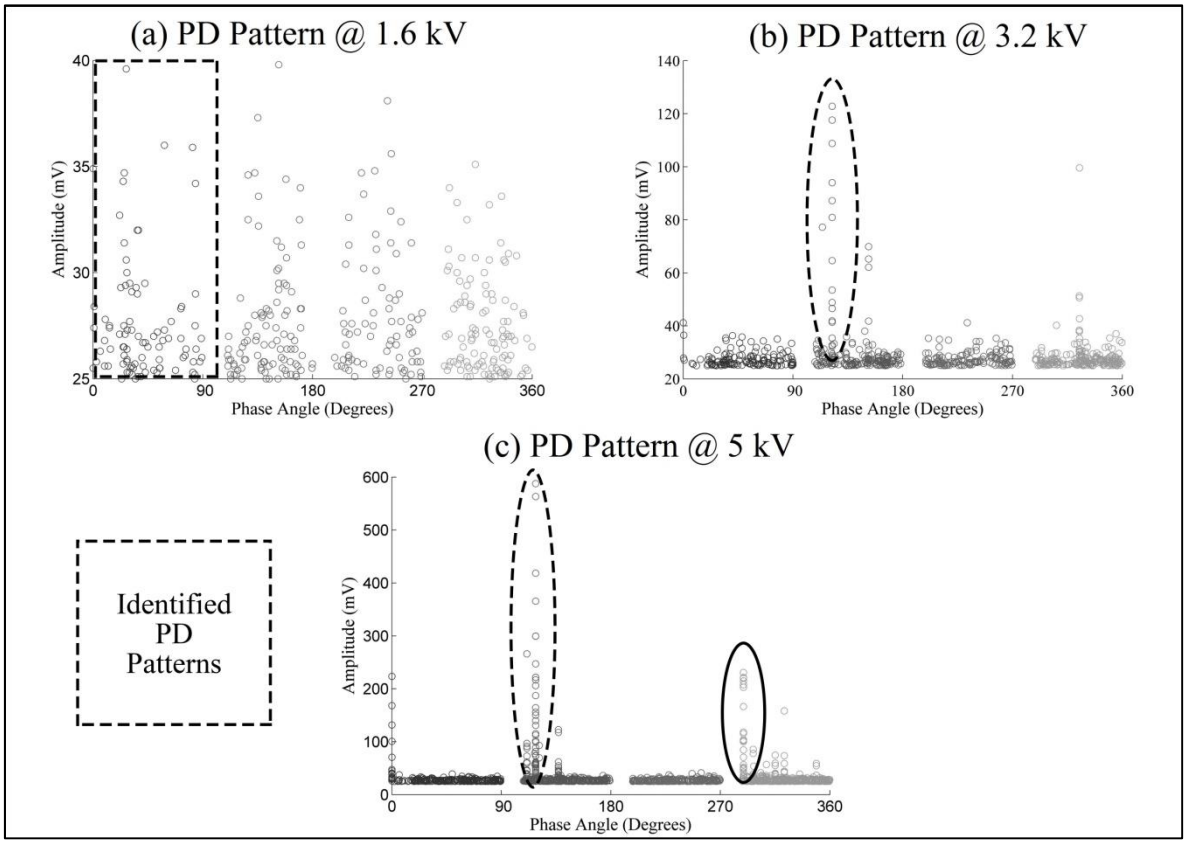

Figure 6-9: PD pattern plots at: (a) 1.6 kV, (b) 3.2 kV and (c) 5 kV

The data of the PD pattern plots at 3.2 kV and 5 kV are somewhat difficult to read due to the amplitude of some of the discharges. The scale has to be adjusted to accommodate all the pulses and for this reason the pulses with smaller amplitudes are plotted in a small area of the total plot. When the pulses with the higher amplitudes are eliminated from the plot, it reveals similar patterns as can be seen in the PD pattern plot at 1.6 kV. The PD pattern plots are used to perform PRPD analysis of the measured data. The patterns are compared to characteristic PD patterns in order to identify the various types of discharges measured in the test specimen.

The PD pattern plots shown in Figure 6-9 were compared to published research as well as characteristic PD patterns in order to be able to determine the types of discharges present in the test specimen. The research work of Hudon and Bélec, presented in [**50**], was used for the purpose of comparison. By analysing the similarities of the discharge patterns obtained from the time domain GUI and that of the research of Hudon and Bélec, it can be seen that both internal PD as well as exciter pulses are present in the test specimen used for the measurements. It is possible to be able to investigate other PD patterns when frequencies above 50 MHz are used for the measurements.

It is also important to record sufficient data in order to be able to perform PRPD analysis of a measured signal, as only a few pulses may not reveal a recognizable pattern. The most important part of PD research is the analysis of the data and for this reason it is vital to have the knowledge of a specialist in order to accurately perform the PRPD analysis. The aim of the study presented in this paper is to do basic research regarding PD and also to develop a measuring system which is able to identify the presence of discharge activity within electrical cables. The PRPD analysis of the data is therefore sufficient for the purposes of this study.

6.4.3. Frequency domain analysis

The MATLAB® program designed for the frequency domain analysis is mainly used for the conversion of the signal from the time domain to the frequency domain. The frequency domain analysis of PD data reveals important characteristics of the measured discharge activity. Some applications also use the frequency domain analysis to determine the location of the fault in the cable. The GUI has a function which can be used to plot the measured signal in the time domain. This is a useful function as it allows the user to observe both the time- and frequency-domain signals side-by-side. It can also be used as a failsafe to ensure that the correct signal is being analysed.

The FFT plot function was used to convert the time domain data of the measured signals of all three input voltages. The FFT plot of the measured signals, at all three input voltages, is shown in Figure 6-10. It can be seen that the three FFT plots are relatively similar and this is due to the fact that all measurements were taken on the same test specimen.

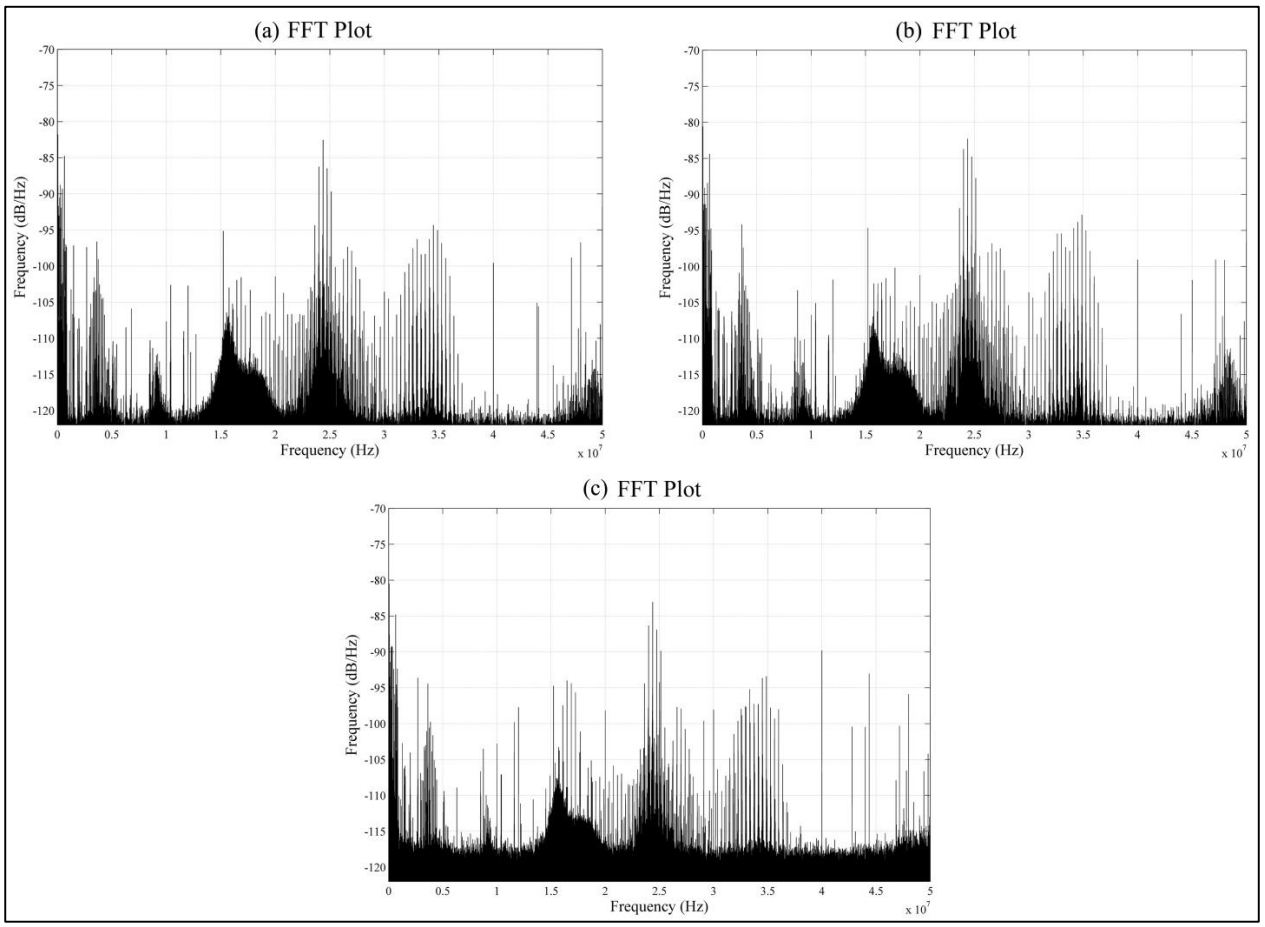

Figure 6-10: FFT plot at: (a) 1.6 kV, (b) 3.2 kV and (c) 5 kV

The similarities of the three FFT plots allow for only one of the FFT plots to be analysed in detail. The frequency analysis is often used to determine the location of the discharge activity within electrical cables. The experimental setup however does not allow for this function to be investigated, due to only the cable termination being tested. The FFT plots of the MATLAB® program show similarities when compared to that of the digital oscilloscope illustrated in Figure 6-6. This then substantiates the accuracy of the designed frequency domain program.

By studying the FFT plot of the measured PD signals it can be seen that the discharges are spread over the entire frequency range, although a large portion of the discharge activity occur between the 15 MHz and 35 MHz range. The FFT plot also indicates the presence of PD activity in the range between 5 MHz and 15 MHz, as well as to the end of the plot at the 50 MHz mark. PD signals measured in power cables often occupy only a small section of the frequency range. This then makes it possible for it to be used to determine the location of the fault. The fact that almost the entire measured frequency

range is covered, testifies to the severity of the discharge activity measured within the test specimen. As the PD severity in a power cable increases to reach a high level, the pulses shown in the FFT plot will continue to grow until most of the frequency range is covered. The digital scope used for the measurements allowed data to be observed up to the 50 MHz mark. It can be useful to implement a scope which is able to also analyse higher frequencies of the measured signals.

6.5.Conclusion

The results obtained by means of the CM system discussed in this dissertation were compared to results from published research as well as models currently used in the industry. The results discussed in "The Importance of Phase Resolved Partial Discharge Pattern Recognition for On-Line Generator Monitoring", were used as one of the reference sources [**50**]. The research presented by Hudon and Bélec shows similarities to the results obtained in this study. It will be impossible to find identical results due to the fact that the measuring system may differ as well as the fact that different test specimens were used. The similarities shown between the two sets of results are still sufficient to validate the results discussed in this chapter.

The CM technique used to obtain the data, discussed in this chapter, is similar to the measuring system used by MARTEC. The fact that the measuring system is similar to one being used in the industry, as well as the fact that the results are based on mathematical and engineering principles supports the validity of the results.

The main objective was to design and implement a CM technique which can be used for the detection of PD activity within the insulation material of medium voltage cables. The results discussed and analysed within this chapter proves that the objective was successfully accomplished.

The purpose of this chapter was to discuss the process of analysing the data obtained from practical PD measurements. The measured data was analysed in both the time- and frequency-domain by means of designed MATLAB® programs. The frequency domain GUI was mainly used to study an FFT plot of the measured signals. The knowledge of a specialist is the most important aspect of any CM technique and can never be ignored. The obtained results were compared to published research as well as results obtained from systems used in the industry in order to validate the accuracy of the results.

Chapter 7 Conclusions and recommendations

The purpose of this chapter is to provide closure to the dissertation. The research and experiments, both simulation and experimental, led to conclusions being formed during the study and are discussed within this chapter. This chapter is also used to formulate recommendations and future work regarding the study. The purpose of the recommendations is to improve the outcomes of this dissertation.

7.1. Conclusions

The problem statement formulated in Section 1.2 stated that the purpose of the project was to investigate the variety of CM techniques and to design a CM technique for electrical cables which makes use of PD measurements. The formulation process of the problem statement led to a number of research objectives defined in Section 1.3. The main research objectives included:

- The investigation of CM
- Modelling of PD simulation models
- Design and implementation of a cable CM technique
- Analysis of measured PD data

The literature study was used as a familiarization process with the concepts of condition monitoring. Emphasis was placed on techniques used for the CM of electrical cables. Various cable CM techniques were identified as plausible solutions for the problem. Further investigations led to the decision that a technique, which uses PD measurements to assess the condition of the cable's insulation material, will be used for the purpose of this study. The scientific methods used to investigate, validate and verify the research objectives were given in Chapter 3 through Chapter 6.

The first research objective addressed was the derivation of mathematical models for simulation purposes. Research indicated that the well-known three-capacitor model is commonly used to derive mathematical models for the representation of PD activity. The three-capacitor model was used for the modelling purposes of two simulation models. The main focus for both models was to be able to accurately simulate PD due to a single void within the insulation material of an electrical cable. The basic three-capacitor model only included the elementary parameters required for the simulation of discharge activity. The simplicity of the model however led to the absence of important elements of discharge activity. The stochastic nature of PD as well as the high frequency model of a power cable

was two of the missing elements which led to the modelling of a second, more comprehensive model. The aim of the comprehensive model was to include more parameters in order to be able to simulate PD activity more accurately. The addition of these parameters also allowed for the investigation of PD characteristics, previously unachievable, with the use of the basic three-capacitor model.

The simulation models were used to simulate PD activity and also to investigate the effect of various parameters on the PD characteristics. The MATLAB® Simulink® environment was used as the simulation platform. Simulations performed by the basic three-capacitor model revealed vital information regarding the phenomena called partial discharge. At this stage of the research very little was known about PD and for this reason the basic model proved to be vital in gaining much needed basic knowledge of PD. As the research progressed shortcomings of the simulations, performed by the basic model, became evident and the need for more comprehensive simulations became evident.

The first parameter to be investigated was the effect of the input voltage on the maximum amplitude of the measured PD signal. It was found that although no definite trend was present, the overall effect was an increase in maximum amplitude when the input voltage was incremented. The effect of the input frequency on the apparent charge of the PD signal is at the moment, a subject much debated among researchers. The simulations performed during this study showed that an increase in input frequency, above the normal 50 Hz operating frequency, resulted in decreased values for the calculated apparent charge.

The most significant result obtained from the simulations was the study of the effect of void size and position on the apparent charge. Results from both models showed that an increased void volume will result in an almost linear increase of the calculated apparent charge of the PD signal. The results obtained from both models were of similar nature and were also compared to results of relevant research. The similarities between published research and simulation results discussed within this dissertation verified the validity of the simulation results.

The literature study presented in this dissertation was used to design a CM technique which can be used to detect the presence of PD activity within medium voltage cables. The IEE Guide for Field Testing and Evaluation of the Insulation of Shielded Power Cable Systems (IEEE std 400™ - 2001) [**48**], along with techniques currently being used within the industry formed the backbone for the design process of the CM technique. The layout of the system and each individual component were discussed in Chapter 4.

The CM technique included two MATLAB® programs, with the purpose to analyse PD data in both the time- and frequency-domain. The design of the system led to the ability of the system to take measurements non-intrusively. The fact that the CM technique is based on systems currently being used within the industry serves as the validation process of the designed system.

The designed system was used to record practical PD data which was then analysed. With the help of MARTEC, it was possible to take measurements on an actual cable joint, taken out of operation due to the fact that PD activity was previously detected within the joint. The measurements were taken at various input voltages in order to study the PD characteristics. The time-domain MATLAB® program was used to determine: the maximum as well as average amplitude of the PD signal, the number of discharges per phase and also the phase patterns of the discharges. The phase patterns were used for basic phase resolved partial discharge (PRPD) analysis of the measured data. The PRPD revealed that both internal PD and exciter pulses were present within the test specimen.

The main function of the frequency domain MATLAB® program is to analyse the measured signal in the frequency domain by means of a FFT analysis. The FFT analyses were used to determine the frequencies at which the discharges were most prominent, as well as the severity of the discharge activity. The CM technique was also designed to use the FFT plot to estimate the location of discharges along the length of the cable. The verification process of the results was based on the comparison of results obtained through analysis of measured data to results of published research and results from techniques used within the industry. It is impossible to find identical results due to a number of reasons, including: different conditions, difference in test specimen and also the fact that the environments where the tests are taken are not identical. This problem was however solved by investigating and comparing trends found in the obtained results. By investigating the trends present in the results of published work it was found that the results discussed in this dissertation showed a number of similarities, this then verifies the accuracy and correctness of the results obtained from analysis of measured data.

7.2. Recommendations

Recommendations as well as future work are discussed in this section. The aim of the recommendations is to improve the outcomes of this dissertation.

7.2.1. Simulation models

The main disadvantage of the simulation models discussed in this dissertation is the inability to simulate PD due to more than one void. Both models make use of only a single void within the insulation material to simulate PD activity. Further research and improved simulation models may accommodate the use of multiple voids as the origin for discharge activity. This will be a useful addition, as it is rarely the case in practical situations where only a single void within the insulation material of the cable is the cause for PD activity.

7.2.2. CM technique

The current CM technique is used to measure PD data on-line and then uses off-line analysis for the PD data. Although this is a technique with the potential to successfully analyse the condition of an electrical cable's insulation, it will certainly be more advantageous to make use of an on-line monitoring technique. On-line CM techniques will allow the engineer to constantly monitor the condition of electrical equipment. The MATLAB® programs are designed in such a way that the source code can be altered with ease to facilitate on-line monitoring with the addition of certain equipment. It is also impossible for a single CM technique to completely analyse the condition of an electrical cable's insulation material. Future work must include the addition of a suitable technique to assist in the analysis of PD data.

7.2.3. Experimental results

The analysis of data can be seen as the most important part of any CM technique. Although it is a relatively easy process to measure PD data, it is far more difficult to accurately interpret the data. The interpretation of PD is done, in some extent, by means of the CM technique, but the expertise of a specialist is still the most important part of this process and can't be ignored. Practical knowledge relating to PD is obtained by performing a variety of experiments in order to investigate the effect of various parameters on the PD characteristics. A work environment where CM is performed on electrical equipment by means of PD measurements is also a good learning ground to gain much needed practical knowledge of PD. The absence of the expertise of a specialist is certainly one of the major disadvantageous of the work presented in this dissertation. As mentioned, it is essential to research the field of PD constantly and gain as much knowledge as possible into the mechanisms of this phenomenon.

7.3. Closure

This research project formed an essential part in gaining knowledge regarding the fairly unknown subject of partial discharge. A variety of CM techniques were researched and the knowledge gained from this work is vital in understanding the operation of monitoring the condition of electrical equipment. The simulations performed in this study revealed information regarding the cause of PD within cables as well as the effect of specific parameters on the PD characteristics. This information aided the understanding of the basic principles of PD. The designed CM technique allowed for the practical investigation of PD within electrical cables. Although simulation results are essential to any research project, they still lack a certain aspect only achievable by practical experiments. The measurement and analysis of actual PD data ensured that the link between theoretical research and practical experiments is present within this dissertation.

Over the course of the study valuable knowledge were gained regarding condition monitoring (CM) of electrical equipment and in particular, techniques using partial discharge (PD). The work presented in this dissertation is my humble contribution to the research field of PD. Condition monitoring of electrical cables are an essential part of electrical engineering and the contribution of research in this field is vital, regardless of the extent of the research. Although the work presented in this dissertation has some shortcomings and may be optimised, the scientific approach implemented to address the problem statement was successful.

List of References

[1] Song Y.H Han Y, "Condition Monitoring Techniques for Electrical Equipment - A Literature Survey," *IEEE Transactions on Power Delivery*, vol. 18, no. 1, pp. 4 - 13, January 2003.

[2] Lofaro R. Villaran M., *Essential Elements of an Electric Cable Condition Monitoring Program*. Upton, NY: Brookhaven National Laboratory, 2010.

[3] Brookhaven National Laboratory, "Assessment of Environmental Qualification Practices and Condition Monitoring Techniques for Low-Voltage Electric Cables," vol. Volume 2, no. 1, February 2001.

[4] Mohamed Alsharif, Peter A Wallace, Donald M Hepburn, and Chengke Zhou, "Partial Discharge Resulting from Internal Degradation in Underground MV Cables: Modelling and Analysis," *IEEE*, vol. 1, no. 1, pp. 1-5, 2009.

[5] J Rohan Lucas, *High Voltage Engineering*, Revised ed., J Rohan Lucas, Ed. Moratuwa, Sri Lanka: Department of Electrical Engineering University of Moratuwa, 2001.

[6] Nigel Hampton, Rick Hartlein, Hakan Lennartsson, Harry Orton, and Ram Ramachandran, "Long-Life XLPE Insulated Power Cable," *Jicable*, vol. I, no. 1, pp. 1-6, 2007.

[7] Institute of Electrical and Electronic Engineers, "The Authoritative Dictionary of IEEE Standard Terms," IEEE, International, International Standard IEEE 100, 2000.

[8] 3M. (2008, January) 3M Electrical Training. [Online]. http://solutions.3m.com/wps/portal/3M/en_US/EMDCI/Home/Support/Training/

[9] I. A. Metwally, "High-voltage power cables plug into the future," *Potentials, IEEE*, vol. 27, no. 1, pp. 18 - 25, Jan - Feb 2008.

[10] Ying Sun. (2010, April) MSE 5320. [Online]. http://electronicstructure.wikidot.com/density-functional-analysis-of-impurities-in-dielectrics

[11] CFC StarTEC LLC. (2005, August) CFC StarTEC LLC. [Online]. http://www.c-f-c.com/specgas_products/sulfurhex_sf6.htm

[12] Stephen Harris. (2012, April) The Engineer. [Online]. http://www.theengineer.co.uk/in-depth/analysis/superconducting-heads-to-the-

cities/1012388.article

[13] RWE. (2012, January) RWE. [Online]. http://www.rwe.com/web/cms/en/113648/rwe/press-news/press-release/?pmid=4007389

[14] S.B. Dalal, R.S. Gorur, and M.L. Dyer, "Aging of distribution cables in service and its simulation in the laboratory ," *Dielectrics and Electrical Insulation, IEEE Transactions on*, vol. 12, no. 1, pp. 139-146, February 2005.

[15] S Grzybowski, P Shrestha, and L Cao, "Electrical Degradation of High Voltage Cable Insulation Energized by Switching Impulses ," in *Electrical Insulation and Dielectric Phenomena, 2008. CEIDP 2008. Annual Report Conference on*, Quebec, QC, 2008, pp. 25-28.

[16] J. Densley, "Ageing mechanisms and diagnostics for power cables - an overview," *Electrical Insulation Magazine, IEEE*, vol. 17, no. 1, pp. 14-22, Jan - Feb 2001.

[17] Brookhaven National Laboratory, "Evaluation of Aging and Environmental Qualification Practices for Power Cables Used in Nuclear Power Plants," January 2003.

[18] Sandia National Laboratory, "Aging Management Guideline for Commercial Nuclear Power Plants - Electrical Cable and Terminations," *National Laboratory for US Department of Energy*, September 1996.

[19] Mohd Qayyuum. (2009, December) TNB Electrical Engineer. [Online]. http://tnbelectricaleng.blogspot.com/2009/12/water-tree-in-xlpe-cable.html

[20] Just Go Technology. (2012, June) Just Go Technology. [Online]. http://www.pci-pcmcia-express.com/P13142-ELECTRICAL-TREEING-IN-HIGH-VOLTAG

[21] Gardner J. B Toman G., "Development of a Non-Destructive Cable Insulation Test," *Workshop on Environmental Qualification of Electric Equipment*, November 1993.

[22] Sandia National Laboratories, "Aging, Condition Monitoring, and Loss-of-Coolant Accident (LOCA) Tests of Class 1E Electrical Cables," *Sandia National Laboratories*, vol. III, no. 1, April 1992.

[23] Paolo F. Fantoni, "Wire System Aging Condition Monitoring and Fault Detection using Line Resonance Analysis," in *OECD Halden Reactor Project*, Halden, Norway, April 2005.

[24] ASTM International, ASTM D638: Standard Test Method for Tensile Properties of Plastics.

[25] ASTM International, ASTM D412: Test Methods for Vulcanized Rubber and Thermoplastic Rubbers and Thermoplastic Elastomers-Tension.

[26] Gillen K.T, "Density Measurements as a Condition Monitoring Approach for Following the Aging of Nuclear Power Plant Cable Materials," in *Radiation Physics and Chemistry*. Exeter, UK: Elsevier Science Ltd, 1999, pp. 429-447.

[27] Warne D. Haddad A., *Advances in High Voltage Engineering*. London, UK: Institution of Electrical Engineering, London, 2004, ch. 4, pp. 139-185.

[28] Chaikin S., "Partial Discharge Testing - Decreasing the Field Failures of High Voltage Components," *HT LLC*, pp. 1-18, March 2001.

[29] Clipper Controls. (2011, April) Clipper Controls. [Online]. http://www.clippercontrols.com/pages/Dielectric-Constant-Values.html#R

[30] ECE Lab. (2012, August) ECE Lab. [Online]. http://www.ecelab.com/schering-bridge.htm

[31] Brown P, "Non-Intrusive Partial Discharge Measurement in High Voltage Switchgear," in *IEE Colloquium on Motors and Condition Assesment Equipment*, London, 1996, pp. 1-10.

[32] Elstein S, Lindner P Lindner M, "High Voltage Engineering," in *Proceedings of International Symposium on High Voltage Engineering*, London, 1999, pp. 4.349-4.352.

[33] Michel Matthieu, "Comparison of Off-Line and On-Line Partial Discharge MV Cable Mapping Techniques," *Conference and Exhibition on Electricity Distribution*, vol. I, no. 1, pp. 1-6, June 2005.

[34] IEC Technical Group, "Partial Discharge Measurements," IEC-Standard, Publication 60270, 2000.

[35] David A. Nattrass, "Partial discharge XVII The early history of partial discharge research," *IEEE Electrical Insulation Magazine*, vol. 9, no. 4, 1993.

[36] Esmaeel Khanahmadloo and S. Mohammad Shahrtash Farhad Haghjoo, "Comprehensive 3-capacitor model for partial discharge in power cables," *COMPEL: The International Journal for Computation and Mathematics in Electrical and Electronic Engineering*, vol. 31, no. 2, pp. 346 - 368, 2012.

[37] Gabe Paoletti and Alex Golubev, "Partial Discharge Theory and Applications to Electrical Systems," in *Pulp and Paper: Industry Technical Conference Record*, 1999, pp. 124 - 138.

[38] Navarrete L.N., Parada A.G. and Miranda A.C. Badillo M.F., "Simulation and analysis of underground power cable faults," in *International Meeting of Electrical Engineering Research*, April 2012, pp. 50-57.

[39] Karmakar S. Sabat A., "Simulation of Partial Discharge in High Voltage Power Equipment," *International Journal on Electrical Engineering and Informatics*, vol. 3, no. 1, pp. 234-247, 2011.

[40] Brussels, M.K. Nayfeh M.H., *Electricity and Magnetism*, 1st ed. New York, NY: Wiley, 1985.

[41] Stratton J.A., *The Electrostatic field*, 1st ed., Du Bridge A., Harnwell G.P. Richtmyer F.K., Ed. New York, NY: McGraw-Hill, 1941.

[42] Niemeyer L. Gutfleisch F., "Measurement and simulation of PD in epoxy voids," *IEEE Transaction on Dielectrics and Electrical Insulation*, vol. 2, no. 5, pp. 729-743, 1995.

[43] Niemeyer L., "A generalized approach to partial discharge modeling," *IEEE Transaction on Dielectrics and Electrical Insulation*, vol. 2, no. 5, pp. 510-528, 1995.

[44] Fileccia Scimemi G., Romano P., Riva Sanseverino E. Candela R., "Analysis of partial discharge activity at different temperatures through an heuristic algorithm," in *IEEE Conference on Electrical and Dielectric Phenomena*, Austin, TX, USA, 1999, pp. 202-205.

[45] C Nyamupangedengu and I.R. Jandrell, "Partial Discharge Spectral Response to Variations in the Supply Voltage Frequency," *IEEE Transactions on Dielectrics and Electrical Insulation*, vol. 19, no. 2, pp. 521 -531, April 2012.

[46] Cheng Y.H., Yan P., Sun Y.H., Shao T. Ren C.Y., "Simulation of Partial Discharge in Single and Double Voids Using SIMULINK," in *Twenty-Seventh International Conference Record of the Power Modulator Symposium*, May 2006, pp. 120-123.

[47] Srinivas N. Ahmed N., "Partial Discharge Severity Assessment in Cable Systems," in *Transmission and Distribution Conference and Exposition*, 2001, pp. 849 - 852.

[48] IEEE Standards, "IEEE Guide for Field Testing and Evaluation of the Insulation of Shielded Power Cable Systems," IEEE Power Engineering Society, New York, NY, Standard 400, 2001.

[49] TiePie engineering. (2012, June) TiePie engineering. [Online]. http://www.tiepie.com/en/products

[50] Bélec M. Hudon C., "The Importance of Phase Resolved Partial Discharge Pattern Recognition for On-Line Generator Monitoring," in *IEEE International Symposium on Electrical Insulation*, Arlignton, Virginia, USA, June 1998, pp. 296 - 300.

Appendix A - Turnitin Report

Digital Receipt

This receipt acknowledges that Turnitin received your paper. Below you will find the receipt information regarding your submission.

The first page of your submissions is displayed below.

Submission author:	HEINO VAN JAARSVELDT
Assignment title:	M.Eng Dissertation - November 20…
Submission title:	20569408:JH_van_Jaarsveldt_205…
File name:	van_Jaarsveldt_20569408_-_Turn…
File size:	1.05M
Page count:	109
Word count:	37,999
Character count:	219,007
Submission date:	13-Nov-2014 01:35PM
Submission ID:	477230594

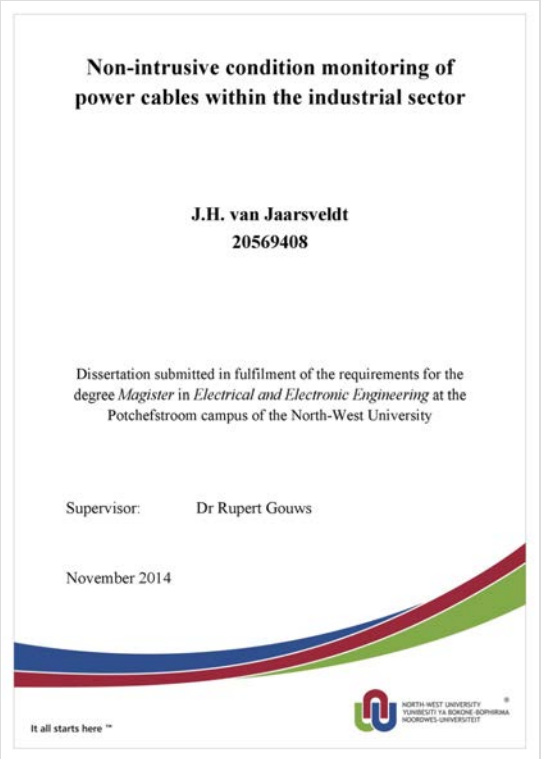

Non-intrusive condition monitoring of power cables within the industrial sector

J.H. van Jaarsveldt
20569408

Dissertation submitted in fulfilment of the requirements for the degree *Magister* in *Electrical and Electronic Engineering* at the Potchefstroom campus of the North-West University

Supervisor: Dr Rupert Gouws

November 2014

It all starts here ™

20569408:JH_van_Jaarsveldt_20569408_-_Turnitin_Version_-_November_2014.docx

ORIGINALITY REPORT

19%	7%	8%	10%
SIMILARITY INDEX	INTERNET SOURCES	PUBLICATIONS	STUDENT PAPERS

PRIMARY SOURCES

1	Submitted to University of Pretoria Student Paper	6%
2	www.nrc.gov Internet Source	3%
3	COMPEL: The International Journal for Computation and Mathematics in Electrical and Electronic Engineering, Volume 31, Issue 2 (2012-02-25) Publication	1%
4	Submitted to Universiti Teknologi MARA Student Paper	<1%
5	Jones, Alan G., Juanjo J. Ledo, Ian J. Ferguson, Jim Craven, Martyn J. Unsworth, Michel Chouteau, and Jessica Spratt. "The electrical resistivity of Canada's lithosphere and correlation with other parameters: Contributions from LITHOPROBE and other programmes", Canadian Journal of Earth Sciences, 2014. Publication	<1%
	Submitted to Higher Education Commission	

Appendix B – SAIEE ARJ Paper

CONDITION MONITORING OF MEDIUM VOLTAGE ELECTRICAL CABLES BY MEANS OF PARTIAL DISCHARGE MEASUREMENTS

H. van Jaarsveldt* and R. Gouws**

*School of Electrical, Electronic and Computer Engineering, North-West University, Private bag X6001, Post-point 288, Potchefstroom, South-Africa, 2520. *E-mail: 20569408@nwu.ac.za*
***E-mail: Rupert.Gouws@nwu.ac.za*

Abstract: The purpose of this paper is to discuss condition monitoring (CM) of medium voltage electrical cables by means of partial discharge (PD) measurements. Electrical cables are exposed to a variety of operational and environmental stressors. The stressors will lead to the degradation of the cable's insulation material and ultimately to cable failure. The premature failure of cables can cause blackouts and will have a significant effect on the safety of such a network. It is therefore crucial to constantly monitor the condition of electrical cables. The first part of this paper is focussed on fundamental theory concepts regarding CM of electrical cables as well as PD. The derivation of mathematical models for the simulation of PD is also discussed. The simulation of discharge activity is due to a single void within the insulation material of medium voltage cross-linked polyethylene (XLPE) cables. The simulations were performed in the MATLAB® Simulink® environment, in order to investigate the effects of a variety of parameters on the characteristics of the PD signal. A non-intrusive CM technique was designed for the detection of PD activity within cables. The CM technique was used to measure and analyse practical PD data. Two MATLAB® programs were designed to analyse the PD data in both the time-domain and frequency-domain.

Keywords: Condition monitoring (CM), partial discharge (PD), cross-linked polyethylene (XLPE) insulation, MATLAB® Simulink®, time- and frequency domain.

1. INTRODUCTION

Electrical networks are interconnections of expensive electrical equipment. Electrical cables are one of the most important parts of any electrical network, as it is used for the transmission of electricity between the variety of electrical equipment. Electrical cables also form an integral part in the safety of any network, as failing cables can lead to the death of employees as well as the damage of expensive equipment. Different types of medium voltage electrical cables are available, each with their own advantages and disadvantages. The type of cable to use is often influenced by the purpose and the physical environment of the cable. Cables are exposed to a variety of environmental and operational stressors which can lead to the degradation of the insulation material and ultimately to cable failure. The level of aging and degradation of electrical cables can be evaluated by means of condition monitoring (CM) techniques [1].

Partial discharge (PD) is classified as both a symptom of degradation as well as a stress mechanism of degradation and will dominate as one of the main degradation mechanisms for medium voltage electrical cables [2]. Due to this, CM techniques, which make use PD measurements, are often used to monitor the condition of electrical cables. PD is the result of localised gasses breakdowns which will occur if the conditions are suitable. A discharge is classified as partial, if the discharge doesn't completely bridge the insulation between two terminals [3].

Since the beginning of the 1990s most energy companies invested in the development of CM techniques. The process of performing CM on electrical equipment can be described as: "Condition monitoring can be defined as a technique or process of monitoring the operating characteristics of a machine in such a way that changes and trends of the monitored characteristics can be used to predict the need for maintenance before serious deterioration or breakdown occurs" [4]. CM techniques are used mainly due to the health of employees and the safe operation of electrical equipment. Any CM technique can be described as an interconnection of the following four main parts:

- Sensor.
- Fault detection.
- Data acquisition.
- Diagnosis.

The choice of sensor is influenced by the physical environment of the equipment being monitored as well as the specific technique used to monitor the equipment. Sensors are used to convert a physical quantity to an electrical signal [4]. The main objective of any CM technique is to detect electrical faults. Fault detection can be described as the process of determining whether a fault is present in equipment being monitored. The data acquisition unit of a CM technique is the link between the measuring of data and the analysis of the measured data. The main purposes of a data acquisition unit are: to amplify the measured signals, the correction of sensor failures and in some cases the conversion of measured

data from analog to digital [4]. The diagnosis of measured data is used to identify trends as well as specific degradation mechanisms [1]. The interpretation of analysed data can be seen as the most important part of any CM technique and is generally performed by a specialist.

The condition of electrical cables needs to be monitored on a regular basis in order to prevent the cables from failing prematurely and causing blackouts. The physical condition of an electrical cable can be determined by the observation, measurement and trending of condition indicators [1]. The ideal cable CM technique adheres to the following desired attributes of a CM technique [5]:

- Non-intrusive and non-destructive.
- Applicable to cable types and materials commonly used.
- Affordable and easy to perform.
- Provides trendable data.
- Capable of measuring property changes that are trendable and that can be correlated to functional performance during normal service.
- Able to identify the location of faults within the cables being tested.
- Able to detect aging and degradation before cable failure.
- Allows a well-defined end condition to be established.

It is impossible for a single technique to adhere to all of the above mentioned desired attributes. A single technique may therefore not be able to completely characterize the condition of an electrical cable. It is important to use a CM program with multiple CM techniques to successfully monitor electrical cables [5].

Electrical detection is a technique commonly used for the detection of PD within electrical cables. Electrical detection of PD can be divided into three groups [2]: 1) the measurement of individual discharge pulses, 2) measurement of total, integrated loss in the insulating material due to discharge activity and 3) the measurement of electromagnetic field effects associated with PD. The technique used to measure individual discharge pulses are commonly used as a CM technique for cables. This technique can be performed by means of a high frequency current transformer (HFCT) connected around the cable. The output of the CT is then measured by means of a digital oscilloscope or similar recording device. The use of a HFCT is a simple and affordable method to perform and also has the safety advantage of being isolated from the generally high operating voltages.

The purpose of this paper is to discuss the design and implementation of a CM technique which make use of PD measurements. The CM technique is focussed on monitoring the condition of medium voltage cables.

2. DESIGN

The purpose of this section is to discuss the design of a cable CM technique, which make use of PD measurements to analyse the condition of electrical cables. The IEEE Guide for Field Testing and Evaluation of the Insulation of Shielded Power Cable Systems will be consulted during the design process of the CM technique [6]. According to the guide PD data can be measured by means of special sensors connected to a splice or termination of the cable. The designed system makes use of a digital oscilloscope to store measured data obtained from the sensors. Designed MATLAB® programs were used to analyse the stored PD data in both the time- and frequency domain. Figure 1 shows an overview of the designed system.

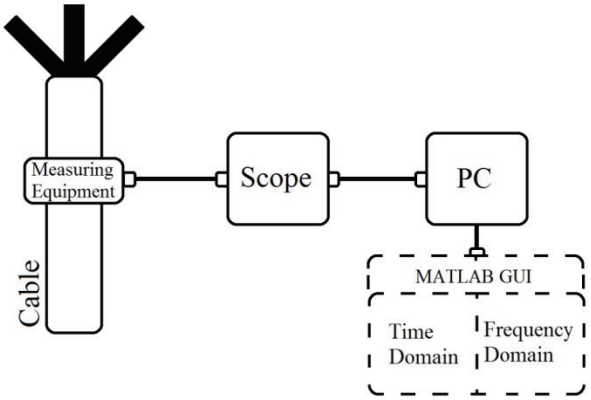

Figure 1: Overview of designed CM technique

An HFCT is used as the sensor device for the detection of PD activity. The physical construction of the HFCT is in the shape of a horseshoe and will allow the user to connect and disconnect the sensor around the cable with ease. The use of an HFCT also isolates the user from the generally high operating voltages and there is also no need for disconnections of cables being tested. The HFCT will be connected directly to a digital oscilloscope. Figure 2 (a) illustrates the commonly used split-core HFCT [7]. An HFCT with the horseshoe structure is shown in Figure 2 (B). Figure 2 illustrates the physical differences between these types of sensors and from this it can be seen that the horseshoe clamp allows for the ease of connection as well as disconnection around cables.

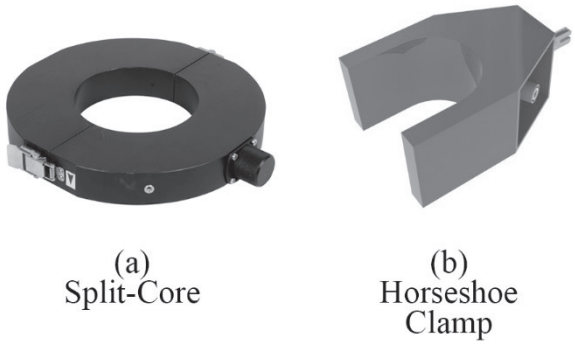

Figure 2: Two HFCT models: (a) split-core [7] and (b) Horseshoe

The system is designed to take PD measurements and store the data on a PC for analysis. The Handyscope HS5, a product of TiePie engineering, will be used as the data acquisition device. The need for a pre-amp is eliminated, due to the sufficient sensitivity of the HS5. The key specifications of the HS5 are shown in table 2.

Table 2: Handyscope HS5 specifications

Product Code	HS5-220
Max. Sampling Speed	200 Ms/s
Bandwidth	250 MHz
Resolution	14bit (0.006%), (16bit enhanced)
Memory	32 M Samples per channel
Accuracy	0.25% DC vertical, 0.1% typical

The PC is used as the device to control the system and also for storage of the recorded data. Two MATLAB® programs were designed to analyse the measured data in both the time- and frequency-domain. The time domain MATLAB® program is designed to display the measured signal in the time domain and to calculate the values for the maximum PD amplitude as well as the average PD amplitude. The time domain program is also used to determine the amount of discharges per phase and the exact position of each discharge within each phase. The results obtained from these two functions are used to perform phase resolved partial discharge (PRPD) analysis of the measured data. The functional flow diagram of these two functions is illustrated in Figure 3.

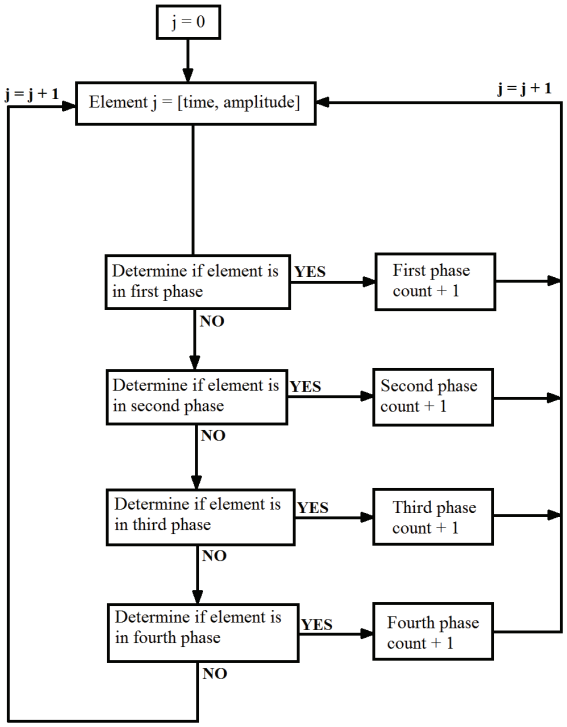

Figure 3: Functional flow diagram of source code

The functional flow illustrates that these two functions will analyse each data point individually. The stored data is in the form of a matrix, with each data point containing two elements: time and amplitude. The time element of each data point is used to determine the specific phase of the measured discharge. The function to determine the amount of discharges per phase will only determine the amount of discharge for a specific phase, as the position of each pulse is not important for this function. PRPD analysis of PD data can be used to determine the source of the discharges. This is an essential part of any CM technique, as different sources may not affect the degradation of the insulation material at the same rate.

A MATLAB® program was also designed for the purpose of analysing the measured data in the frequency domain. The transformation process is used to convert a signal from the time domain to the frequency domain and vice versa, this can also be seen as the most important concept of frequency domain analysis. A built-in fast Fourier transform (FFT) of MATLAB® is used for the transformation purposes of the CM technique. FFT functions are commonly used to convert time domain data to the frequency domain by computing the discrete Fourier transform (DFT) of the signal. The functional flow of a FFT function is shown in Figure 4.

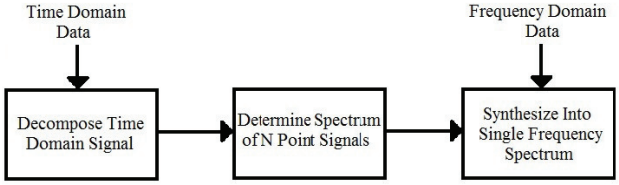

Figure 4: Functional flow diagram of an FFT function

The first step of the FFT function is to decompose an N point signal into N single point signals. This is then used to determine the spectrum of each individual point. The final step of the FFT function is to synthesize the N frequency spectra into a single frequency spectrum.

The frequency domain analysis of the measured data will be used to determine at which frequencies the discharge activity is more prolific. The FFT plot can also be used to determine the severity of PD activity as well as the location of the fault.

3. SIMULATED PARTIAL DISCHARGE RESULTS

3.1 Introduction

The purpose of this section is to discuss the derivation of mathematical models for the simulation of PD. The development of electrical models to study the behaviour of PD activity within the insulation of electrical cables started in 1932, when Germant and Philippoff developed the simplest electrical representation of a defect within the insulation [8]. Research, over the years, lead to the improvement of this original model. The simulations discussed in this paper will be based on this well-known three-capacitor model. The first simulation model will be designed with only the basic parameters required to simulate the occurrence of discharge activity within the insulation material of an electrical cable. The simplicity of this model will cause a lack in accuracy and will also prevent the investigation of certain specific PD

characteristics. This led to the derivation of a more comprehensive simulation model.

It is essential that both models are able to accurately simulate PD activity within medium voltage cables. The chosen parameters of the simulation models are therefore very important and careful consideration is taken before choosing the simulation parameters. Cross-linked polyethylene (XLPE) has become the globally preferred insulation material for medium voltage electrical cables. This is due to the many advantages of XLPE, including: improved impact strength, dimensional stability, tensile strength and an improved resistance to aging [9]. For this reason XLPE will be used as the insulation material for both simulation models. PD in electrical cables generally occurs due to cavities within the insulation material of the cable [10]. Both models simulate PD activity due to a single void within the insulation material of an electrical cable. The dimensions of the void also play an essential part in assuring the accuracy of the simulation models. Voids within XLPE insulation typically have a volume of 10 mm^3, with a radius between 1 mm and 2 mm and a height between 2 mm and 3 mm [11]. This was considered when the dimensions of the voids, for both simulation models, were chosen.

3.2 Basic three-capacitor model

The type of void will have a unique effect on the PD characteristics and will therefore be the main focus of the basic three-capacitor simulation model. The chosen void parameters are also the most important factors for PD characterization. A capacitor circuit was used to model the insulation material as well as the void for the basic simulation model. The capacitor configuration shown in Figure 5 illustrates the three "zones" of the simulation model, including: the void, the insulation in the vicinity of the void and the rest of the healthy insulation [12].

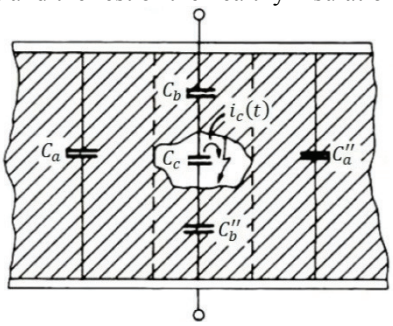

Figure 5: Capacitor configuration for basic model [12]

The derived capacitor circuit was used to design a simulation model in the Simulink® environment of MATALB®. The electrical circuit, on which the Simulink model is based, is illustrated in Figure 6. The main component of the simulation model is the capacitor configuration consisting of the three capacitors, (C_c), (C_b) and (C_a). The parallel RLC branch in the circuit will act as the input impedance to which the measuring equipment will be connected. A high voltage filter (Z) is added to the circuit for the reduction of background noise.

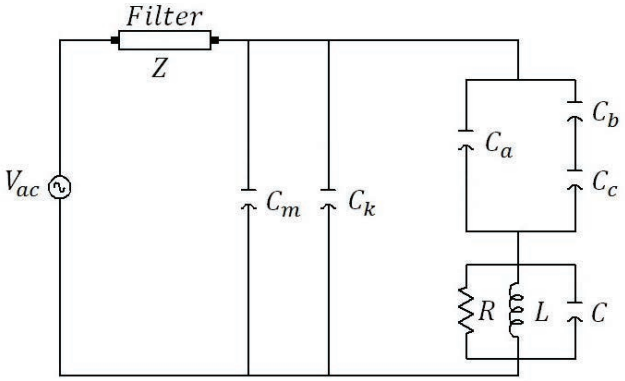

Figure 6: Derived circuit for the basic simulation model

The equations for the three capacitors of the basic simulation model will only be influenced by the permittivity of the insulation material (ε_r), the permittivity of free space (ε_0) and the dimensions of the void. The capacitance value of the capacitor associated with the void is given by [12]:

$$C_c = \frac{\varepsilon_0 \times r^2 \times \pi}{h} \tag{1}$$

The capacitance values for the healthy part of the insulation and the part of the insulation material in the vicinity of the void is calculated by means of the following two equations [12]:

$$C_a = \frac{\varepsilon_0 \times \varepsilon_r \times (a - 2b) \times b}{c} \tag{2}$$

$$C_b = \frac{\varepsilon_0 \times \varepsilon_r \times r^2 \times \pi}{h} \tag{3}$$

These three equations were used to determine the values for the capacitors required for the simulation of PD by means of the basic three-capacitor simulation model.

The first set of simulations was performed in order to study the effect of the input voltage on the maximum amplitude of the measured PD signal. The input voltage was incremented from 7 kV to 50 kV with a constant void size. The results from these simulations are depicted in the graph shown in Figure 7.

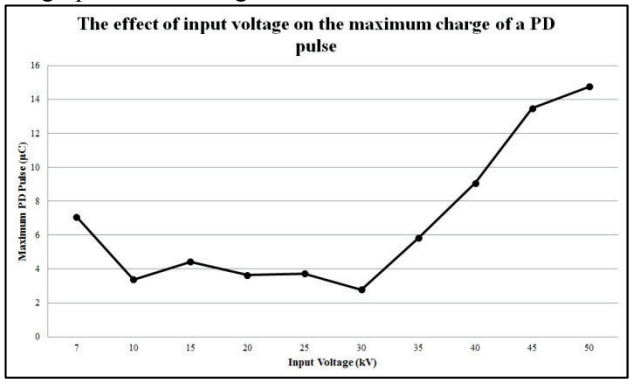

Figure 7: Effect of input voltage on the maximum PD amplitude

From the graph it can be seen that the resulting PD magnitudes, for input voltage between 10 kV and 30 kV, varies between 2 μV and 5 μV. An unusual high maximum PD amplitude is present at an input voltage of 7 kV. The conclusion can be made that the maximum PD amplitude will remain relatively constant for a range of input values. As the input voltage is increased beyond the 30 kV mark, the maximum amplitude also increases. It can therefore be said that an increase in input voltage will result in increased maximum amplitudes of the measured PD signal.

The correlation between the void size and the determined apparent charge was also investigated by means of a set of simulations. The void dimensions included a constant height of 3 mm and the radius of the void was incremented in sizes of 0.5 mm from 1 mm to 5 mm. The input voltage was kept at a constant value for all of the simulations. The change in void parameters for each simulation will result in different capacitance values of the test object. Equations (1), (2) and (3), were used to determine the capacitors of the test object for each of the simulations. The results of this set of simulations are shown in Figure 8.

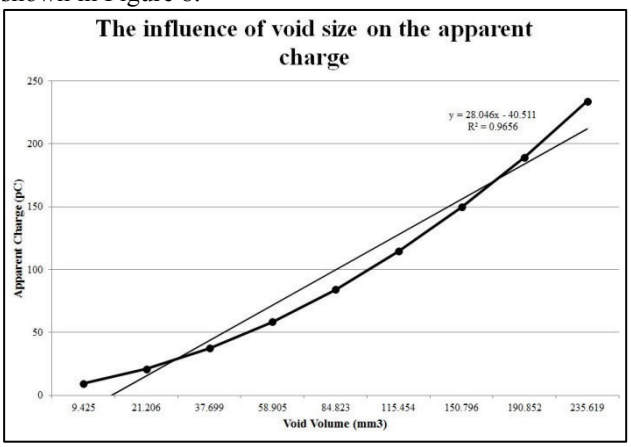

Figure 8: Correlation between void size and apparent charge

A study of the results shown in the graph led to the conclusion that, the correlation between void size and apparent charge is almost linear. A trendline was fitted to the data to be able to determine the coefficient of determination (R^2). The determined coefficient of determination was $R^2 = 0.9656$. The R^2 value indicates that the trendline is a close representation of the actual data. From this the conclusion can be made that a larger void volume will result in an almost linear increase in calculated apparent charge values; this will then result in more severe PD activity within the cable. The equation of the trendline, $y = 28.046x - 40.511$, can be used with the calculated apparent charge value to determine an estimate void size.

The basic three-capacitor simulation model was also used to study the effect of the input frequency on the apparent charge of the PD signal. The results are shown in Figure 9.

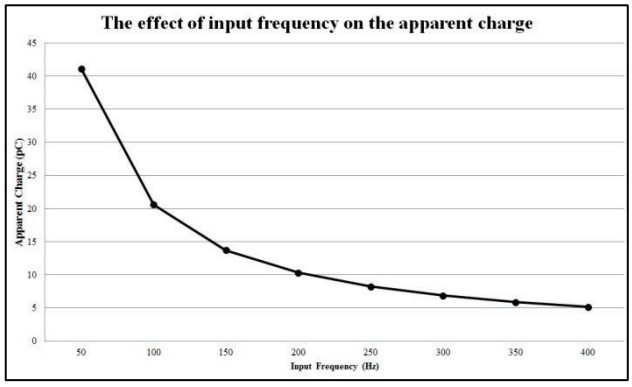

Figure 9: The effect of input frequency on the apparent charge

Published research showed that there is no trend in the effect of input frequencies below 50 Hz on PD characteristics [13]. Input frequencies between 50 Hz and 400 Hz were therefore used for this set of simulations. From the graph it is clear that the input frequency has a definite effect on the apparent charge of the measured signal. As the input frequency is increased above the normal operating frequency of 50 Hz, the apparent charge will decrease. The input frequency will also have an effect on other PD characteristics, such as: PD inception voltage, PD signal magnitude and rise and fall times [13].

3.3 Comprehensive simulation model

The comprehensive simulation model is an improvement of the basic simulation model and will therefore be based on the same principles. The improvements of the comprehensive model resulted in a more complex simulation model. Figure 11 shows the cross sectional view of the basic structure of a medium voltage electrical cable [14].

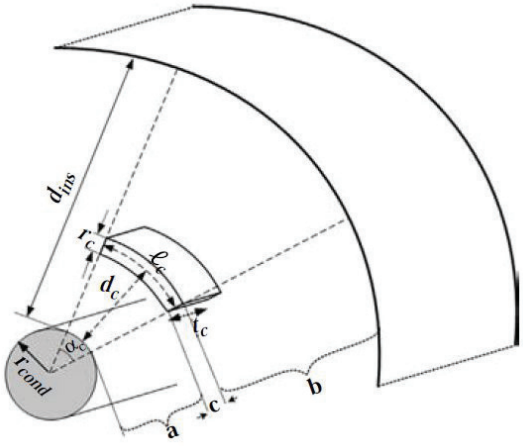

Figure 11: Capacitor configuration comprehensive simulation model [14]

The model shown in Figure 11 was used to derive an electrical circuit which was used to perform the simulations associated with the comprehensive three-capacitor model.

The electrical circuit which was used to create the Simulink® model for the comprehensive simulations is shown in Figure 12.

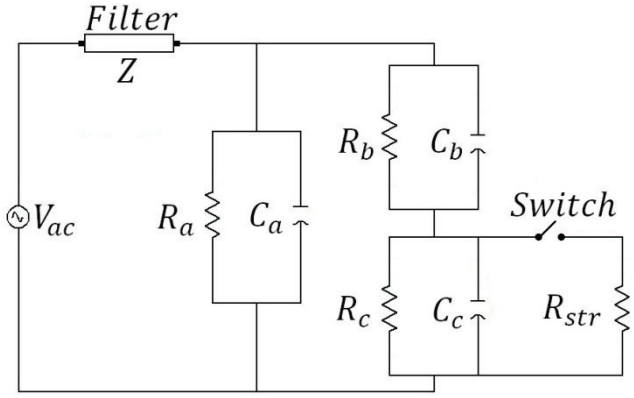

Figure 12: Derived circuit for the basic three-capacitor simulation model

It is clear that the circuit used for the comprehensive simulations has distinct similarities to the circuit used for the basic simulations. The void capacitor is denoted by (C_c), the capacitor of the insulation in the vicinity of the void by (C_s) and the capacitor of the healthy insulation by (C_p). The improvements of the comprehensive model led to the addition of resistors associated with each of the capacitors of the test object. The void resistor is given by (R_c), the resistor for the insulation in the vicinity of the void by (R_s) and the resistor for the rest of the healthy insulation by (R_p). The streamer resistance of the circuit is denoted by (R_{str}). A voltage controlled switch was used to initiate the occurrence of PD activity for this simulation model.

The insulation in the vicinity of the void is divided into two parts, "a" and "b", the capacitor values for both parts are calculated by means of the following equations [14]:

$$C_a = \frac{\varepsilon_{ins}}{\ln\left(\left(r_{cond} + d_c - {}^{r_c}/_2\right)/r_{cond}\right)} \cdot \frac{l_c}{(r_{cond} + d_c)} \cdot t_c \quad (4)$$

$$C_b = \frac{\varepsilon_{ins}}{\ln\left((r_{cond} + d_{ins})/(r_{cond} + d_c + {}^{r_c}/_2)\right)} \cdot \frac{l_c}{(r_{cond} + d_c)} \cdot t_c \quad (5)$$

The capacitance value for the insulation in the vicinity of the void is calculated by means of equation (4) and equation (5) as the equivalent series capacitance value of (C_a) and (C_b):

$$C_s = \frac{C_a C_b}{C_a + C_b} \quad (6)$$

The resistance of part "a" and part "b" of the insulation can be determined by means of the following derived equations [14]:

$$R_a = \frac{1}{\sigma_{ins}} \cdot \frac{r_{cond} + d_c}{l_c t_c} \cdot \ln\left(\frac{r_{cond} + d_c - r_c/2}{r_{cond}}\right) \quad (7)$$

$$R_b = \frac{1}{\sigma_{ins}} \cdot \frac{r_{cond} + d_c}{l_c t_c} \cdot \ln\left(\frac{r_{cond} + d_{ins}}{r_{cond} + d_c + r_c/2}\right) \quad (8)$$

The resistance value for the insulation material in the vicinity of the void is found by means of the equivalent series resistance value of (R_a) and (R_b):

$$R_s = R_a + R_b \quad (9)$$

The capacitance value for the rest of the healthy insulation is calculated by means of the following equation [14]:

$$C_p = \frac{2\pi\varepsilon_{ins}}{\ln((r_{cond} + d_{ins})/r_{cond})} \cdot L \quad (10)$$

The resistance value for this part of the insulation can be found by means of similar assumptions used to determine the value of (C_p) [14]:

$$R_p = \frac{1}{2\pi L\sigma_{ins}} \cdot ln\left(\frac{r_{cond} + d_{ins}}{r_{cond}}\right) \quad (11)$$

The capacitance value of the capacitor associated with the void is determined with the following equation [14]:

$$C_c = \frac{\varepsilon_0}{\ln\left((r_{cond} + d_c + {}^{r_c}/_2)/(r_{cond} + d_c - {}^{r_c}/_2)\right)} \cdot \frac{l_c}{(r_{cond} + d_c)} \cdot t_c \quad (12)$$

The resistance value of the resistor associated with the void is then determined by means of:

$$R_c = \frac{1}{\sigma_c} \frac{r_{cond} + d_c}{l_c t_c} \ln\left(\frac{r_{cond} + d_c + r_c/2}{r_{cond} + d_c - r_c/2}\right) \quad (13)$$

The first set of simulations performed by means of the comprehensive simulation model was used to study the effect of the input voltage on the apparent charge of the PD signal. For this set of simulations the void size was kept constant and the input voltage was incremented by 0.5 kV from 6.6 kV to the final value of 11 kV. The results are shown in Figure 13

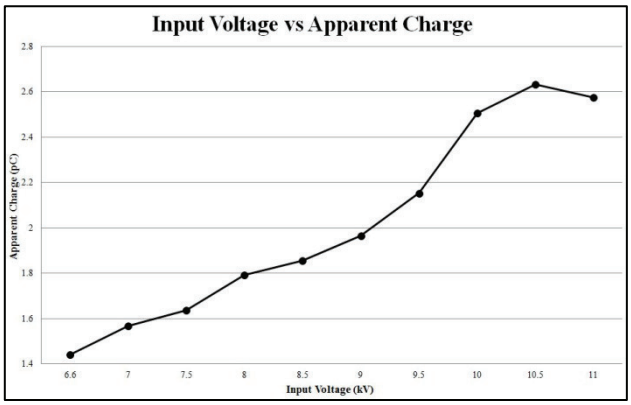

Figure 13: Correlation between input voltage and apparent charge

From Figure 13 it can be seen that an increase in input voltage will result in increased values for the apparent charge. There is however no direct trend between these two parameter. The basic simulation model as well as published work from other researchers yielded similar results.

The comprehensive model can be used to study the effect of both void size and position on the apparent charge. Three different void positions with the exact same void volume were used for this investigation. The three positions included: 1) a void in the middle of the insulation, 2) a void close to the conductor as well as 3) a void near the sheath of the cable. The following equations were used to calculate the position of each void [14]:
Close to the conductor:

$$d_c = 0.15 d_{ins} \quad (14)$$

Middle of insulation:

$$d_c = 0.5 d_{ins} \quad (15)$$

Near the sheath:

$$d_c = 0.85 d_{ins} \quad (16)$$

The length of the void (l_c) was incremented from 1 mm to 5 mm while both the height (r_c) and width (t_c) were kept constant. The simulations for all three the void positions were conducted and the results obtained from each set of simulations were used to draw a graph to show the effect of void volume and void positions on the same graph. The results are shown in Figure 14.

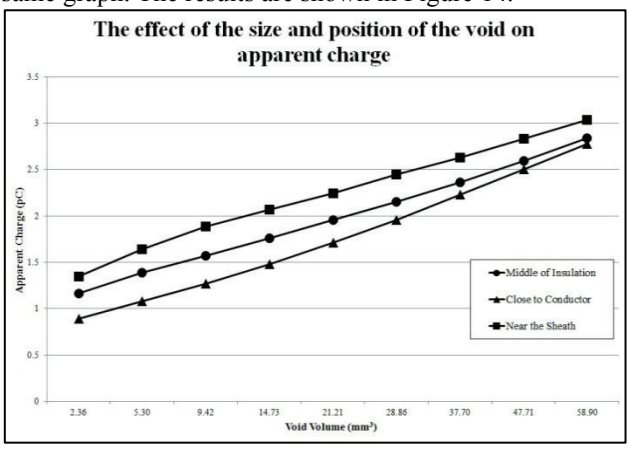

Figure 14: Effect of void parameters on the apparent charge

The graphs in Figure 14 show that an increased void volume will result in an increased value for the calculated apparent charge of the PD signal. The results obtained by means of the basic simulation model were similar to the results obtained from the comprehensive model. The coefficients of determination for the three positions are: middle of the insulation R^2 = 0.9983, close to the conductor R^2 = 0.9943 and near the outer sheath of the cable R^2 = 0.9958. It is thus confirmed that an increased void volume will result in an almost linear increase in apparent charge of the PD signal. The position of the void has an influence on the amplitude of the apparent charge.

The simulations discussed in this paper were used to investigate the effect of a variety of parameters on PD characteristics. The results obtained from both the basic and the comprehensive simulation models show similarities when compared. Results obtained from published research were also compared to the simulation results discussed in this paper. The similarities between results from published research and the results discussed in this paper verify the validity of the simulation models.

4. EXPERIMENTAL SETUP AND RESULTS

4.1 Introduction

The designed CM technique discussed in Section 2 of this paper was used to measure and analyse practical PD data. The experimental setup as well as the analysis of the measured data will be discussed in this section. The purpose of the designed CM technique is only to detect the presence of discharge activity within medium voltage cables and to analyse the measured PD data to some extent. It is necessary to utilize a number of CM techniques as well as the expertise of a specialist for the complete analysis of PD data. The complete CM technique can be divided into a number of stages which must be completed in order to be able to detect the presence of PD within the insulation material of electrical cables. A functional flow diagram of the required steps is illustrated in Figure 15.

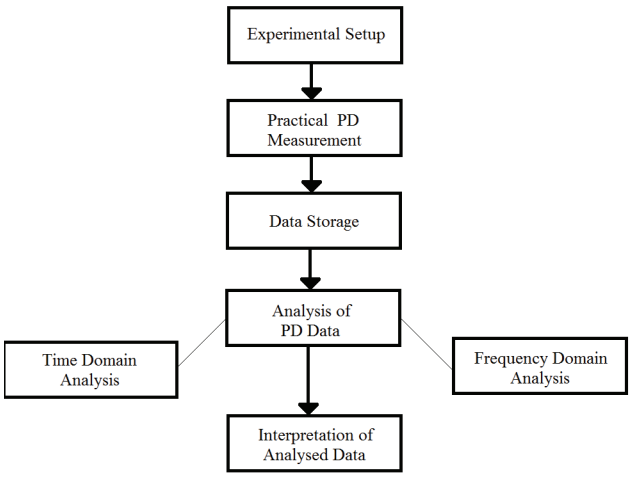

Figure 15: Flow diagram of the stages for the CM technique

The first stage of the CM technique includes the experimental setup of measuring equipment and the test specimen. The next stage is to perform accurate PD measurements on the test specimen. The data obtained from the measurements is then stored for analysis. MATLAB® programs are used to analyse the PD data in the time- and frequency-domain. The final step of the CM technique is to interpret the analysed data. This is the most important step of the entire process and is also the part where the expertise of a specialist is required for the correct interpretation of analysed PD data.

4.2 Experimental setup

The experimental setup of the CM technique includes the combination of measuring equipment and test specimen required for the measuring of practical PD data. The experimental setup of the measuring equipment is shown in Figure 16.

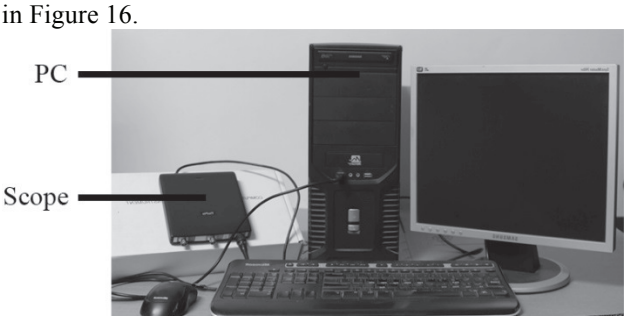

Figure 16: Experimental setup of measuring equipment

The measuring equipment includes a PC, used to control the system as well as to act as storage device for the measured data, and the digital oscilloscope which acts as the data acquisition unit of the CM technique.

A cable termination was used as the test specimen for the measurement of practical PD data. The cable termination was taken out of operation due to the fact that severe levels of discharge activity were detected within this section of the cable. The test specimen is shown in Figure 17.

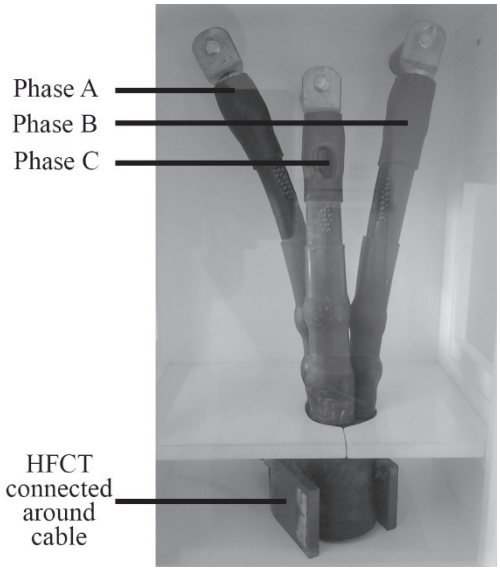

Figure 17: Cable termination

The connection of an HFCT around the cable can be seen in Figure 17. The cable termination is connected to a high voltage variac for the supply of variable input voltages. Sets of measurements were taken at input voltages of 1.6 kV, 3.2 kV and 5 kV. The different levels of input voltage facilitate the study of the effect of input voltage on PD characteristics.

5.3 Analysis of PD data

The process of measuring PD data can be seen as a relatively easy process to perform. The analysis of the measured data is however far more difficult. Modern CM techniques can be used to analyse measured PD data to some extent, but CM techniques are still dependent on the expertise of a specialist for successful analysis of the condition of electrical equipment.

The HS5 scope was used to store the measured data in ".mat" files, which can be accessed by the designed MATLAB® programs. The time domain analysis of the measured data includes: the study of the PD signal over time, the calculation of maximum and average PD amplitude, the calculation of the amount of discharges per phase as well as the ability to indicate the phase patterns of discharges. The time domain program was used to store and analyse data for three cycles (60 ms) of the input voltage. The graphical user interface (GUI) for the designed time domain MATALAB® program is shown in Figure 18.

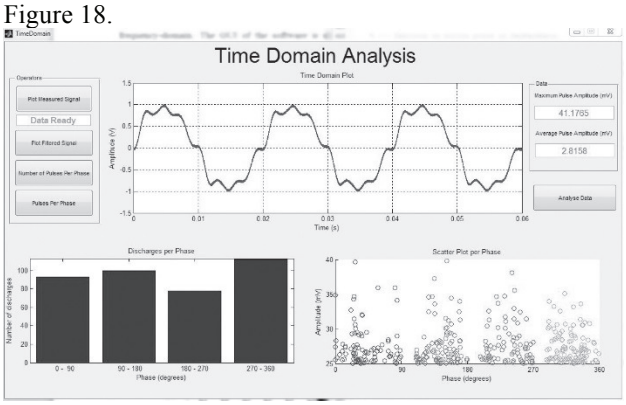

Figure 18: Time domain GUI of MATLAB program

The function to determine the number of discharges per phase was used to analyse the measured data. The results obtained from this function are given in Table 2.

Table 2: Amount of PD pulses per phase

Input voltage (kV)	First phase	Second phase	Third phase	Fourth phase
1.6	93	100	78	112
3.2	140	189	137	214
5	274	356	218	365

The numerical values were also used to construct a histogram of the results in order to be able to study the correlation between the input voltage and the number of discharges per phase. The histogram is shown in Figure 19.

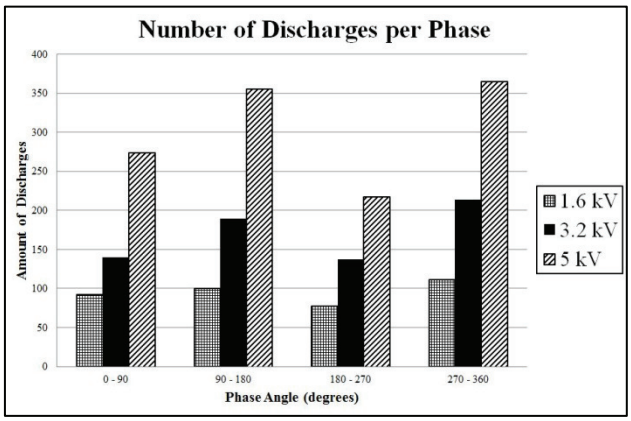

Figure 19: Histogram of amount of PD pulses per phase

From this graph it can be seen that a common trend for all the input voltages are present. The conclusion was made that an increased input voltage will result in increased amounts of discharges per phase. This trend is also present in the results obtained from the simulation models. The graph shows a significant increase in the number of discharges per phase at the 5 kV input voltage. This can be a result of the level of degradation of the cable being tested. When the 5 kV level is reached the input voltage is at such a level that PD activity reaches a critical level and will therefore cause a significant increase in various PD characteristics.

The phase pattern of the measured PD data is shown in Figure 20. The obtained PD patterns are compared to characteristic PD patterns in order to perform PRPD analysis of the measured data.

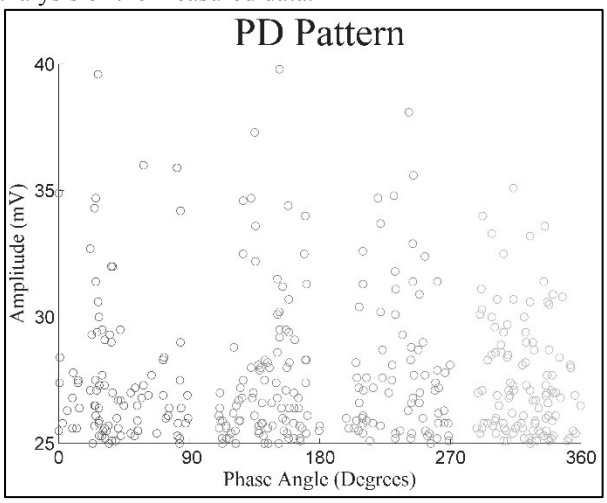

Figure 20: Phase plot of PD patterns at 1.6 kV

The plot shown in Figure 20 was compared to published research as well as characteristic PD patterns to be able to determine the types of discharges present within the test specimen. By means of comparison to the work of Hudon and Bélec [15], it was determined that both internal PD as well as exciter pulses is present within the test specimen. The measurements were taken up to a maximum bandwidth of 50 MHz; it is possible that other PD patterns may be visible if data samples are taken above the 50 MHz bandwidth. PD patterns may be clearer if more samples are taken at each measurement. The reason for this is that insufficient samples may not be enough to reveal a recognizable pattern.

The most important part of the frequency domain analysis is the ability to perform FFT analysis of the recorded time domain signals. The GUI for the frequency domain MATALAB® program is illustrated in Figure 21

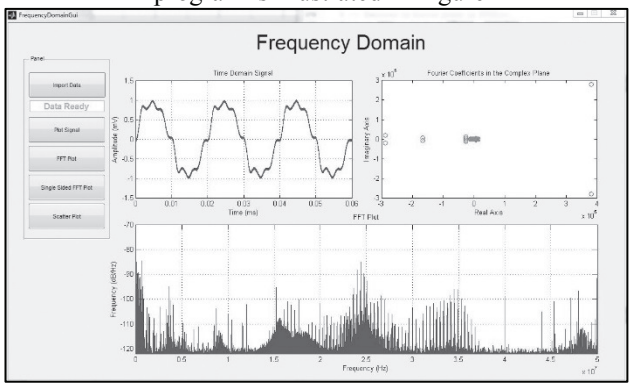

Figure 21: Frequency domain GUI of the MATLAB program

The FFT function is an algorithm which is used to compute the DFT of time domain data. The DFT is a useful operation, but computing it directly from the definition can be a time consuming operation. An FFT is used to compute the same result, but with improved speed. The FFT plot of the measured signal, at 1.6 kV, is shown in Figure 22.

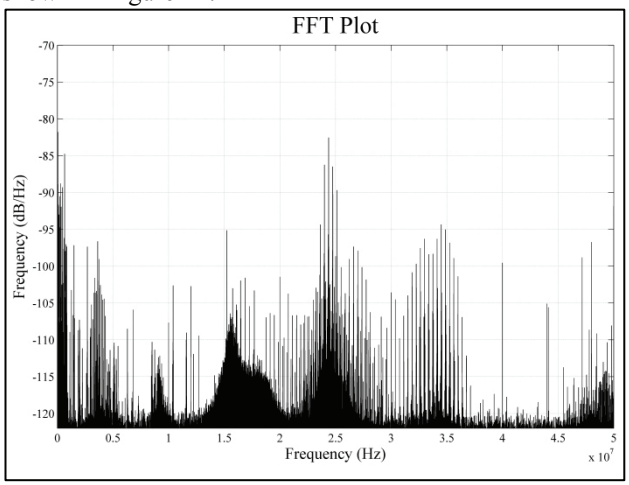

Figure 22: FFT plot at 1.6 kV

Frequency analysis of PD data associated with electrical cables is often used to determine the location of the discharge activity. The FFT plot shown in Figure 22 shows that the discharges are spread over the entire frequency range. A large portion of the discharges are however present between 15 MHz and 35 MHz. The fact that discharges are present in large portions of the measured frequency range testifies to the severity of the measured discharge activity. If the severity of PD activity within a power cable increases to reach a high level, the pulses shown in the FFT plot will continue to grow until most of the frequency range is covered.

5. CONCLUSION

A CM technique was designed which can be used to monitor the condition of electrical cables by means of PD measurements. The CM technique consists of: a sensor, a data acquisition unit and a PC. The type of sensor used for this technique is an HFCT with a physical structure representing a horseshoe. The use of an HFCT as the sensor ensures the safety of this technique, due to the fact that the measuring equipment is isolated from the typically high operating voltages. The data acquisition unit of this technique was a digital oscilloscope. The Handyscope HS5 was chosen due to a number of advantages of this scope. The final component of the CM technique is the PC. The PC is used to control the system and also to act as storage device for measured PD data. Two MATLAB® programs were designed to perform the analysis of measured PD data in both the time- and frequency-domain.

Simulation models were used to simulate the occurrence of PD activity within medium voltage electrical cables. The PD activity is due to a single void within the insulation material of the cable. Research indicated that the well-known three-capacitor model is commonly used to derive mathematical models for the representation of PD activity. The basic three-capacitor simulation model was derived with only the basic required parameters to be able to simulate PD activity. The simplistic approach of this model led to the inability to investigate the effects of a variety of parameters on the PD characteristics. This and reduced accuracy were the main reasons for the development of a more comprehensive model. The comprehensive model is able to investigate a number of crucial PD parameters. The comprehensive model also includes the stochastic nature of PD. The results obtained from the simulations discussed in this paper were used to gain knowledge regarding the phenomenon known as PD.

The designed CM technique was used to measure practical PD data. The test specimen used for the experimental results was a cable termination, taken out of operation due to the fact that discharge activity was previously detected in this component. The measured data was analysed in the time domain in order to determine: the maximum and average amplitudes of the recorded signal, the amount of discharges per phase as well as to plot the phase patterns of the PD pulses. The phase patterns are used to perform PRPD analysis of the measured PD data. This is done by comparing the obtained patterns to characteristic PD patterns as well as patterns of published research. The frequency domain program is used to analyse the measured time domain data in the frequency domain. An FFT function is used to convert the time domain data to the frequency domain. The FFT plots of the measured data were used to investigate: the frequencies at which the discharge activity is most prolific and the severity of the discharge activity.

6. REFERENCES

[1] M. Villaran and R. Lofaro, *Essential Elements of an Electric Cable Condition Monitoring Program*, 1st ed. Upton, NY: Brookhaven National Laboratory, 2010.

[2] A. Haddad and D. Warne, *Advances in High Voltage Engineering*. London, UK: Institution of Electrical Engineering, London, 2004, ch. 4, pp. 139-185

[3] S. Chaikin, "Partial Discharge Testing - Decreasing the Field Failures of High Voltage Components," *HT LLC*, pp. 1-18, March 2001.

[4] Y. Song and Y.H. Han, "Condition Monitoring Techniques for Electrical Equipment - A Literature Survey," *IEEE Transactions on Power Delivery*, vol. 18, no. 1, pp. 4 - 13, January 2003.

[5] Brookhaven National Laboratory, "Assessment of Environmental Qualification Practices and Condition Monitoring Techniques for Low-Voltage Electric Cables," vol. 2, no. 1, February 2001.

[6] IEEE Standards, "IEEE Guide for Field Testing and Evaluation of the Insulation of Shielded Power Cable Systems," IEEE Power Engineering Society, New York, NY, Standard 400, 2001.

[7] Techimp. (2013, June) Techimp Systems. [Online]. http://www.techimp.com/systems/Products/Sensors/PDSensors.aspx

[8] D.A. Nattrass, "Partial discharge XVII The early history of partial discharge research," *IEEE Electrical Insulation Magazine*, vol. 9, no. 4, 1993.

[9] I. A. Metwally, "High-voltage power cables plug into the future," *Potentials, IEEE*, vol. 27, no. 1, pp. 18 - 25, Jan - Feb 2008.

[10] N. Ahmed and N. Srinivas, "Partial Discharge Severity Assessment in Cable Systems," in *Transmission and Distribution Conference and Exposition*, 2001, pp. 849 - 852.

[11] C.Y. Ren, Y.H. Cheng, P. Yan, Y.H. Sun, and T. Shao, "Simulation of Partial Discharge in Single and Double Voids Using SIMULINK," in *Twenty-Seventh International Conference Record of the Power Modulator Symposium*, May 2006, pp. 120-123.

[12] A. Sabat and S. Karmakar, "Simulation of Partial Discharge in High Voltage Power Equipment," *International Journal on Electrical Engineering and Informatics*, vol. 3, no. 1, pp. 234-247, 2011.

[13] C. Nyamupangedengu and I.R. Jandrell, "Partial Discharge Spectral Response to Variations in the Supply Voltage Frequency," *IEEE Transactions on Dielectrics and Electrical Insulation*, vol. 19, no. 2, pp. 521 -531, April 2012.

[14] F Haghjoo, E Khanahmadloo, and S.M. Shahrtash, "Comprehensive 3-capacitor model for partial discharge in power cables," *COMPEL: The International Journal for Computation and Mathematics in Electrical and Electronic Engineering*, vol. 31, no. 2, pp. 346 - 368, 2012.

[15] C. Hudon and M. Bélec, "The Importance of Phase Resolved Partial Discharge Pattern Recognition for On-Line Generator Monitoring," in *IEEE International Symposium on Electrical Insulation*, Arlignton, Virginia, USA, June 1998, pp. 296 - 300.

Appendix C – MATLAB® GUIs

MATLAB® GUIs

The results obtained from both the time- and frequency-domain GUIs are shown in this appendix. The measured PD data at the three input voltages (1.6 kV, 3.2 kV and 5 kV) were analysed by means of the designed MATLAB® programs. The time domain results, at 1.6 kV, obtained by means of the MATLAB® programs are shown in Figure .

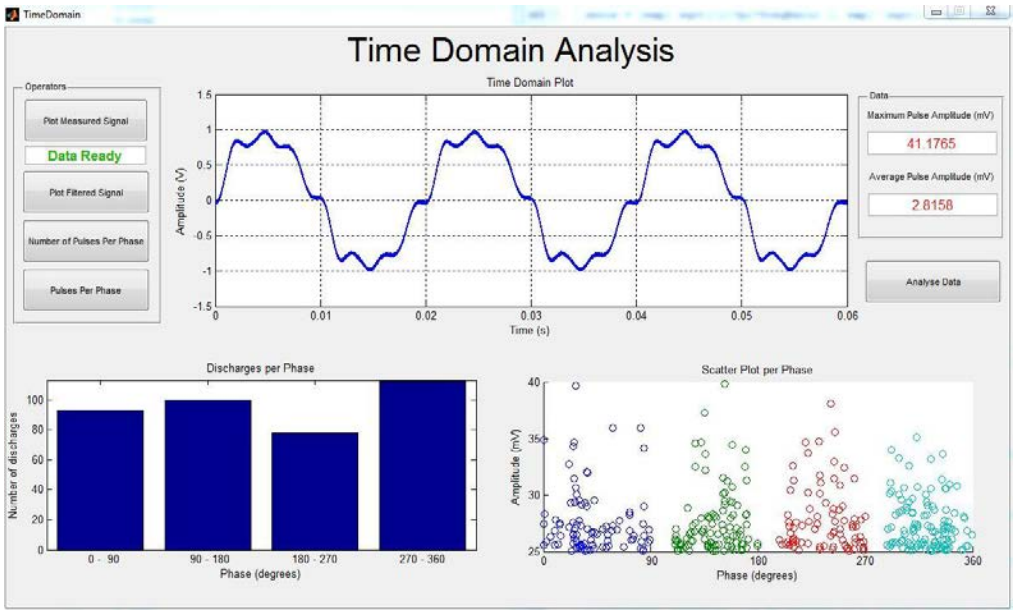

Figure A: Time domain GUI results at input voltage of 1.6 kV

The frequency domain results, at 1.6 kV, obtained by means of the MATLAB® programs are shown in Figure .

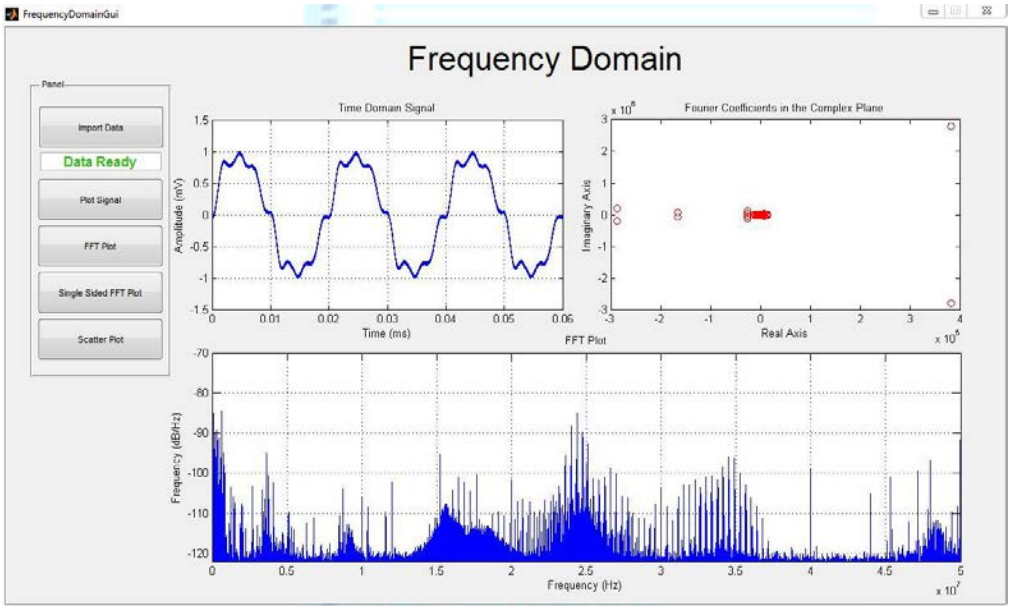

Figure B: Frequency domain GUI results at input voltage of 1.6 kV

Figure CC shows the time domain results, at 3.2 kV, obtained by the time domain MATLAB® GUI. Similarities between the results at 1.6 kV and 3.2 kV are expected due to the same test specimen being used for both sets of measurements. There are also a number of differences present. The shape of the recorded signal is slightly different and also has a larger amplitude, this is due to the fact that the PD is more severe at this level of voltage.

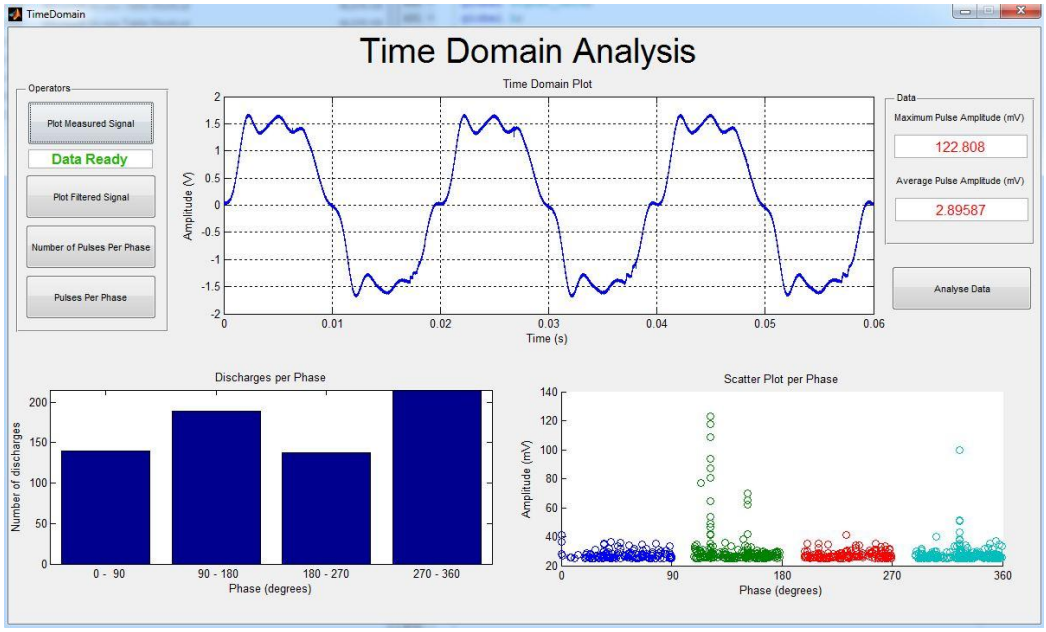

Figure C: Time domain GUI results at input voltage of 3.2 kV

The frequency domain results of the measured data, at 3.2 kV, are shown in Figure . The FFT plot of this data again shows similarities to the data at 1.6 kV. By investigating the two FFT plots it can be seen that the amplitude at 3.2 kV is larger as well as the level of PD being more severe.

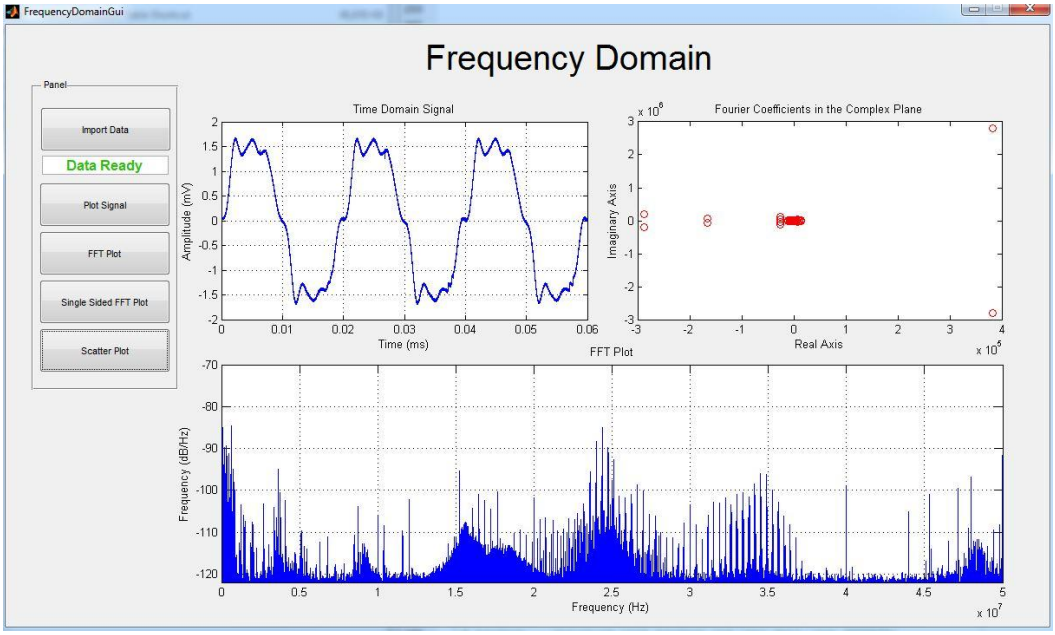

Figure D: Frequency domain GUI results at input voltage of 3.2 kV

The time domain data, at 5 kV, shows some distinct variations when compared to the data of the other two input voltages. Figure shows the results of the time domain GUI of the data measured at 5 kV. It can be seen that the recorded signal has some unique deformities when compared to the other two signals. The amplitude as well as the number of pulses at 5 kV are higher than at the other two input voltages. This is due to the level of PD, at 5 kV, within the test specimen.

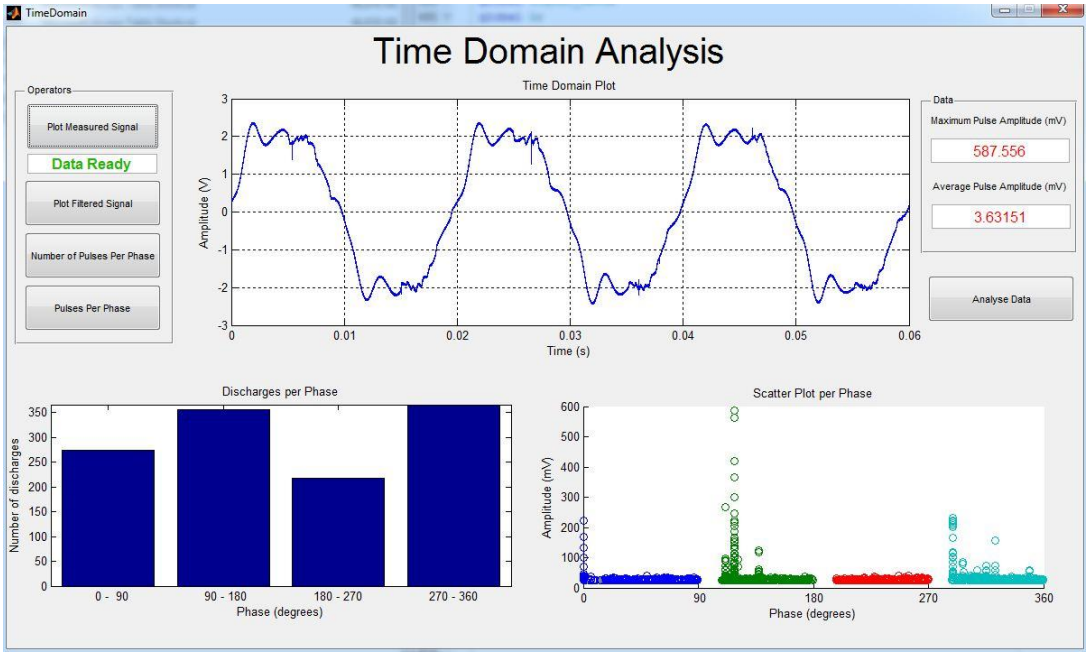

Figure E: Time domain GUI results at input voltage of 5 kV

Figure shows the results obtained by means of the frequency domain MATLAB program of the measured data at 5 kV.

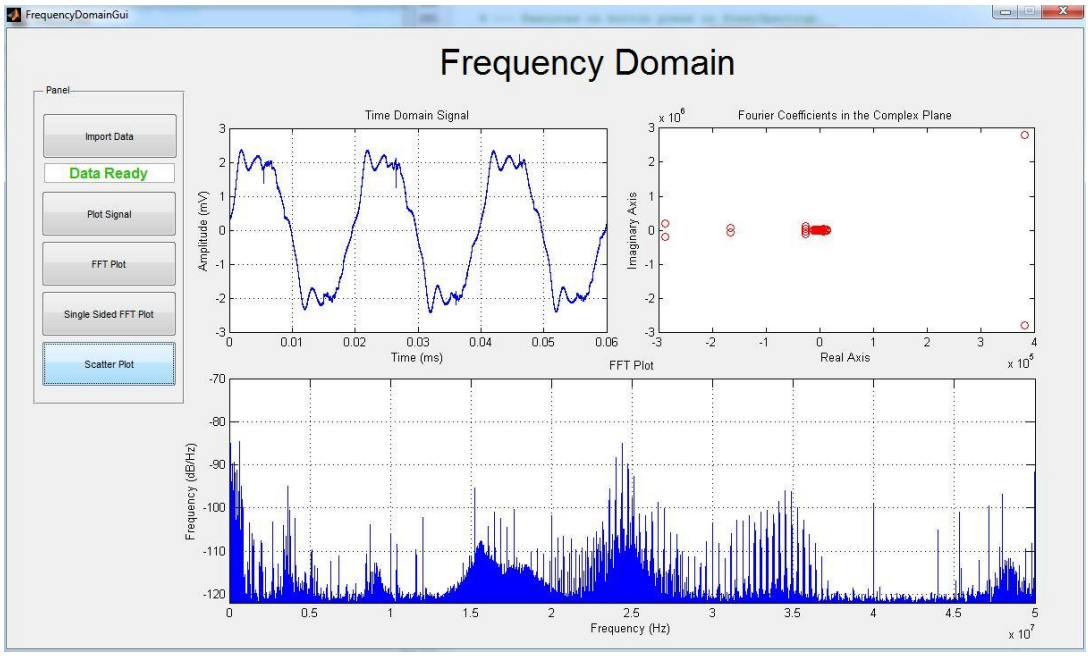

Figure F: Frequency domain GUI results at input voltage of 5 kV

Appendix D – Data CD

A data CD is attached to the dissertation with additional information, relevant to the study. The data CD contains the following:

- Project Documents
- Research Papers
- MATLAB® Programs
- MATLAB® Simulink® Models
- Datasheets
- Photo's